CHAPTER 3

EXTRACTION OF METALS FROM SPENT LITHIUM ION BATTERIES

Extraction of metals from spent lithium ion batteries

Considering the metals of importance for lithium ion batteries, it is desired to extract not only the cobalt but other metals such as Li, Ni and Mn also from the cathodic active material of the end-of-the life batteries. The present study is mainly focused on the sulfuric acid leaching of such metals in absence or presence of a reductant.

3.1 Leaching of metals from the cathode material in absence of reductant

Effect of temperature, time, acid concentration and pulp density has been investigated in order to optimise the parameters while studying the kinetics of leaching. In order to understand the extraction behaviour of metals by the hydrometallurgical process, examining the thermodynamic aspects particularly the stability regions of different phases in the aqueous solutions would be useful.

3.1.1 *Thermodynamic aspects of the metals in cathode active material*

Although, the Eh-pH diagrams of lithium and nickel under normal conditions are available in literature (Schweitzer and Pesterfield, 2010), but for the concentrations generally found in spent LIBs, Pourbaix diagrams for these systems are reconstructed (FactSage® 6.4) and are shown in Fig. 3.1a (0.1 M Li) and Fig. 3.1b (0.1 M Ni).

The Eh-pH diagrams of Co-H_2O and Mn-H_2O systems are particularly important to discuss in view of indifferent leaching behaviour of their higher valence states which exhibit the stability region for the redox couple: Co(II) - Co(III) and Mn(II) - Mn(IV). Therefore, the Eh-pH diagrams for both metals with concentrations generally found in the spent batteries, have been redrawn at 298 K and 1 atm pressure using data from various sources (Schweitzer and Pesterfield, 2010; Pourbaix, 1966) including that of FactSage® 6.4 software.

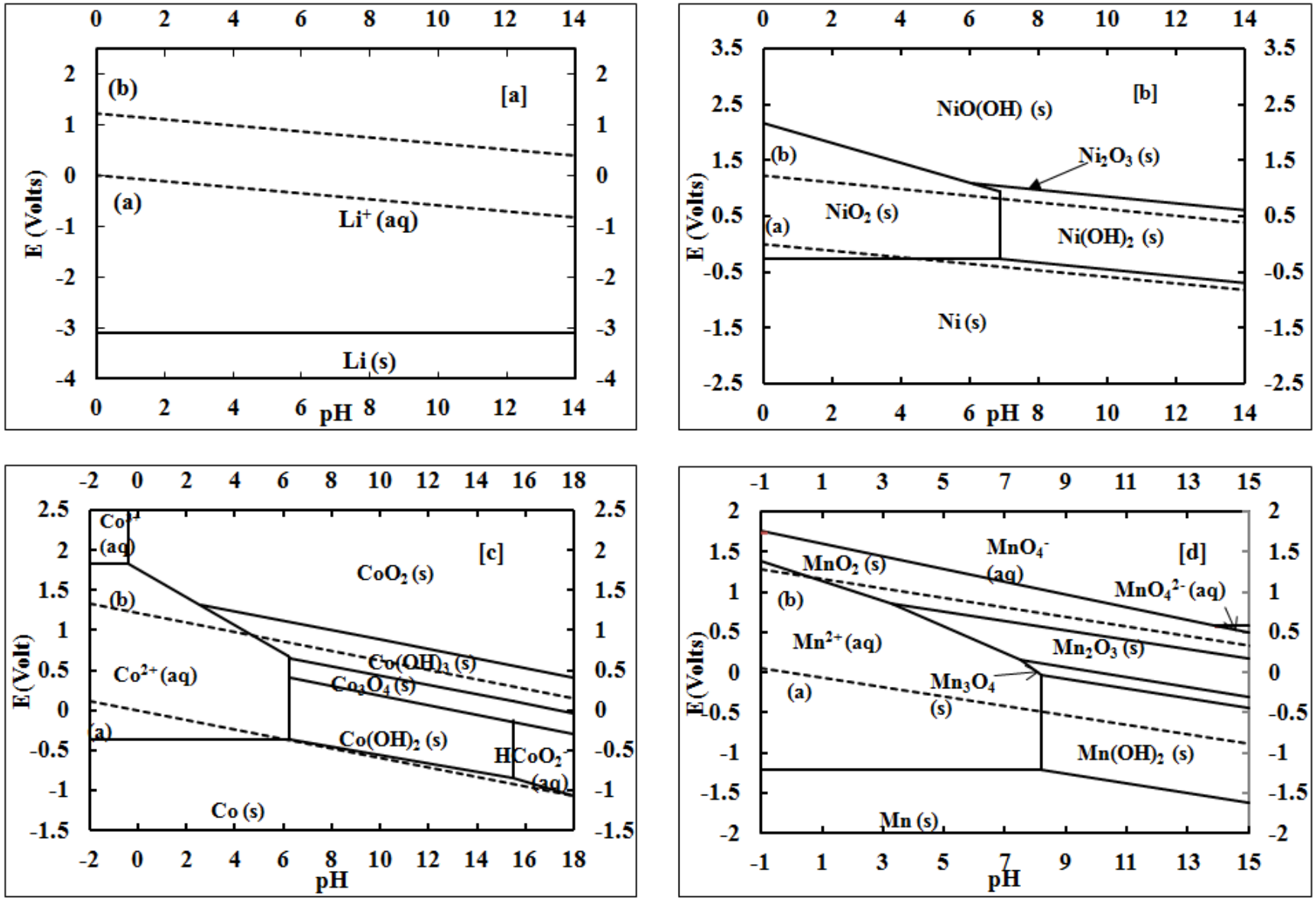

Fig. 3.1: Eh-pH diagram for [a] Li-H_2O, [b] Ni- H_2O, [c] Co- H_2O and [d] Mn- H_2O system at 298 K

The Eh-pH diagram of Co-H_2O system at 0.5 M Co is incorporated in Fig. 3.1c. As mentioned above, Co(III) oxide present as $LiCoO_2$ in the cathode material has to dissolve in sulfuric acid. Co^{3+} phase cannot dissolve even in strong acid until redox potential reaches to ~ +1.84 V. This region falls above the line (b), which is difficult to achieve under the normal leaching conditions. However, if cobalt is available as Co(II) which is possible by reducing Co(III), it can be solubilized in acid as its stability region extends till pH 6.3. $Co(OH)_3$ can be reduced to $Co(OH)_2$ through Co_3O_4 in alkaline solution also at the higher pH and can be reductively leached (Co^{2+}) in an acid. In the Eh-pH diagram of Mn-H_2O system (0.1 M Mn), the domain of stable Mn phases is within the stability region of water (Fig. 3.1d), whose lower limit is indicated by line (a). Manganese (II) can thus be dissolved in entire acidic region. In order to dissolve Mn(IV) [MnO_2] phase which is also a part of $Li_2CoMn_3O_8$ [a spinel structure containing Mn(III) and Mn(IV)] in the spent batteries, a very strong reducing condition and strong acid solutions are required to form soluble Mn(II) phase. At pH > 3.2, Mn(IV) can however, be solubilized as Mn(II) under relatively lower redox conditions through the formation of an intermediate phase viz., Mn_2O_3(s).

3.1.2 *Leaching of metals using different acids:* In order to study the efficacy of different acids for the leaching of cathode active material, the concentration of acids such as HCl and H_2SO_4 was varied from 0.5 to 3 M at 368 K and 50 g/L pulp density (PD) for 240 min. As can be seen from Fig. 3.2a the recovery of all the metals increased with increase in HCl concentration. On the other hand the leaching of metals viz., Li, Ni and Mn was almost constant (Fig. 3.2b) with H_2SO_4 in the concentration range 1-3 M. Within 240 min, 93.4% Li, 66.2% Co, 96.3% Ni and 50.2% Mn were leached out with 3 M H_2SO_4 as compared to the leaching of 91% Li, 64.1% Co, 87.5% Ni and 68.6% Mn with 3 M HCl under the similar conditions. Hence further optimization experiments were performed using 1 M H_2SO_4 which was preferred over HCl due to the high metal yields. Experiments with nitric acid were however, avoided to alleviate the gaseous pollution (NO_x) and need of specific material of construction.

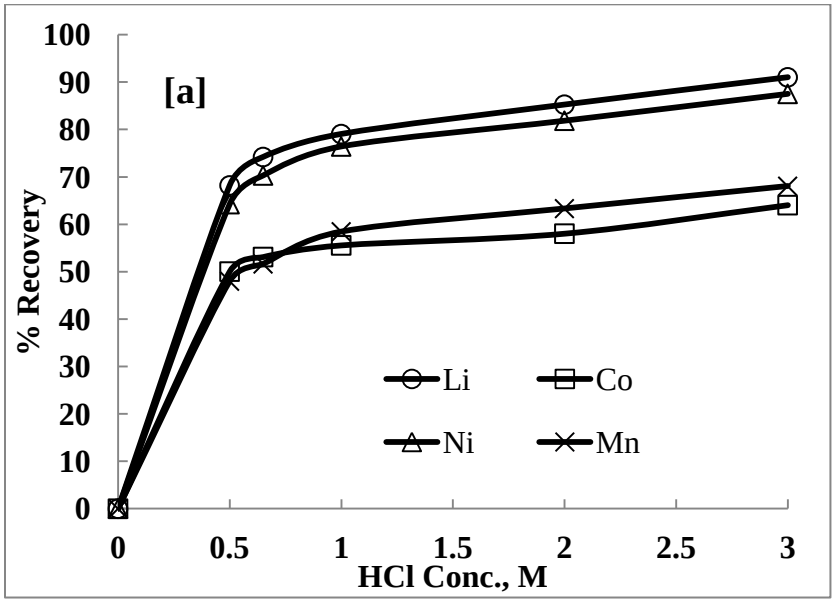

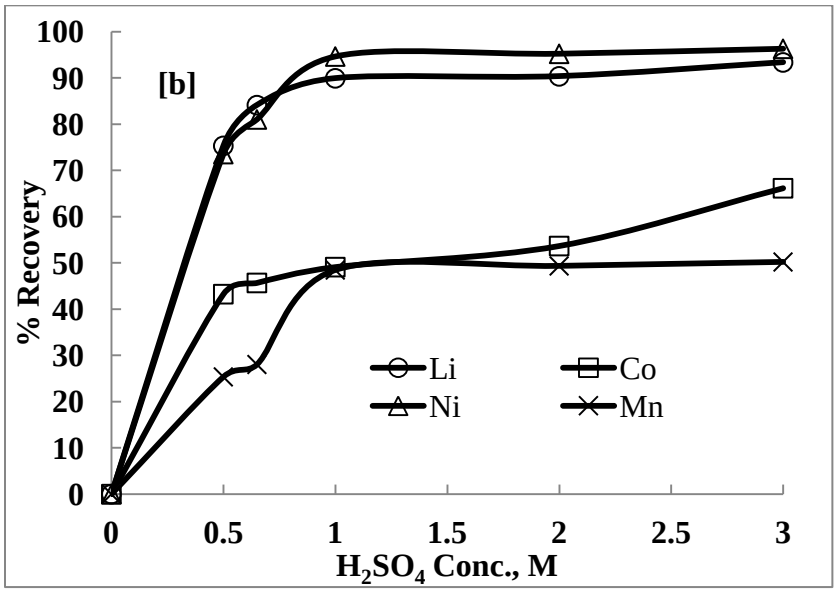

Fig. 3.2: Effect of acid concentration on the leaching of cathode active material (a) HCl, (b) H_2SO_4, 368 K, 50 g/L pulp density, 240 min.

3.1.3 *Effect of time on the leaching of metals:* Leach recovery of metals (Li, Co, Ni and Mn) in 1 M H_2SO_4 at 368 K and 50 g/L pulp density with time (0 – 300 min) is shown in Fig. 3.3. The increase in leaching time improved the dissolution of all metals. Besides, the extent of dissolution of the metals was high in 180 min except for manganese and cobalt. Leaching of 89.9% Li, 94.7% Ni and only ~49% Co and Mn was recorded in 240 min with 1 M H_2SO_4. Lower recovery of the cobalt and

manganese may be attributed to the higher oxidation states of cobalt and manganese such as Co^{3+} and Mn^{4+} which are not soluble in acid. The redox potential (E_{SCE}) of the solution was found to be >900 mV over the leaching period of 120 min.

As such the leaching efficiency of cobalt depends on the concentration of reductant used. Reductant converts Co(III) or Mn(IV) to the +2 state for effective dissolution and subsequent recovery by standard methods (Lee and Rhee, 2003; Pagnanelli et al., 2014). It is evident from the Eh-pH diagram of Co-H_2O system (Fig. 3.1d) that the soluble Co^{3+} phase can be formed by the oxidation of Co^{2+} in strong acidic media at around +1.84 V. The Co(II) remains stable in solution in the pH range 1-6.3. Similarly in the case of Mn (Fig. 3.1d), direct reduction of Mn(IV) to Mn^{2+} can be possible only in very stringent conditions (Schweitzer and Pesterfield, 2010).

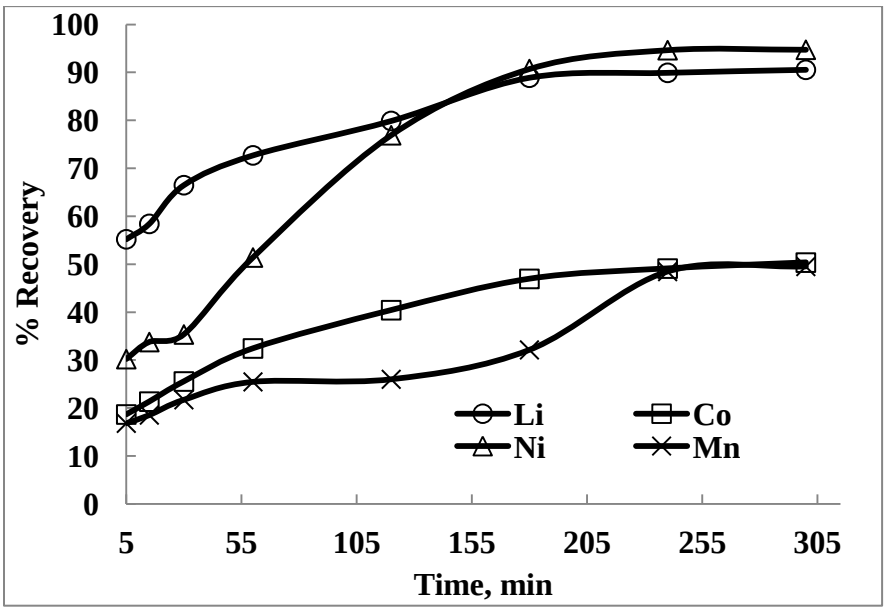

Fig. 3.3: Effect of time on the leaching of metals using 1 M H_2SO_4 at 368 K and 50 g/L pulp density.

3.1.4 *Effect of stirring speed*: Effect of stirring speed on the leaching of metals present in the cathode active material was studied using 1 M H_2SO_4 at 368 K and 50 g/L pulp density for 240 min. The dissolution of the metals show only minor increase after 250 rpm and the leaching efficiency remained unchanged after 500 rpm (Fig. 3.4). Therefore, a stirring speed of 500 rpm was maintained during the subsequent leaching

experiments which was found to be sufficient to keep the particles under suspension and minimize the diffusion layer of lixiviant around the powder being leached out.

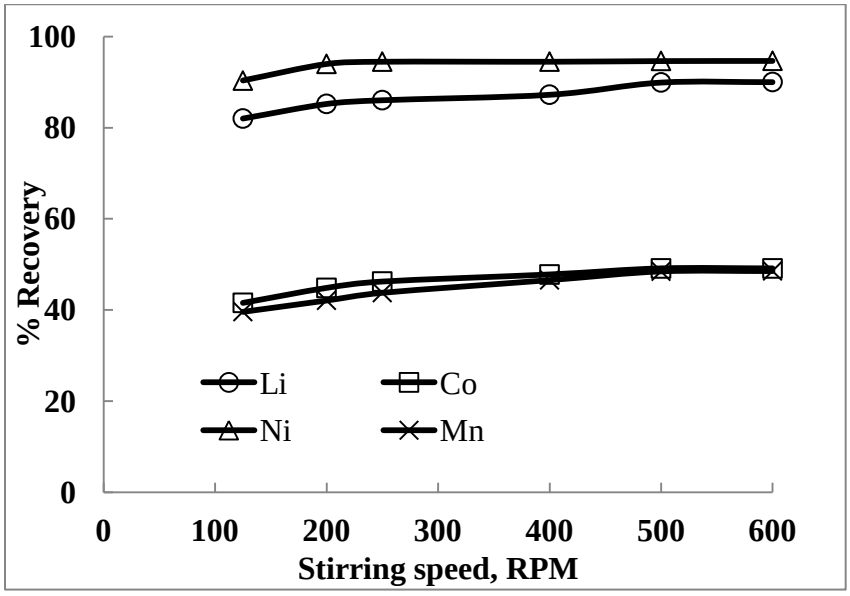

Fig. 3.4: Effect of stirring speed on the recovery of metals from cathode active material using 1 M H_2SO_4 at 368, 50 g/L PD and 240 min

3.1.5 *Effect of pulp density on the leaching of metals:* Fig. 3.5 shows almost similar leaching efficiency of all the metals when the pulp density is maintained in the range 5 - 50 g/L. In particular, ~90.6% Li, 95.9% Ni and only about 50% of Co and Mn were recovered at 5 g/L pulp density while increasing pulp density to 100 g/L lowered the leaching to 83.4% Li, 46.4% Co, 89.6% Ni and 42.3% Mn. The lower pulp density could increase the concentration of metal ions in the leach solution, strengthen mass transfer and accelerate the leaching rate (Rubisov et al., 2000). But the lower pulp density would lead to increased volume of the leach liquor which is not favorable for subsequent metal separation and recovery. Hence 50 g/L pulp density was taken as optimum for rest of the experiments.

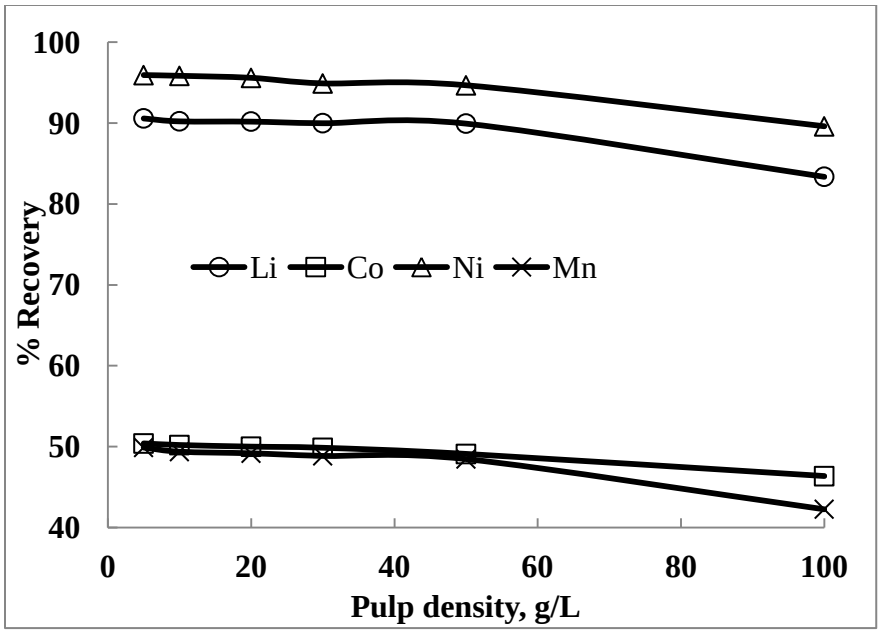

Fig. 3.5: Effect of pulp density on the leaching of cathode active material using 1 M H_2SO_4 at 368 K in 240 min.

3.1.6 *Effect of temperature on the leaching of metals:* Effect of temperature on the leaching efficiency of the valuable metals was studied in 1 M H_2SO_4 at a pulp density of 50 g/L for 240 min of leaching time. Results (Fig. 3.6) show that percentage recovery of all metals increased with increase in temperature. At 308 K only 76.4% Li, 43.3% Co, 85.7% Ni and 40% Mn were recovered which increased to about 90% Li, 49% Co, 94.6% Ni and 48.5% Mn at 368 K. The thermodynamic feasibility of leaching of $LiCoO_2$, the major phase of cathode material with H_2SO_4 solution at 368 K is evident from equation (3.1):

$$4LiCoO_{2(s)}+6H_2SO_{4(aq)}\rightarrow 4CoSO_{4(aq)}+2Li_2SO_4+6\,H_2O+O_{2(g)},\ \Delta G^{o}_{368} = -748.0\ kJ \quad (3.1)$$

The above results further affirm that some reductant is necessary to reduce Co(III) and Mn(IV) present in the material to the lower oxidation state to improve the leaching even at higher temperature (368 K). XRD analysis of the leach residue (Table 3.1) also shows the presence of unreacted phases which could be leached out under stringent conditions.

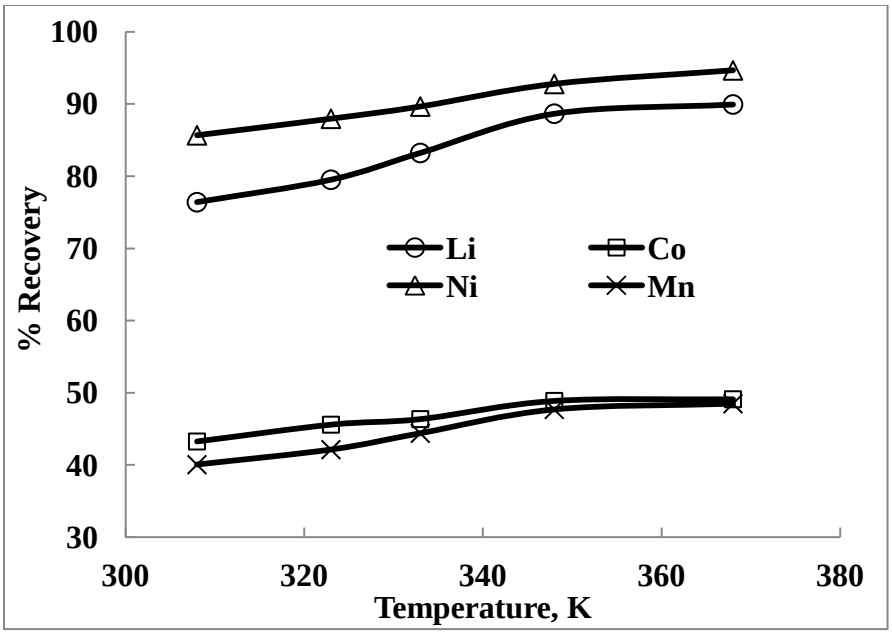

Fig. 3.6: Effect of temperature on the leaching of cathode active material using 1 M H_2SO_4 at 50 g/L in 240 min.

Effect of varying temperature with time on the leaching of metals is shown in Fig. 3.7. The rate of dissolution has steadily increased till 240 min and thereafter changed slightly. The low recovery of manganese can be attributed to the lower solubility of Mn(IV) present in the spinel structure of $Li_2CoMn_3O_8$ as discussed in the thermodynamic section (Fig. 3.1d) under the experimental conditions maintained here. The percentage leaching of different metals can be utilized to examine the kinetics of leaching while applying the standard rate equations.

3.1.7 *Kinetics of leaching*: Data on the extraction of different metals at varying temperature were tested using shrinking core models (Levenspiel, 1999) particularly the chemical control [$1-(1-x)^{1/3} = k_c.t$ ---(1.17)] and diffusion control [$1-(2/3)x-(1-x)^{2/3} = k_{d.}\, t$ ---(1.18)] kinetic expressions described in Chapter 1. The leaching data show poor fit to these models as shown in Figs. 3.8 and 3.9; this is evident from the low values of R^2 (0.76 to 0.98). However, the kinetic data fitted well to the empirical model based on the logarithmic rate law [$(-\ln(1-x))^2 = k_l.\, t$---(1.20), Chapter 1] controlled by the surface layer diffusion of the lixiviant (Kim et al., 2011). The plots of '$(-\ln(1-x)^2$ *vs* t' at different temperatures show (Fig. 3.10 a, b, c, d) the best fit of kinetic data to the logarithmic equation which is inferred from the high R^2 values like

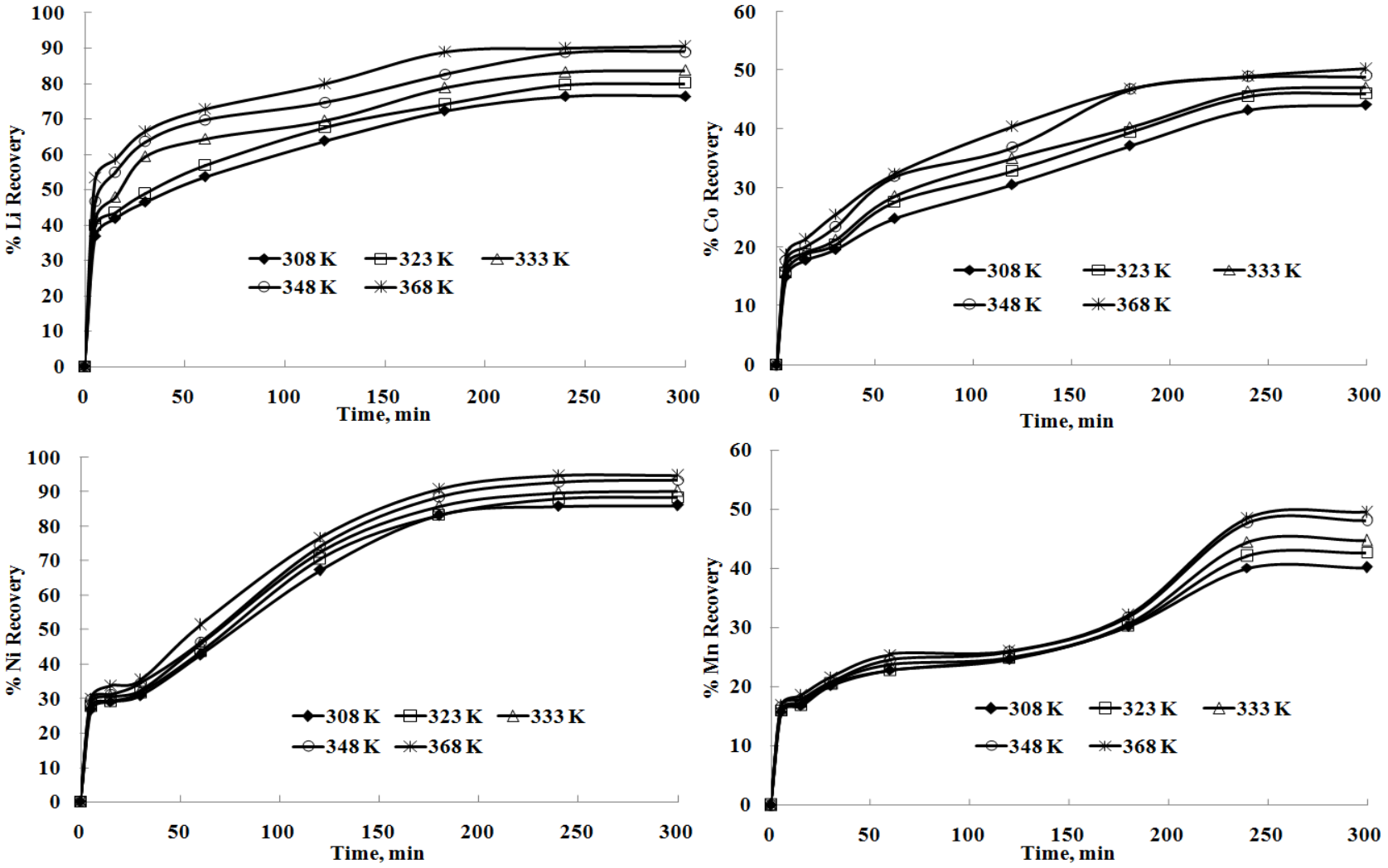

Fig. 3.7: Recovery of Li, Co, Ni and Mn from spent cathode active material at various temperatures using 1M H_2SO_4 at 50 g/L in 240 min

0.97- 0.98 for Li, 0.98 for Co, and 0.96-0.99 for Ni. Due to different oxidation states of manganese present in the spent battery and spinel structure of the manganese containing phase, the leaching data did not fit well to the model used.

The values of the specific rate constant obtained from the kinetic data corresponding to the empirical model (Fig. 3.10) were used for making the Arrhenius plot [Eq. 1.21 ($k = A\ e^{-Ea\ /\ RT}$), Chapter 1] and to estimate the activation energy values for the leaching of different metals (Fig. 3.11). Activation energy (kJ/mol) was calculated to be 16.4 for Li, 7.4 for Co and 18.5 for nickel in the temperature range 308-368 K. The E_a values are well within the range for dissolution of metals following the logarithmic expression (Kim et al., 2011). The mechanism of leaching through the surface layer diffusion of the reactant can be substantiated by analyzing the change in phases (by XRD) and morphological features (by SEM) of leach residues as compared to the untreated sample.

3.1.8 *Characterization of the leach residue:* The XRD patterns of the leach residues are shown in Fig. 3.12, besides the XRD of cathodic material while the identified phases (major and minor) are listed in Table 3.1. Upon leaching with 1 M H_2SO_4 at 368 K and 50% PD in 60 min the major phases were identified to be $LiCoO_2$, $(Li_{0.65}Ni_{0.05})(NiO_2)$, NiO_2 and with CoF_4 being minor, illustrated the dissolution of lithium and other metals with decreased ratio of lithium in the respective products (Fig. 3.12a). The reduced amount of residue obtained in 120 min of leaching and the XRD phase analysis of the same (Table 3.1) indicate the conversion of lithium and nickel bearing phases originally present in the material (Fig. 3.12b). Along with major phases like $LiCoO_2$ and NiO_2, the non-stoichiometric entities such as $(Li_{0.65}Ni_{0.05})(NiO_2)$, and $(Li_{0.55}Ni_{0.05})(NiO_2)$ were observed to be the major and minor phases, respectively. $CoFeF_5.7H_2O$ was also observed in minor amounts. While the residue in 240 min of leaching had major phases- $(Li_{0.09}Ni_{0.01})(NiO_2)$, CoF_4 and $LiCoO_2$, the minor phases being $Li_{0.06}NiO_2$ and $CoFeF_5.7H_2O$ (Fig. 3.12c). $LiCoO_2$ in the residue did not react completely because of the presence of Co^{3+} ions without using a reducing agent. Some reduction of Co(III) with Mn(III) could also take place

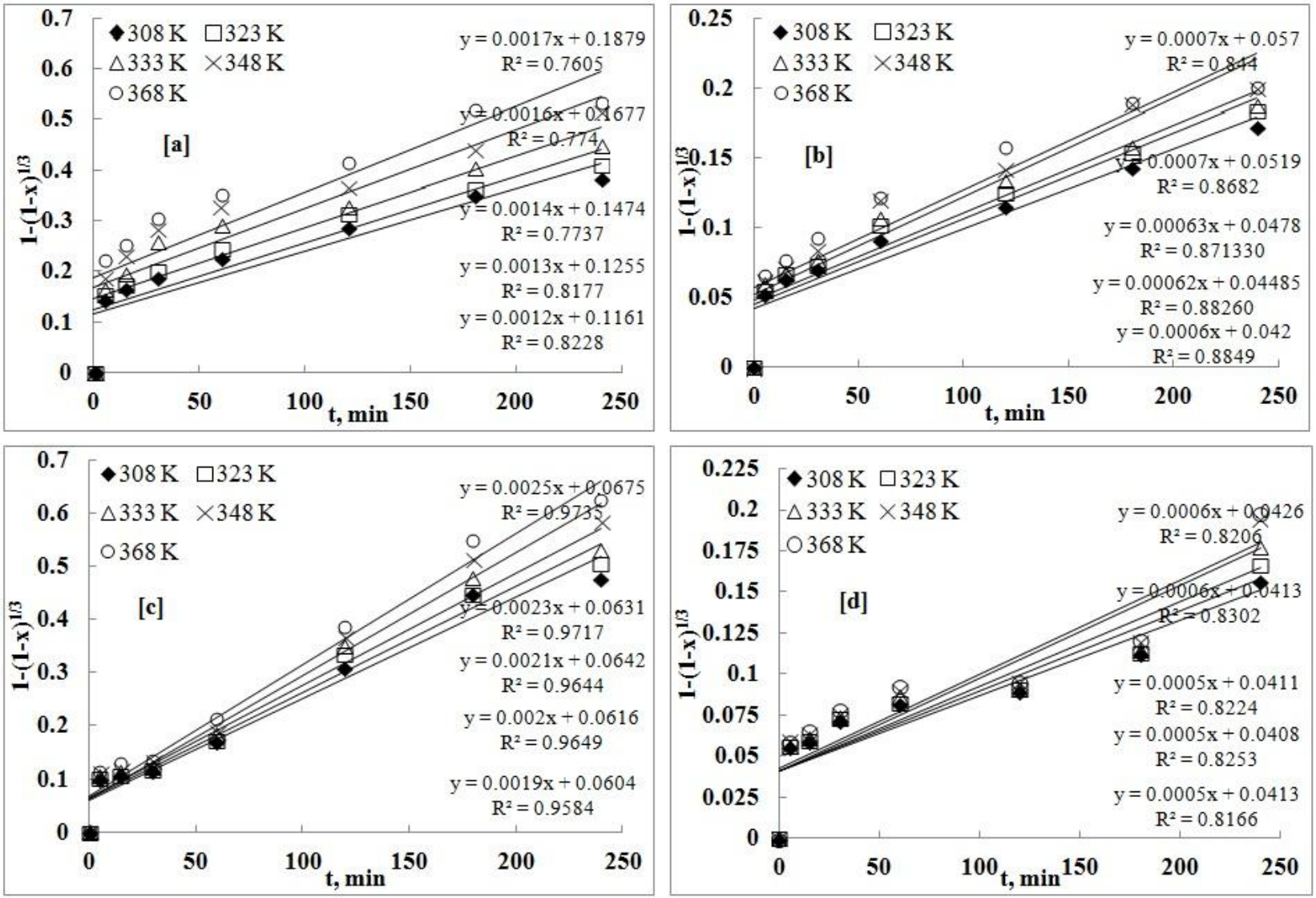

Fig. 3.8: Chemical controlled kinetic model for the leaching of metals (a- Li, b-Co, c-Ni, d-Mn) in temperature range (308 - 368 K)

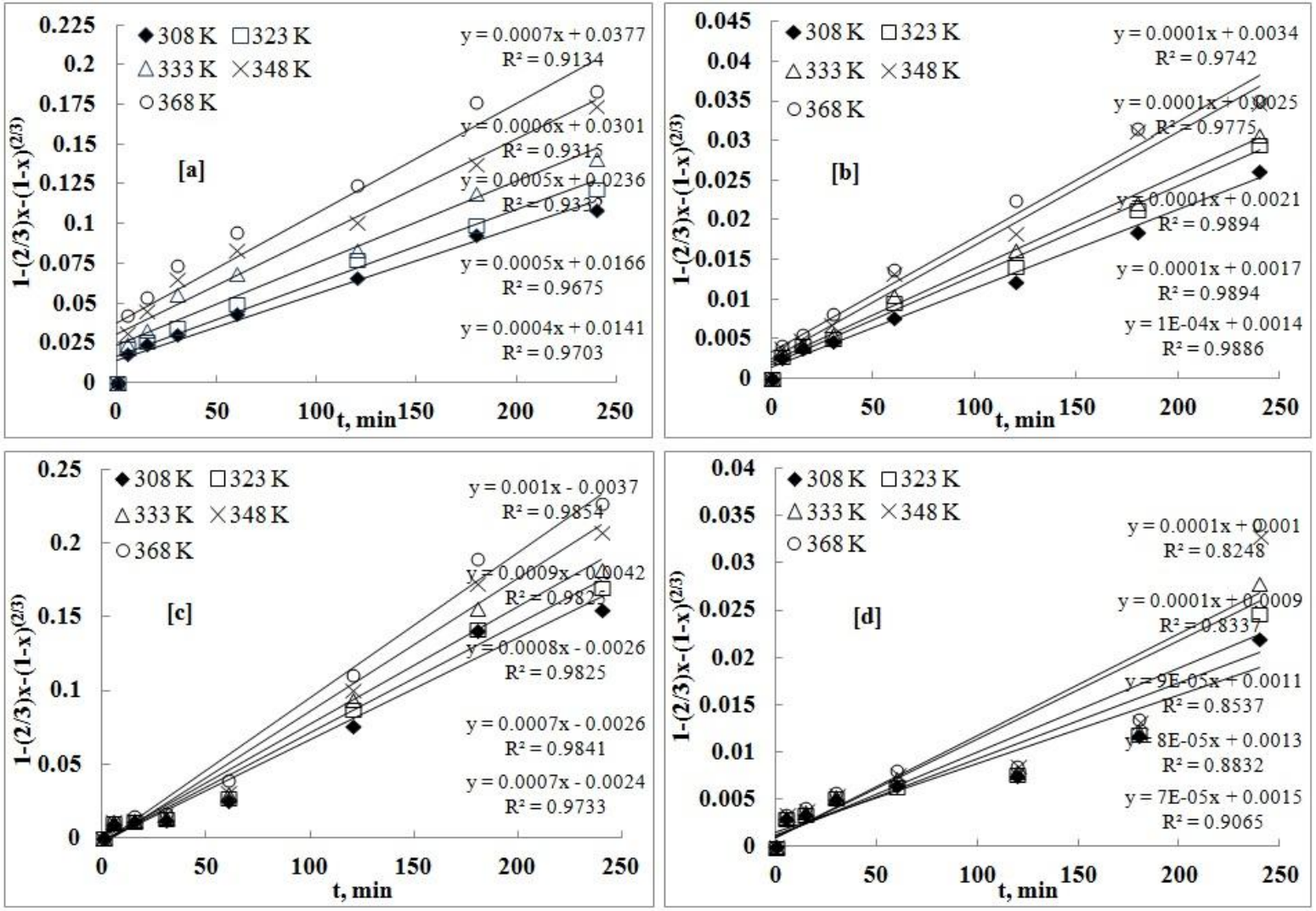

Fig. 3.9: Diffusion controlled kinetic model for the leaching of metals (a- Li, b-Co, c-Ni, d-Mn) in temperature range (308-368 K)

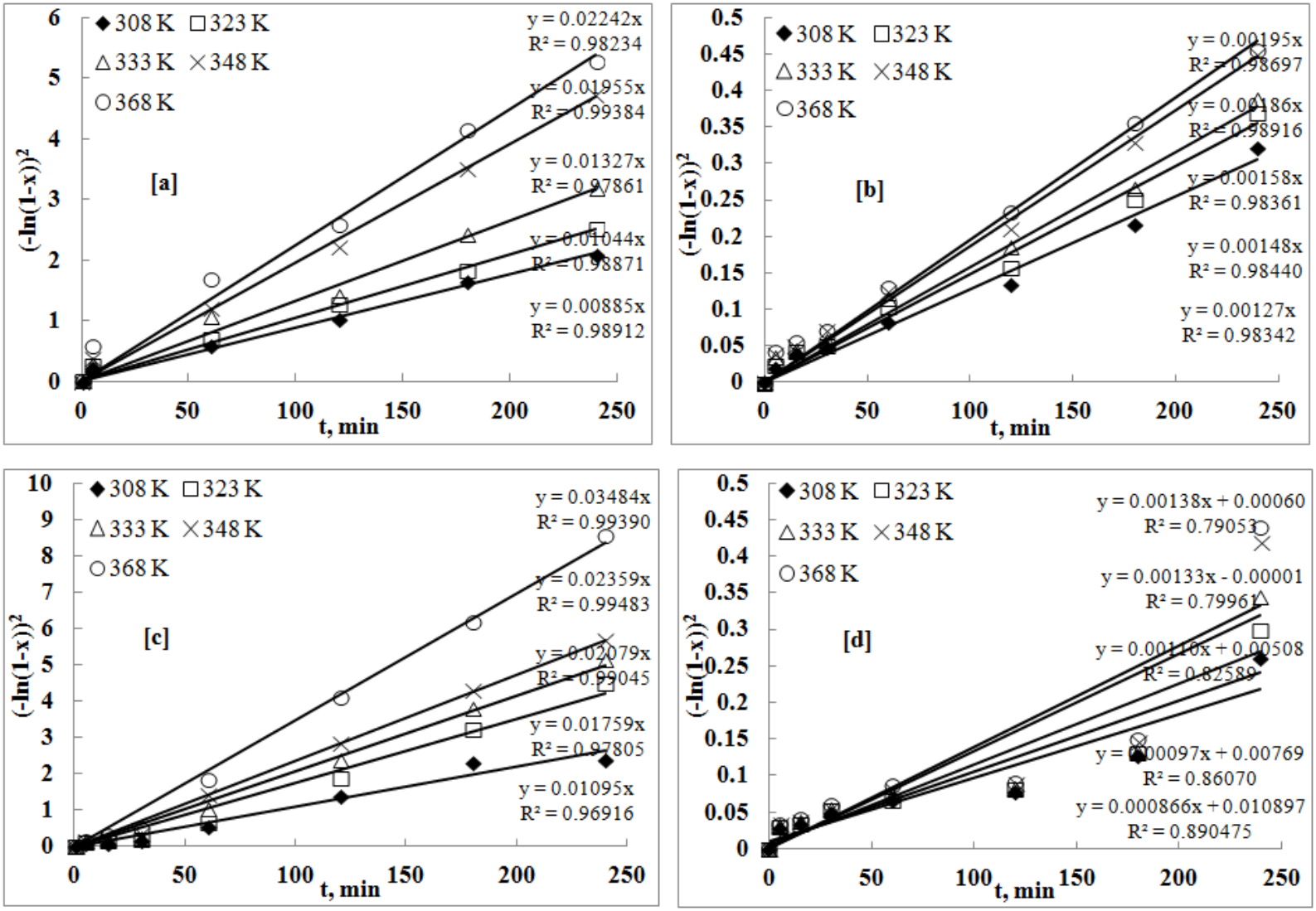

Fig. 3.10: Empirical model for kinetics of leaching metals (a- Li, b-Co, c-Ni, d-Mn) in temperature range (308-368 K)

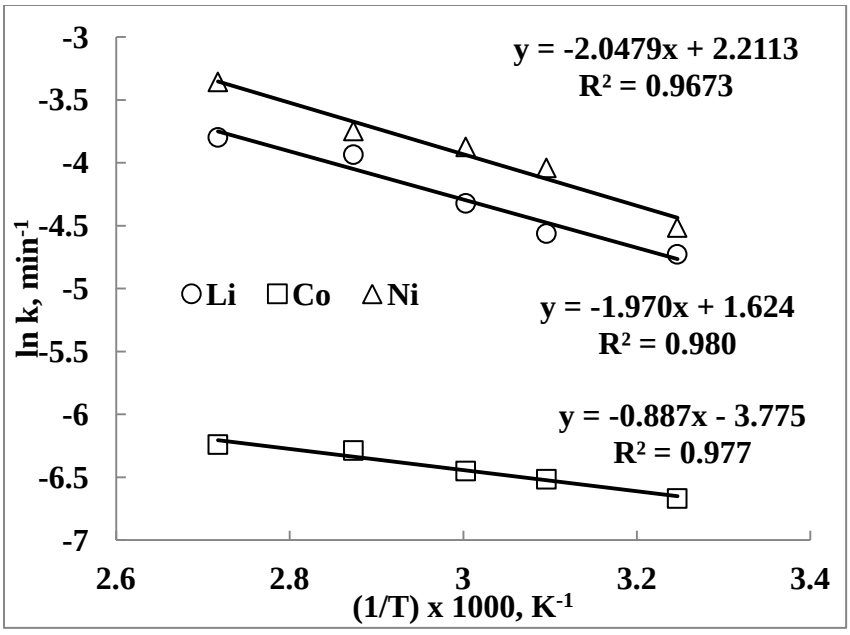

Fig. 3.11: Arrhenius plot for empirical kinetic model applied for lithium, cobalt and nickel.

as observed in the leach residue (Table 3.1) in view of the redox reaction which is evident from the E^o values [Mn(III) → MnO_2, E^o +0.95; Co(III) → Co(II), E^o +1.82]. The XRD patterns also show the progressive reduction in the intensities of major peaks in the residue obtained with time.

The SEM images of the residues obtained in leaching at 368 K under the optimum conditions at different time intervals (60-240 min) are shown in Fig. 3.13 which can be compared with the SEM image of the untreated cathodic material (Fig. 3.13a). Lithium is not detected by SEM. The residue of 60 min leaching (Fig. 3.13b) depicts the morphology with the localized corrosion observed for particle-1 along with reduction in size of particles, besides the low cobalt content (Fig. 3.13b) in more corroded particle (point 3). Fig. 3.13c exhibits the morphology of the leach residue in 120 min which is much more corroded with still lower metal content. In particular, particles 2 and 3 might be transformed by the leaching of lithium and some cobalt, with remaining white porous phase rich in Co(III).

Residue obtained in 240 min (Fig. 3.13d) reflects the wide spread corrosion with lower levels of the metal constituents analyzed by EDAX. Thus cobalt content was lowered in most reacted particles; Co being < 30% at point 1. The presence of small amount of manganese can also be seen at point 1. A minimum change on the

surface with minor reaction around the edges can be seen in Fig. 3.13d at point 3 for a Co-rich particle of smaller size which is essentially a Co(III) phase. Maximum recovery of metals such as Co, Li, Ni and Mn observed in 240 min of leaching, is thus corroborated by the SEM-EDAX and XRD studies. Surface corrosion of the particles with time supports the applicability of logarithmic rate law controlled by the surface diffusion of the lixiviant, sulfuric acid on the particles of cathode material.

Table 3.1: XRD phase analysis of cathodic material and leach residues at different time interval. [Conditions: 1 M H_2SO_4, 368 K and 50% PD]

Sample	**Major phase**	**Minor phase**
Cathode active material	$LiCoO_2$,$Li_2CoMn_3O_8$, $(Li_{0.85}Ni_{0.05})(NiO_2)$	$(Li_{0.69}Ni_{0.01})(NiO_2)$, CoF_4
Leach residue in 60 min	$LiCoO_2$, $(Li_{0.65}Ni_{0.05})(NiO_2)$, NiO_2	$(Li_{0.49}Ni_{0.01})(NiO_2)$, CoF_4
Leach residue in 120 min	$LiCoO_2$, $(Li_{0.65}Ni_{0.05})(NiO_2)$, NiO_2	$CoFeF_5.7H_2O$, $(Li_{0.55}Ni_{0.05})(NiO_2)$
Leach residue in 240 min	$LiCoO_2$, $(Li_{0.09}Ni_{0.01})(NiO_2)$, CoF_4	$Li_{0.06}NiO_2$, $CoFeF_5.7H_2O$

To increase the leaching efficiency, use of different reductants has been reported (Lee and Rhee, 2003; Chen et al., 2015). The hydrogen peroxide is often used as a reductant during the leaching. The H_2O_2 or other reductant reduces Co^{3+} to Co^{2+} and Mn^{4+} to Mn^{2+} in the spent LIBs, which are favourably solubilized compared to using only acid as leaching agents (Lee and Rhee, 2003; Zhu et al., 2012). The sulfuric acid leaching of cathodic material is therefore, investigated in the presence of two reductants, viz., $NaHSO_3$ and H_2O_2 and parameters are optimized. Also the kinetics and mechanism of the metal dissolution are stressed upon and are supported by the XRD and SEM-EDAX studies.

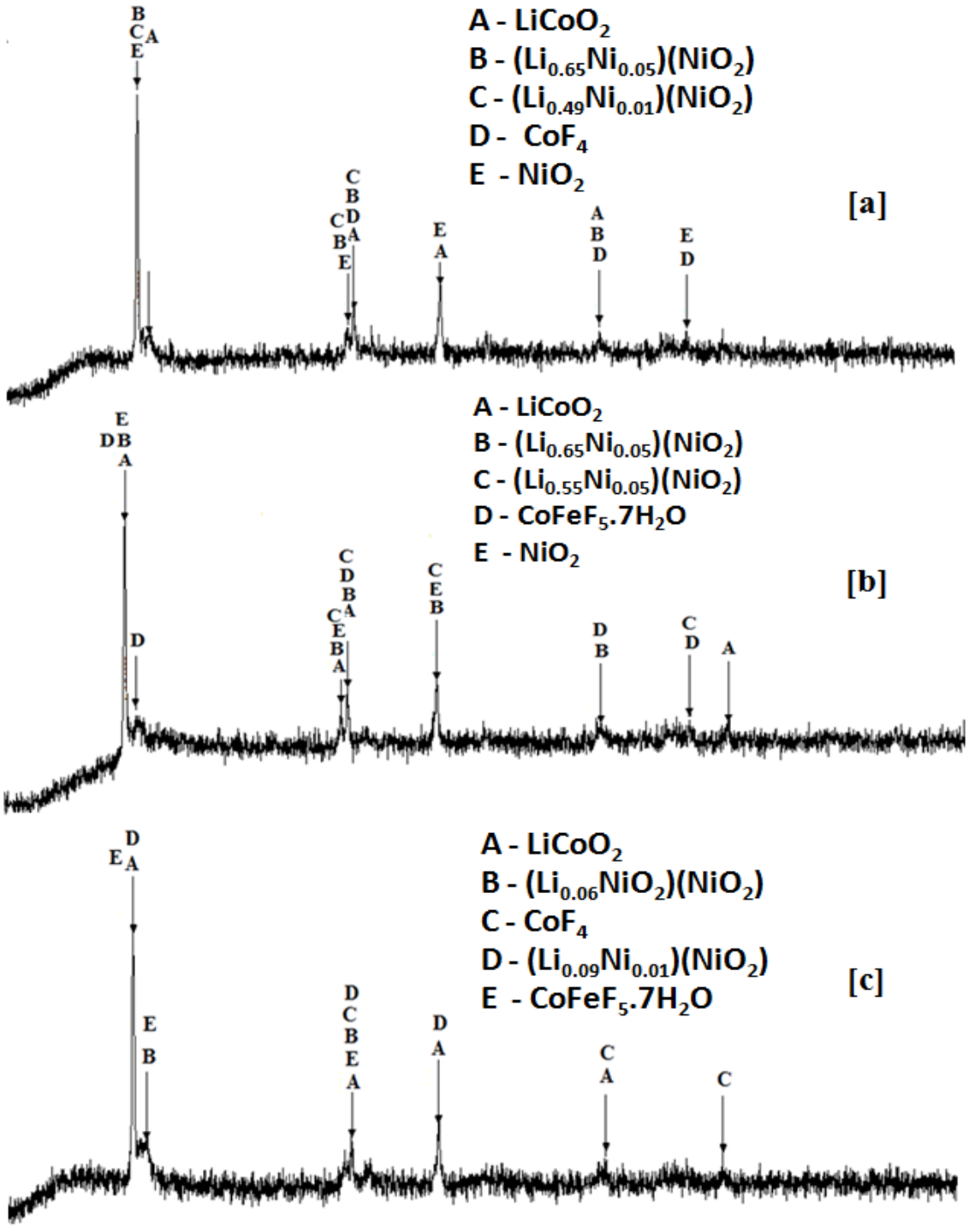

Fig. 3.12: XRD pattern of the residues obtained in leaching at 368 K and 50 g/L PD in 60 min (a), 120 min (b), and 240 min (c).

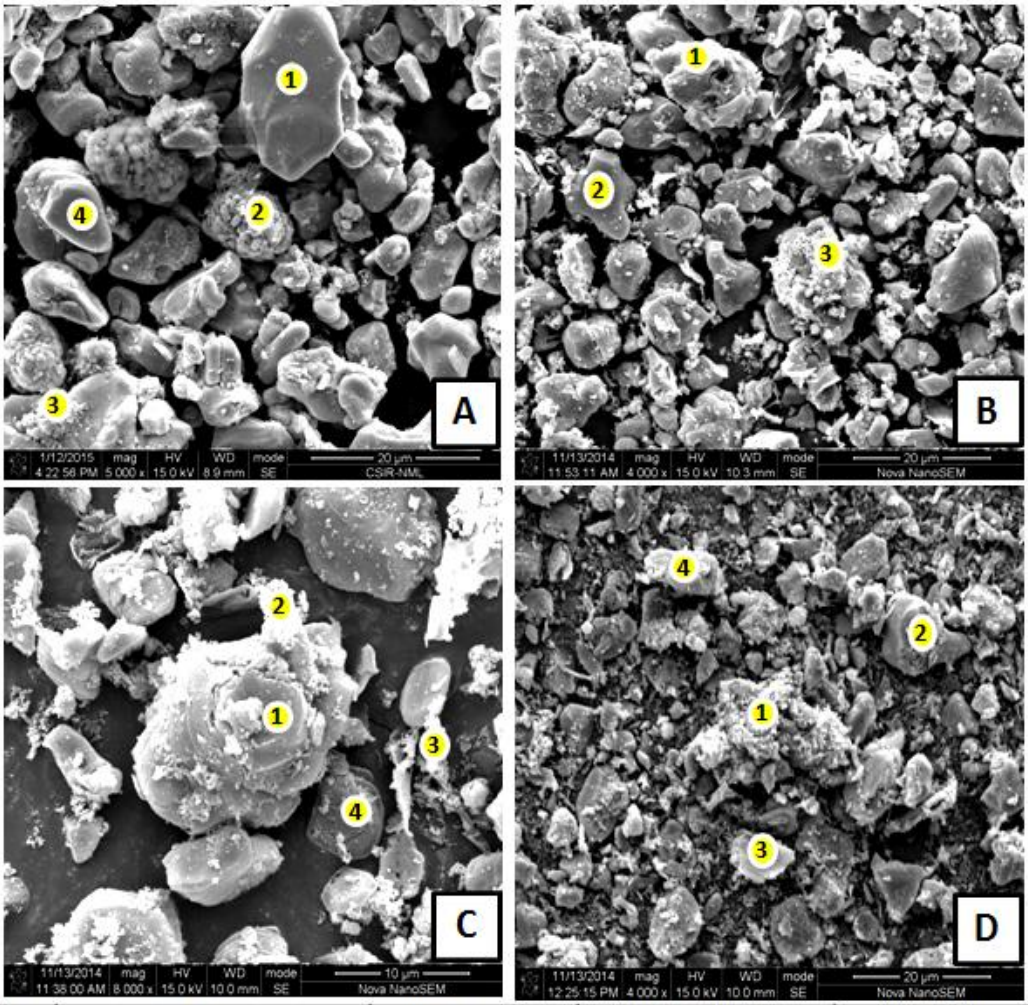

Element	(A) Head				(B) at 60 min			(C) at 120 min				(D) at 240 min			
(wt%)	P-1	P-2	P-3	P-4	P-1	P-2	P-3	P-1	P-2	P-3	P-4	P-1	P-2	P-3	P-4
C K	nd	nd	47.3	nd	02.1	04.1	16.7	05.1	27.9	56.2	09.6	49.5	06.2	04.2	07.9
O K	22.8	32.1	13.2	18.8	14.1	11.7	18.3	17.4	17.6	10.7	13.8	13.1	19.2	14.6	25.9
Al K	00.8	00.9	00.5	00.7	00.7	00.9	00.6	00.8	00.7	00.7	00.9	00.7	00.9	00.9	01.1
Mn K	00.4	18.6	00.6	00.8	00.6	00.5	00.8	00.7	01.4	01.4	00.4	00.9	00.9	00.8	00.8
Co K	71.8	24.2	34.2	73.8	76.2	75.2	56.6	68.5	40.8	16.3	71.8	27.9	64.8	72.0	56.9
Ni K	02.1	20.2	01.8	02.4	02.5	02.2	02.5	02.1	02.4	02.8	00.4	02.2	02.7	02.5	01.9
Cu K	01.7	03.1	01.7	02.5	03.9	05.4	04.6	05.4	09.2	11.9	03.2	05.7	05.2	05.1	05.5

Fig. 3.13: SEM-EDAX analysis of head sample (A) and residues in 60 min (B), 120 min (C) and 240 min (D) leaching with 1 M H_2SO_4 at 368 K and 50% PD

3.2 Leaching of metals from the cathode material in presence of sodium bisulfite as a reductant

In view of the stability and storage problem of the H_2O_2, an alternate and novel reducing agent-sodium bisulfite has been applied to recover constituent metals from the cathodic material.

3.2.1 *Effect of $NaHSO_3$ concentration on the leaching of metals:* The effect of reductant concentration on the metal dissolution was examined by varying the concentration of $NaHSO_3$ in the range 0 - 0.25 M. Other parameters maintained during the leaching include: temperature 368 K, H_2SO_4 concentration 1 M, pulp density 20 g/L, stirring speed 500 rpm and time 240 min. The addition of sodium bisulfite has significantly improved the extent of metal leaching as shown in Fig. 3.14. The results also illustrate that the leaching efficiency of metals increases from 49.1 to 77.1% for Co, 48.5 to 85.3% for Mn, 94.7 to 95.2% for Ni, and 89.9 to 92.1% for Li in absence (Fig. 3.3) and presence of the reducing agent at 0.075 M concentration, respectively. The optimum amount of $NaHSO_3$ for the high dissolution of metals is thus found to be 0.075 M.

Increase in the recovery of cobalt / manganese is attributed to the reduction of Co^{3+} to Co^{2+} and Mn^{+4} to Mn^{2+} states, both in the divalent forms dissolve readily in H_2SO_4 as reported elsewhere (Lee and Rhee, 2003; Sun and Qiu 2012). While sodium bisulfite helped in the dissolution of cobalt and manganese by reducing them to their lower oxidation states, the leaching of lithium is also promoted because of its association with the same oxide phases (Table 2.1) as that of cobalt and manganese. Interestingly the leaching behavior of Li and Ni in the spent LIBs is almost similar which may be attributed to the fact that they hardly undergo reduction process unlike cobalt and manganese. As such $NaHSO_3$ may play a limited role in the leaching of Ni(II) containing non-stoichiometric phases with spinel structure, although reduction of very minor amount of Ni(III) formed during the process of charge-discharge cycle may not be ruled out. The SEM images of the residues in the subsequent images have shown a decrease in the particle size of the powder after the leaching and decrease in the elemental distribution. The presence of reductant (0.075 M $NaHSO_3$) during the

leaching in 1 M H_2SO_4 at 368 K has decreased the redox potential value, E_{SCE} to ~400 mV after 240 min of leaching as compared to the E_{SCE} of >900 mV recorded in absence of any reductant.

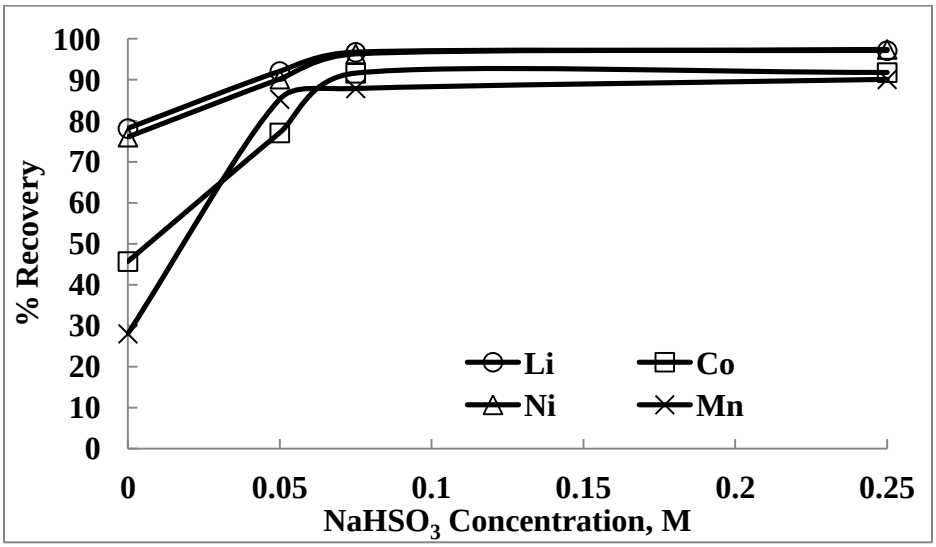

Fig. 3.14: Effect of $NaHSO_3$ concentration on the leaching of metals from cathodic powder in 1 M H_2SO_4 at 368 K and 20 g/L pulp density in 240 min.

3.2.2 *Effect of time:* The effect of time (0 – 300 min) on the leaching efficiency of metals was examined using 1 M H_2SO_4 and 0.075 M $NaHSO_3$ at 368 K and 20 g/L pulp density. It is apparent that with increase in leaching time, dissolution of all the metals increased (Fig. 3.15). The optimum dissolution of the metals was observed in 240 min with successive decrease in the amount of constituent metals, and thereafter leaching of the metals remained almost unchanged. About 96.7% Li and Ni, 91.6% Co, and 87.8% Mn were extracted in 240 min with 1 M H_2SO_4 in the presence of $NaHSO_3$. The rate of leaching of cobalt was observed to be slow which was related to the conversion of Co(III) to Co(II) from the $LiCoO_4$ phase with $NaHSO_3$. The leaching of lithium was also promoted because of its association with cobalt which further justifies the slow rate of leaching of Co-Li and need of a reductant.

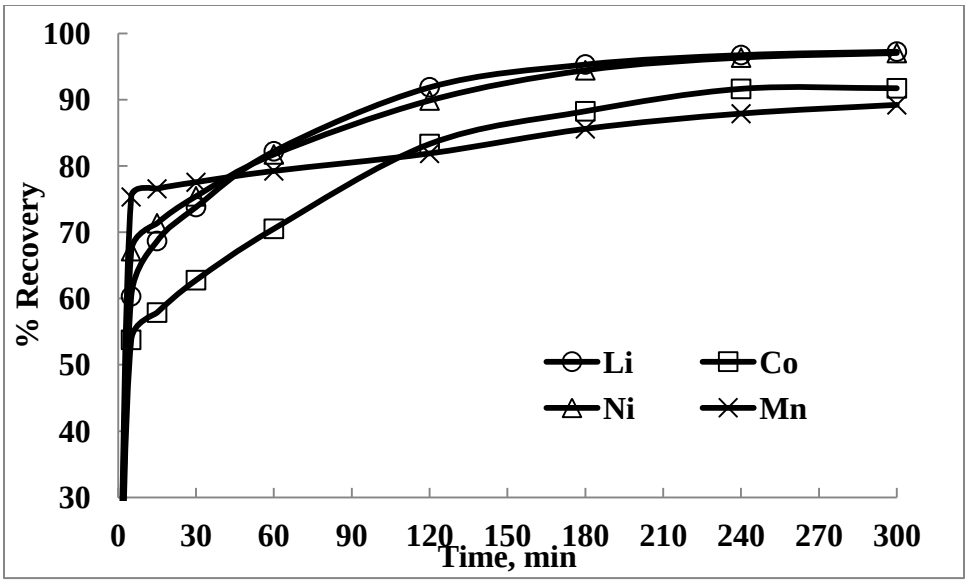

Fig. 3.15: Effect of time on the leaching of metals using 1 M H_2SO_4 and 0.075 M $NaHSO_3$ at 368 K and 20 g/L pulp density.

3.2.3 *Effect of pulp density:* The effect of pulp density (5 - 50 g/L) on the leaching efficiency of the metals was studied in 1 M H_2SO_4 and 0.075 M $NaHSO_3$ for 240 min at 368 K. Results given in Fig. 3.16 clearly show that the leaching of all the metals decreases with increase in the pulp density. These data also infer that the dissolution of these metals is nearly constant in the pulp density range of 5 -20 g/L. In particular, about 97% Li and Ni, 93% Co and 89% Mn were leached out at 5 g/L pulp density and increasing the pulp density to 50 g/L lowered the metal dissolution to 93%, 85 %, 92.4% and 83.7% for Li, Co, Ni and Mn, respectively. Beyond 20 g/L pulp density which is higher compared to the literature reports (Lee and Rhee, 2002; Lee and Rhee, 2003; Li et al., 2010a; Li et al., 2010b; Shuva and Kurny, 2013; Li et al., 2011a; Li et al., 2011b; Chen et al., 2011; Chen et al., 2014c), the recovery decreases due to the lower concentration of the lixiviant available in the mixture. Hence 20 g/L pulp density can be taken as optimum value for rest of the experiments.

3.2.4 *Effect of temperature:* Effect of temperature on the leaching of valuable metals was also studied using 1 M H_2SO_4 and 0.075 M $NaHSO_3$ at a pulp density of 20 g/L for a fixed leaching time of 240 min. Results presented in Fig. 3.17 show that 84.4% Li, 65.6% Co, 82.2% Ni and 73.6% Mn can be leached out at room temperature (308

K). The leaching efficiency of the metals increased with increase in temperature. At 348 K, 94.6% Li, 87.6% Co, 95.8% Ni and 80.7% Mn were leached out. When the temperature was further increased to 368 K, the recovery of Li, Co, Ni and Mn increased marginally to 96.7%, 91.6%, 96.4% and 87.9%, respectively. It was further observed that the recovery of Mn slightly increased with increase in temperature from 323 to 348 K.

On examining the leaching of various metals with time (Fig. 3.18) at a particular temperature, it was observed that the rate of dissolution steadily increased till 180 min and thereafter change in leaching pattern was marginal till 240 min. The recovery of metals increased with increase in temperature and time except for manganese in the temperature range 323-348 K as mentioned above, which also increased beyond 348 K. The dissolution patterns of different metals can be utilized to examine the kinetics of leaching while applying the rate equations/models.

To determine the mechanism of leaching by $NaHSO_3$, a thermodynamic study using data from the HSC Chemistry 7.14 was performed to predict the probability of reactions (Eqs. 3.2-3.5) in the system. The values of standard Gibbs free energy change (ΔG^o) for the dissolution of Li, Co, Mn and Ni were also determined at 368 K and other temperatures.

$$4LiCoO_2 + 2NaHSO_3 + 5H_2SO_4 = 4CoSO_4 + 2Li_2SO_4 + 6H_2O + Na_2SO_4 \quad \Delta G^o_{368} = -1025.9 \text{ kJ} \qquad (3.2)$$

$$4Li_2CoMn_3O_8 + 3NaHSO_3 + 3.5H_2SO_4 = 4CoSO_4 + Li_2SO_4 + 5H_2O + 1.5Na_2SO_4 + 6LiMn_2O_4 \quad \Delta G^o_{368} = -815.1 \text{ kJ} \qquad (3.3)$$

$$4LiNiO_2 + 2NaHSO_3 + 5H_2SO_4 = 4NiSO_4 + 2Li_2SO_4 + 6H_2O + Na_2SO_4 \quad \Delta G^o_{368} = -1149.9 \text{ kJ} \qquad (3.4)$$

$$CoF_4 + 4\ NaHSO_3 + O_2 = CoSO_4 + 2\ Na_2SO_4 + 4\ HF + SO_2, \quad \Delta G^o_{368} = -214.8 \text{ kJ} \qquad (3.5)$$

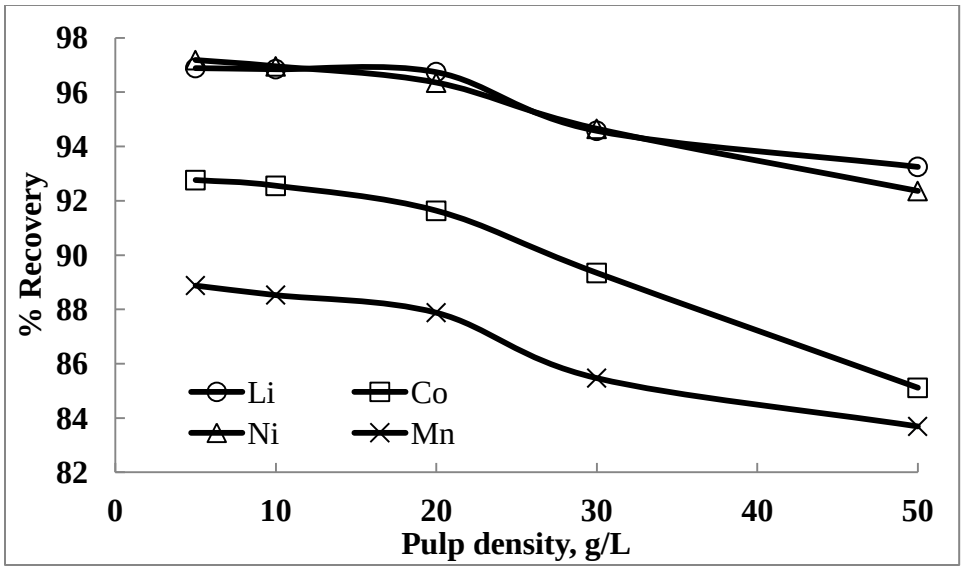

Fig. 3.16: Effect of pulp density on the leaching of cathode active material using 1 M H_2SO_4 and 0.075 M $NaHSO_3$ at 368 K in 240 min.

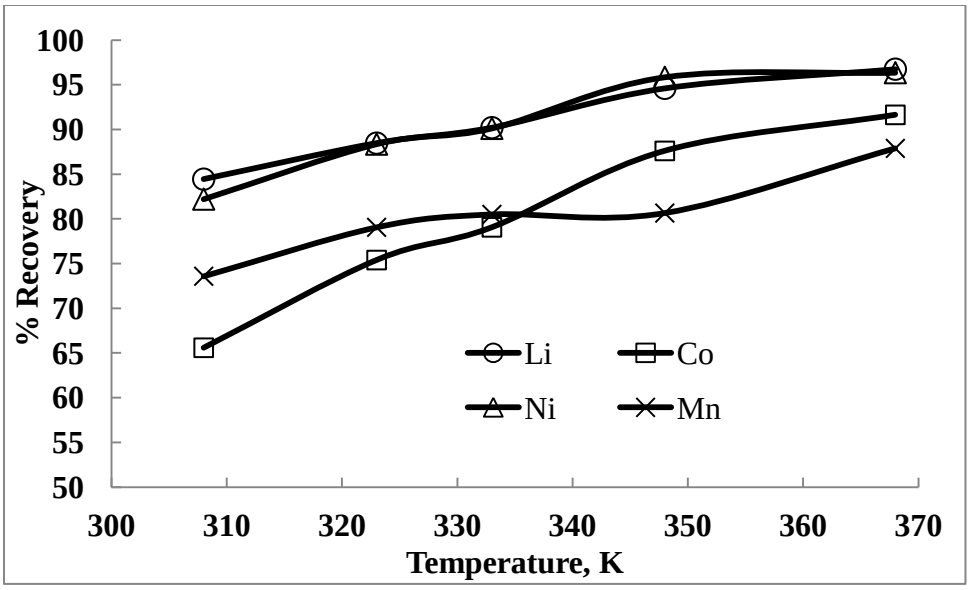

Fig. 3.17: Effect of temperature on the leaching of metals from the cathode material using 1 M H_2SO_4 and 0.075 M $NaHSO_3$ in 240 min at 20 g/L pulp density.

Table 3.2: ΔG^o for chemical equations in temperature range 308–368 K

T (K)	ΔG^o values for the equations 3.2-3.5 (kJ)			
	Eq. 3.2	**Eq. 3.3**	**Eq. 3.4**	**Eq. 3.5**
308	-1041.1	-832.2	-1141.6	-264.7
323	-1037.4	-828.1	-1144.8	-256.8
333	-1034.9	-825.2	-1146.1	-248.5
348	-1031.1	-820.9	-1148.3	-231.8
368	-1025.9	-815.1	-1149.9	-214.8

It can be clearly seen from Table 3.2 that the higher changes in the negative free energy values for Eqs. 3.2 and 3.4 make the reactions thermodynamically feasible with the chemical entities being potentially leachable in sulfuric acid with the presence of sodium bisulfite.

3.2.5 *Kinetics of leaching:* To understand the nature of interaction between the particles of cathode powder sample and the reductant (sodium bisulfite), an attempt was made to fit the kinetic data obtained from the leaching experiments at different temperatures in the shrinking core models based on the surface chemical and diffusion control models (Chapter 1, Eqs. 1.17 & 1.18). Kinetic data show poor fit to both the models (Figs. 3.19 and 3.20). In fact the correlation coefficients for most metals were not more than 0.94 and 0.87, respectively for the chemical and diffusion control models. Kinetic data were thus analyzed by using an empirical model (Eq. 1.20, Chapter 1) for the leaching which is goverened by the logarithmic rate law (Levenspiel, 1999; Kim et al., 2011).

The results obtained for the leaching of Li, Co and Ni at different temperatures (Fig. 3.18) give straight lines when $(-\ln(1-x))^2$ *vs.* t is plotted (Fig. 3.21 a-d). The plots for the three metals clearly show the best fit to this model which is evident from the high values of correlation coefficients (R^2 >0.98). Similar to the leaching kinetics discussed in section 3.1.6, the leaching data for manganese did not fit well to the empirical model in this case also and hence the plot is not shown. Different oxidation states and spinel structure of the manganese containing phases (Xiaong et al., 2012), make them less amenable to the prevailing leaching conditions.

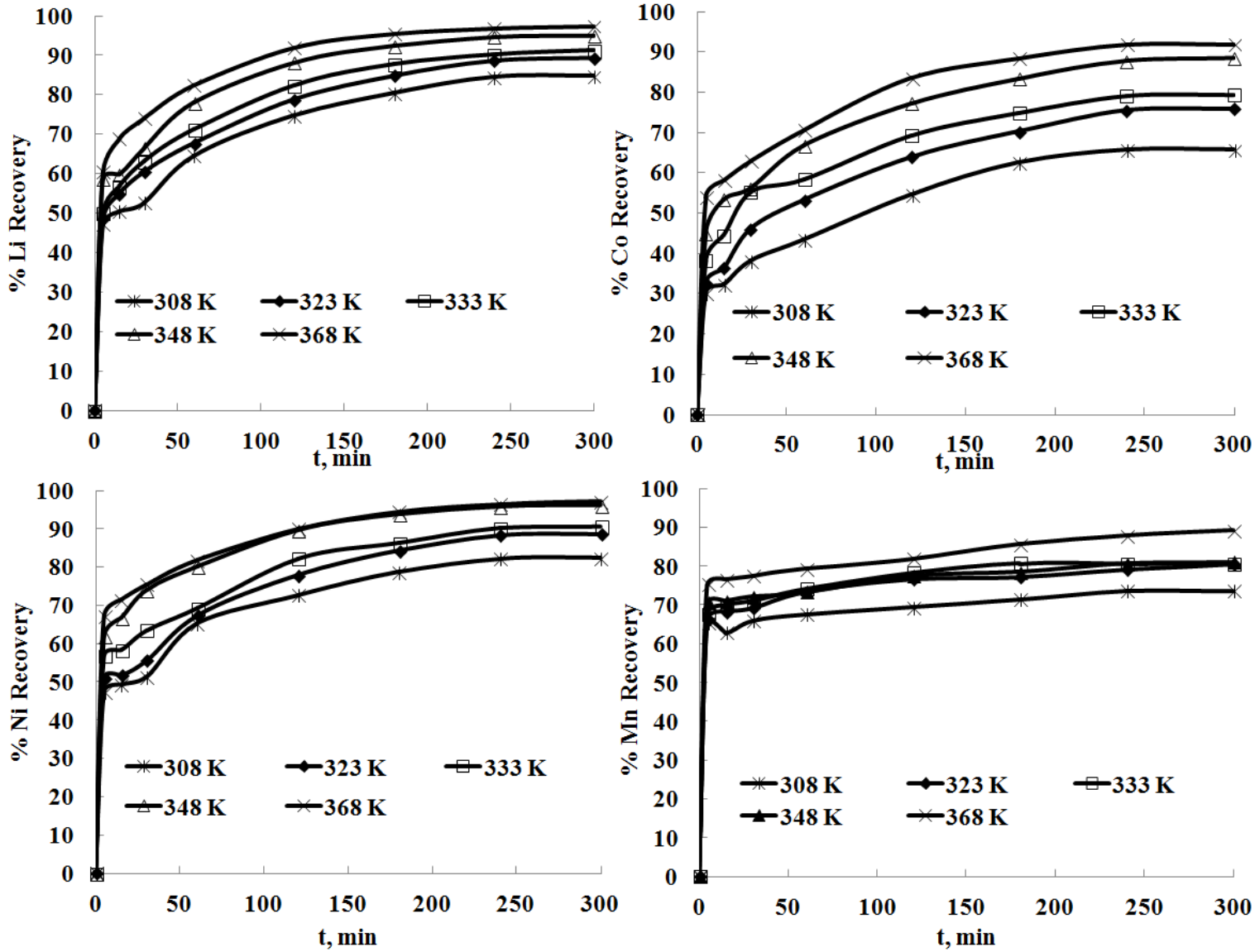

Fig. 3.18: Effect of temperature on the recovery of different metals from LIBs at different time intervals (1 M H_2SO_4 and 0.075 M $NaHSO_3$ at 20 g/L pulp density)

The plots of ln k vs.1/T are shown in Fig. 3.22 which have high correlation coefficients (>0.97). The activation energy values (E_a) calculated from the Arrhenius plots are found to be 20.4, 26.8 and 21.7 kJ / mol for Li, Co and Ni, respectively. The activation energy values fall within the range obtained earlier for the empirical model (Kim et al., 2011). This further suggests that the leaching of metals from the cathodic material follows the mechanism involving the reaction of lixiviant through diffusion on the surface of the particles.

3.2.6 Characterization studies: The leach residues obtained from the experiments were characterized using XRD phase analysis (Table 3.3). From the phase identification, it is clear that the intensity of the major phases is reduced progressively in different residues. Both the major [$LiCoO_2$, $Li_2CoMn_3O_8$, $(Li_{0.85}Ni_{0.05})(NiO_2)$] and minor phases [$(Li_{0.69}Ni_{0.01})(NiO_2)$ and CoF_4] identified in the untreated sample undergo changes during the acid leaching in the presence of sodium bisulfite. On leaching the material in 60 min, the major phases identified were $Li_{0.5}Co_{1.02}O_2$, $(Li_{0.69}Ni_{0.01})(NiO_2)$, which illustrated the dissolution of lithium and other metals with decreased ratio of lithium in the respective intermediate products. However, the major phase viz., $Li_2CoMn_3O_8$ present in the untreated sample was detected as the minor phase in 60 min of leaching. Increase in the recovery of metals with time is also reflected in the XRD analysis of the residues in which the Li and Ni contents dropped in the non-stoichiometric entities such as $(Li_{0.69}Ni_{0.01})(NiO_2)$ and $(Li_{0.09}Ni_{0.01})(NiO_2)$ identified as the major phases in 120 and 180 min of leaching, respectively. Other phases containing the lower ratio of lithium and nickel are also present along with that of cobalt-containing compound in the minor amount.

In 240 min, the amount of the leach residue was found to be very small and therefore, several experiments were conducted under the similar conditions to generate sufficient amount of residue for XRD and SEM studies. In this residue the non-stoichiometric phases comprising of very low contents of lithium and nickel were observed due to almost complete leaching of the metals. Manganese was however, present as a minor phase in the form of MnO_2. Interestingly, a new nickel containing minor phase such as $NiFeF_5.7H_2O$ was noticed with the progress of the leaching in 180 and 240 min, which was not reflected in the XRD of untreated cathode material.

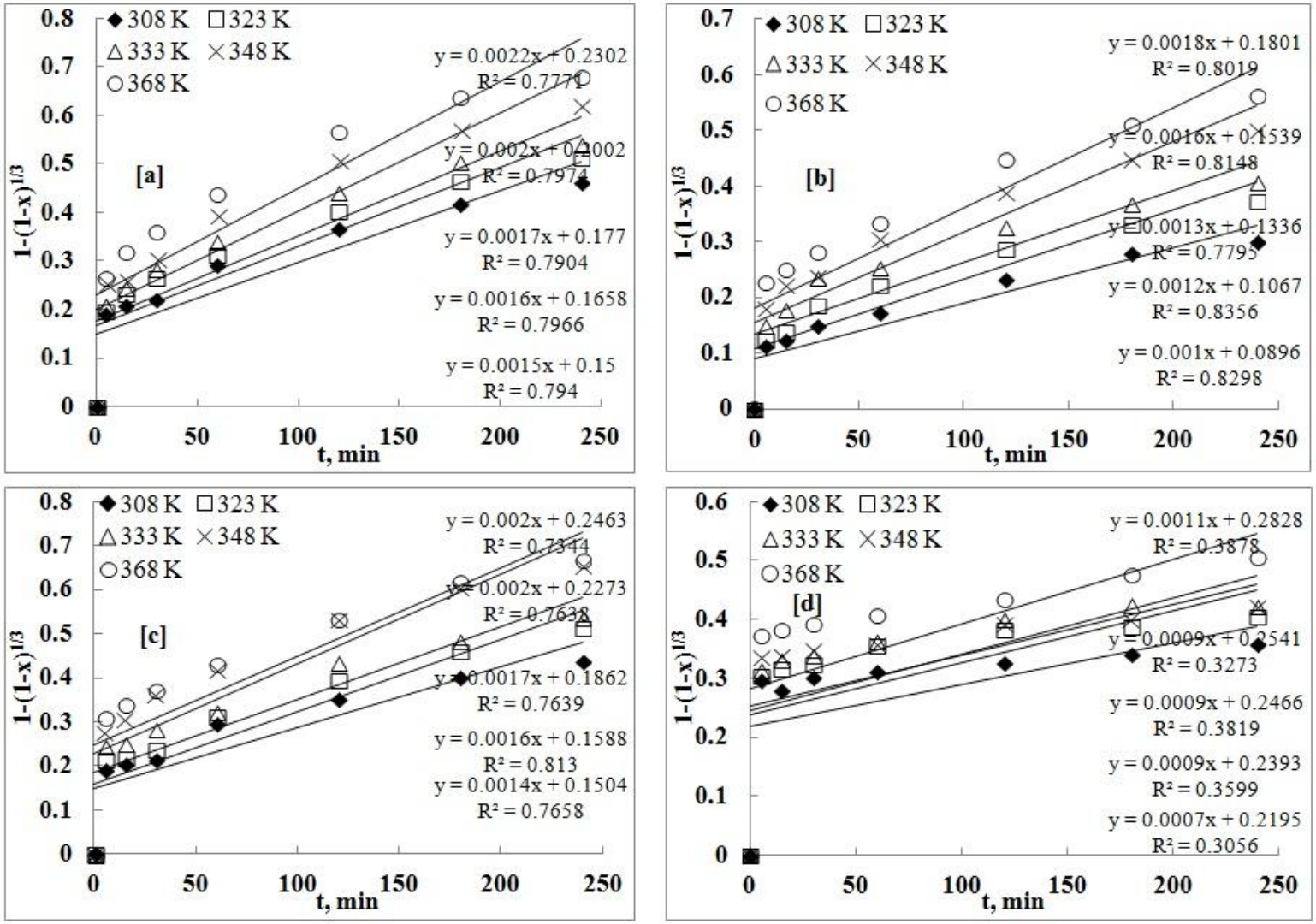

Fig. 3.19: Chemical controlled kinetic model for the leaching of metals (a- Li, b-Co, c-Ni, d-Mn) by $NaHSO_3$-H_2SO_4 in temperature range (308-368 K)

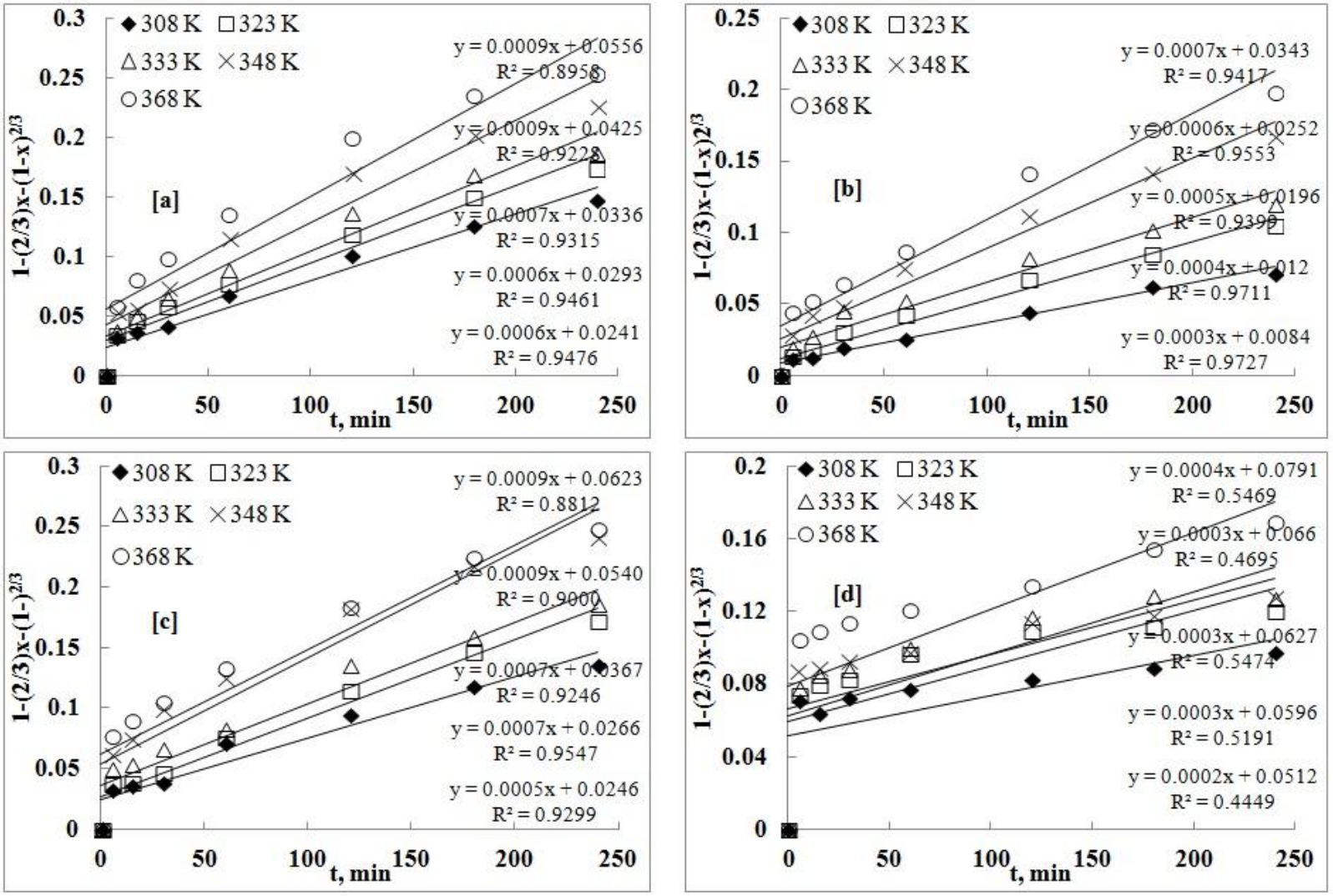

Fig. 3.20: Diffusion controlled kinetic model for the leaching of metals (a- Li, b-Co, c-Ni, d-Mn) by $NaHSO_3$-H_2SO_4 in temperature range (308-368 K)

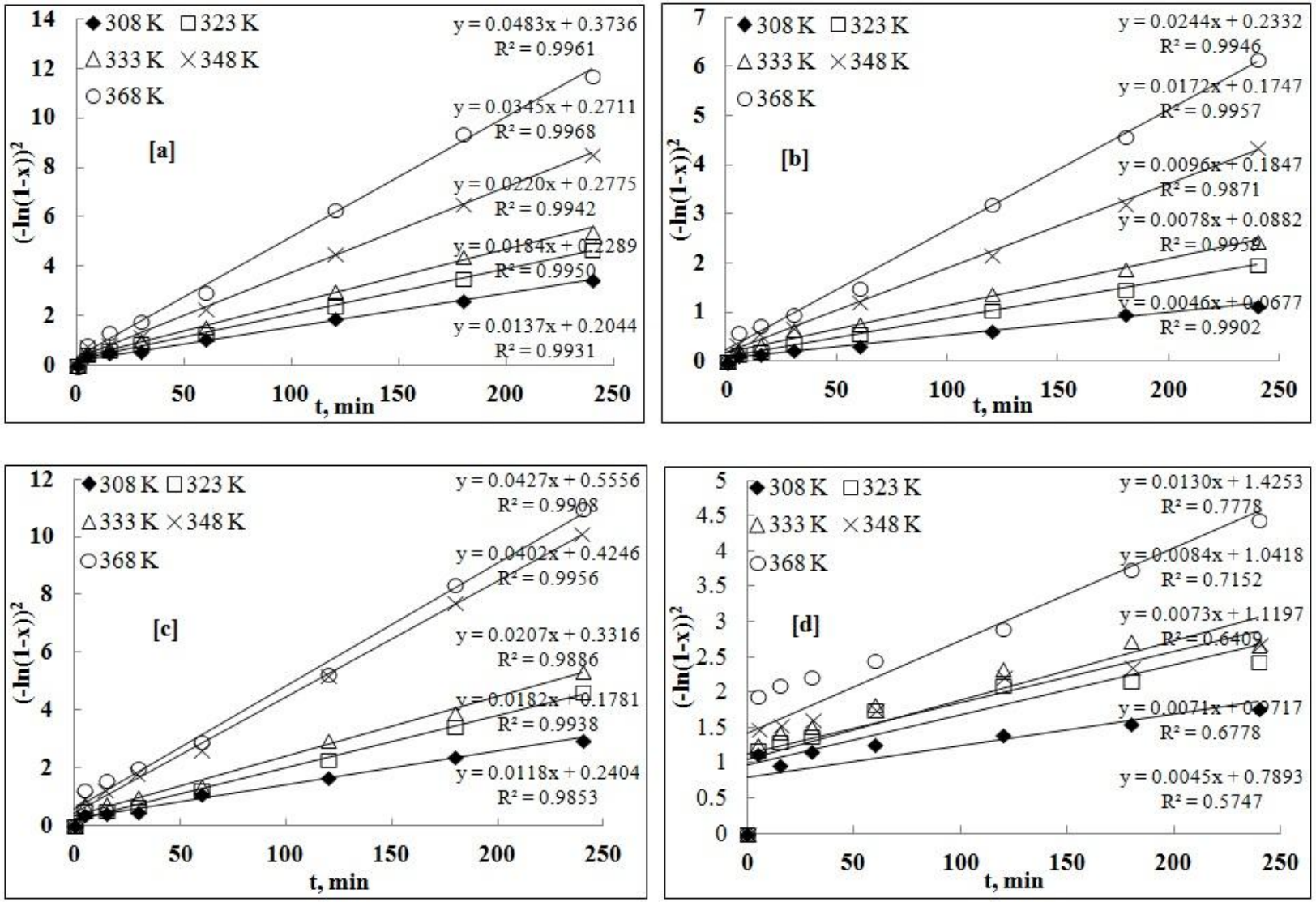

Fig. 3.21: Empirical model for the leaching of metals (a- Li, b-Co, c-Ni, d-Mn) by $NaHSO_3$-H_2SO_4 in temperature range (308-368 K)

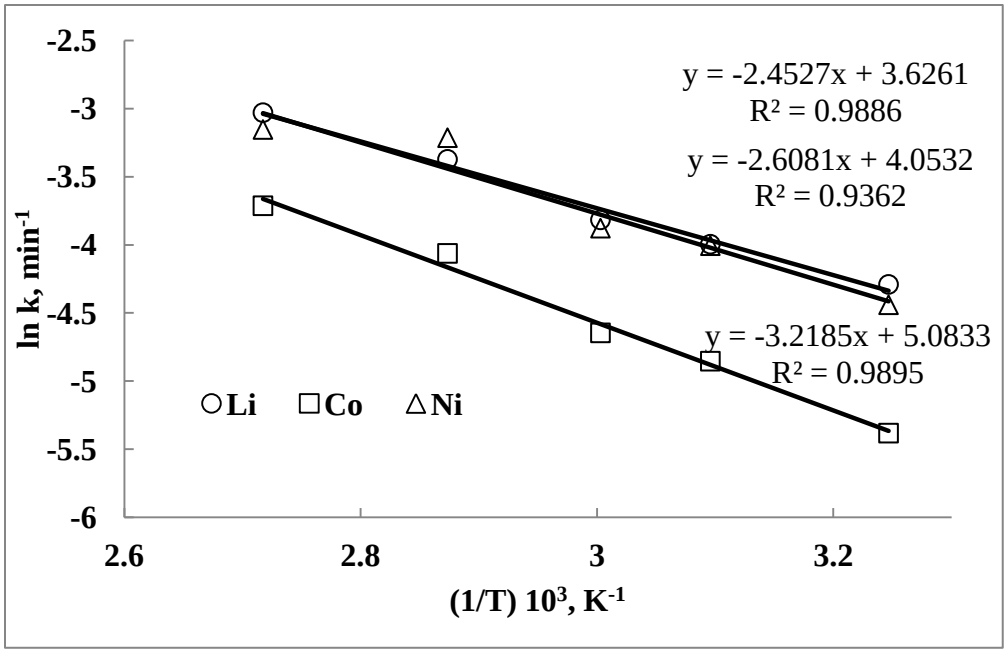

Fig. 3.22: Arrhenius plot for the leaching of the metals from LIBs in the temperature range 308-368 K

The leaching of metals with time was further examined by comparing the change in the elemental distribution of cathodic sample with that of the leach residues (Table 3.3). EDAX data clearly show a progressive decrease in the average content of most metals (Co, Ni, Mn) in the residues as the leaching progressed with time (60-240 min). While Fig. 2.4 shows the SEM of the untreated sample, SEM of the residue obtained in 240 min at 368 K under the optimum conditions is given in Fig. 3.23. In the untreated sample (Fig. 2.4), $LiCoO_2$ particles are present in irregular morphologies along with large number of secondary particles. The very high recovery of metals such as Co, Li, Ni and Mn is corroborated by a decrease in particle size, change in morphological features with corroded and spongy surface (Fig. 3.23) and mapping of the metals along with low elemental distribution in the EDAX (Table 3.3) of the leach residue. The characterization of the cathode material and the residues by SEM-EDAX studies and XRD phase analysis with time thus provides evidence on the mechanism of leaching of valuable metals, which proceeds through the surface diffusion of the lixiviant on the reacting particles. The logarithmic rate law representing the kinetic data is thus supported by the characterization studies.

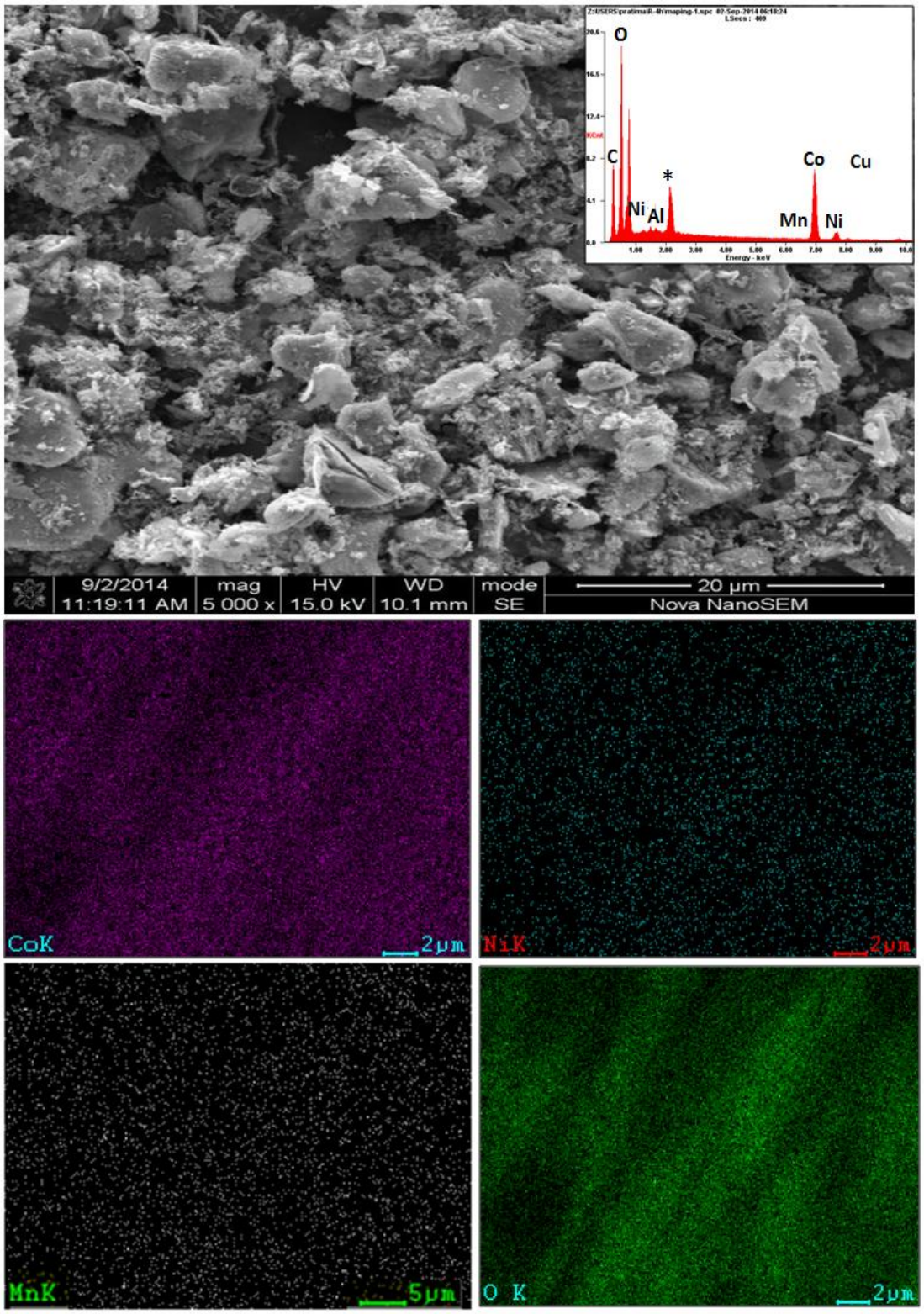

Fig. 3.23: SEM-EDAX analysis of residue at 240 min with mapping of constituent elements

Table 3.3: XRD phase identification and EDAX analysis of the leach residues at different time with elemental distribution
(Conditions: 1 M H_2SO_4 & 0.075 M $NaHSO_3$, 368 K, 20 g/L PD) {nd: not-detected}

Sample	Major Phases	Minor Phases	Average elemental analysis by SEM-EDAX (%)			
			Li	Co	Ni	Mn
Leach residue in 60 min	$Li_{0.5}Co_{1.02}O_2$, $(Li_{0.69}Ni_{0.01})(NiO_2)$	$(Li_{0.59}Ni_{0.01})(NiO_2)$, $Li_2CoMn_3O_8$	Nd	66.68	2.37	0.78
Leach residue in 120 min	$(Li_{0.69}Ni_{0.01})(NiO_2)$	$(Li_{0.59}Ni_{0.01})(NiO_2)$, $Li_{0.5}Co_{1.02}O_2$,$NiFeF_5.7H_2O$, $Li_2CoMn_3O_8$, $Li_{0.05}Mn_2O_4$	Nd	57.61	1.82	0.78
Leach residue in 180 min	$(Li_{0.09}Ni_{0.01})(NiO_2)$	$(Li_{0.59}Ni_{0.01})(NiO_2)$, $Li_{0.445}(Li_{0.03}Co_{0.97})O_2$, $NiFeF_5.7H_2O$, MnO_2	Nd	45.95	1.51	0.67
Leach residue in 240 min	--	$(Li_{0.09}Ni_{0.01})(NiO_2)$, $NiFeF_5.7H_2O$, MnO_2	Nd	36.50	1.48	0.58

3.3 Leaching of metals from the cathode material in presence of H_2O_2 as a reductant

In order to compare the leaching efficiency including the kinetics using the two reductants- $NaHSO_3$ and H_2O_2, the experiments were also performed with the latter. The effect of various parameters like reductant concentration, pulp density, temperature and time, was investigated and results are discussed.

3.3.1 *Effect of H_2O_2 concentration on the leaching of metals:* In order to examine the effect of reductant concentration on the extent of metal dissolution, the concentration of H_2O_2 was varied in the range 0.5-10 (v/v)%. Other parameters maintained during the leaching include: temperature-368 K, H_2SO_4 concentration-1 M, pulp density-20 g/L and time-240 min. The addition of reductant significantly improved the leaching efficiency of metals as shown in Fig. 3.24. The effect of H_2O_2 on the dissolution of metals with 1 M H_2SO_4, indicates the increase in leaching efficiency from 55.6% to 80.2% for cobalt and 53.2% to 85.9% for manganese as the H_2O_2 amount was increased from 0.25% to 5% (Fig. 3.24). No significant increase in the leaching

efficiency was observed with more than 5% H_2O_2. Increase in the recovery of cobalt and manganese is attributed to the reduction of Co^{3+} to Co^{2+} and Mn^{4+} to Mn^{2+} states, which are readily dissolved in H_2SO_4 (Lee and Rhee, 2003). As with $NaHSO_3$, the lithium and nickel have followed almost similar leaching behavior with H_2O_2 also since they hardly undergo reduction process unlike cobalt and manganese. Hence for other optimization experiments the concentration of H_2O_2 was taken as 5%.

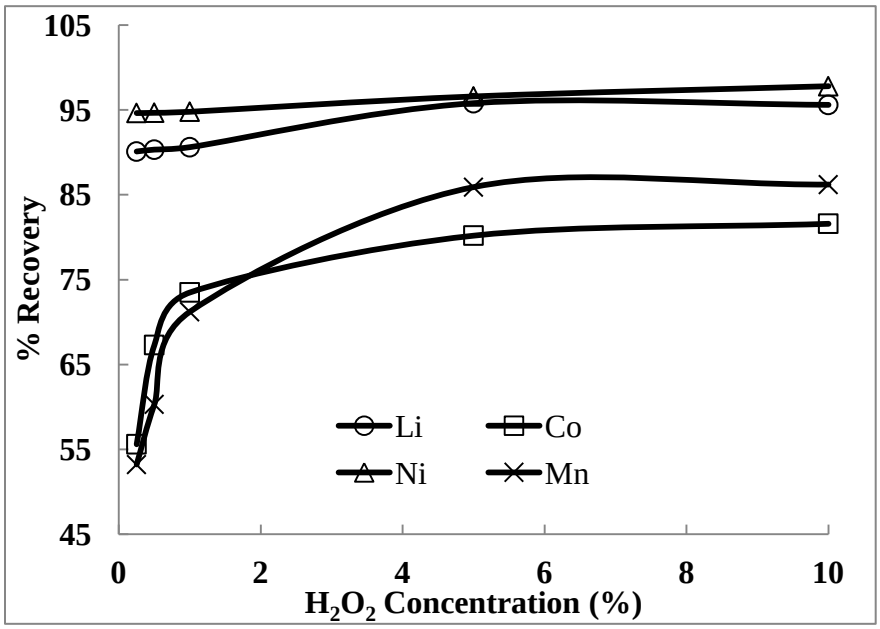

Fig. 3.24: Effect of concentration of H_2O_2 on the leaching of Li, Co, Ni and Mn from cathode active material using 1M H_2SO_4, 20 g/L pulp density at 368 K in 240 min

The leaching characteristics could be predicted by the Eh-pH diagrams for the hydrogen peroxide system also. Fig. 3.25 depicts the stability diagram of the individual metal ions in the presence of other constituents at 368 K for the H_2O_2 system (HSC Chemistry 7.14). For an instance, the stability domain of soluble phases of Li for sulfuric acid leaching in presence of H_2O_2 as a reductant is incorporated in the system Li-Co-Mn-Ni-S-H_2O (Fig. 3.25a) drawn at 368 K. Similarly the stability regions for other metals (Co, Ni and Mn) can be seen (Figs. 3.25 b,c,d).

The effect of a reducing agent on the metal recoveries was investigated while comparing the redox potential value determined against saturated calomel electrode (SCE). In the absence of any reducing agent, the E_{SCE} of the solution could reach >900 mV over the leaching period of 120 min as mentioned in section 3.1. Addition

of 5% H_2O_2 in 1 M H_2SO_4 at 368 K drastically decreased the E_{SCE} of the solution to 580 mV in 240 min, which further dropped to ~400 mV when 0.075 M $NaHSO_3$ was present as the reductant in the lixiviant at this temperature in 240 min of leaching. This clearly infers that the concentration of reducing agent has a positive effect on the metal extraction only up to a certain extent [5% H_2O_2 (Fig. 3.26) and 0.075 M $NaHSO_3$ (Fig. 3.15)]; above this range the reaction rate becomes less dependent on reductant's concentration and the mass transfer of reducing agent from solution to particles may no longer be the rate controlling mechanism (Stuurman et al., 2014).

The leaching behaviou of metals under the system sulfuric acid-H2O2 was also assessed thermodynamically (HSC Chemistry 7.14). The values of ΔG^o were calculated (Table 3.4) for the dissolution of Li, Co, Mn and Ni (Eqs. 3.6-3.8) at 308-368 K.

$$2LiCoO_2 + 3H_2O_2 + 3H_2SO_4 = 2CoSO_4 + Li_2SO_4 + 6H_2O + 2O_2, \quad \Delta G^o_{368} = -651.2 \text{ kJ} \qquad (3.6)$$

$$Li_2CoMn_3O_8 + H_2O_2 + 3H_2SO_4 = CoSO_4 + Li_2SO_4 + 4H_2O + O_2 + 2MnO_2 + MnSO_4 \quad \Delta G^o_{368} = -421.6 \text{ kJ} \qquad (3.7)$$

$$2LiNiO_2 + 3H_2O_2 + 3H_2SO_4 = 2NiSO_4 + Li_2SO_4 + 6H_2O + 2O_2, \quad \Delta G^o_{368} = -646.1 \text{ kJ} \qquad (3.8)$$

Table 3.4: ΔG^o for chemical equations in the temperature range 308–368 K

T (K)	ΔG^o values for the equations 3.6-3.8 (kJ)		
	Eq. 3.6	**Eq. 3.7**	**Eq. 3.8**
308	-642.9	-419.3	-640.9
323	-644.9	-419.9	-642.2
333	-646.2	-420.2	-642.9
348	-648.3	-420.8	-644.3
368	-651.2	-421.6	-646.1

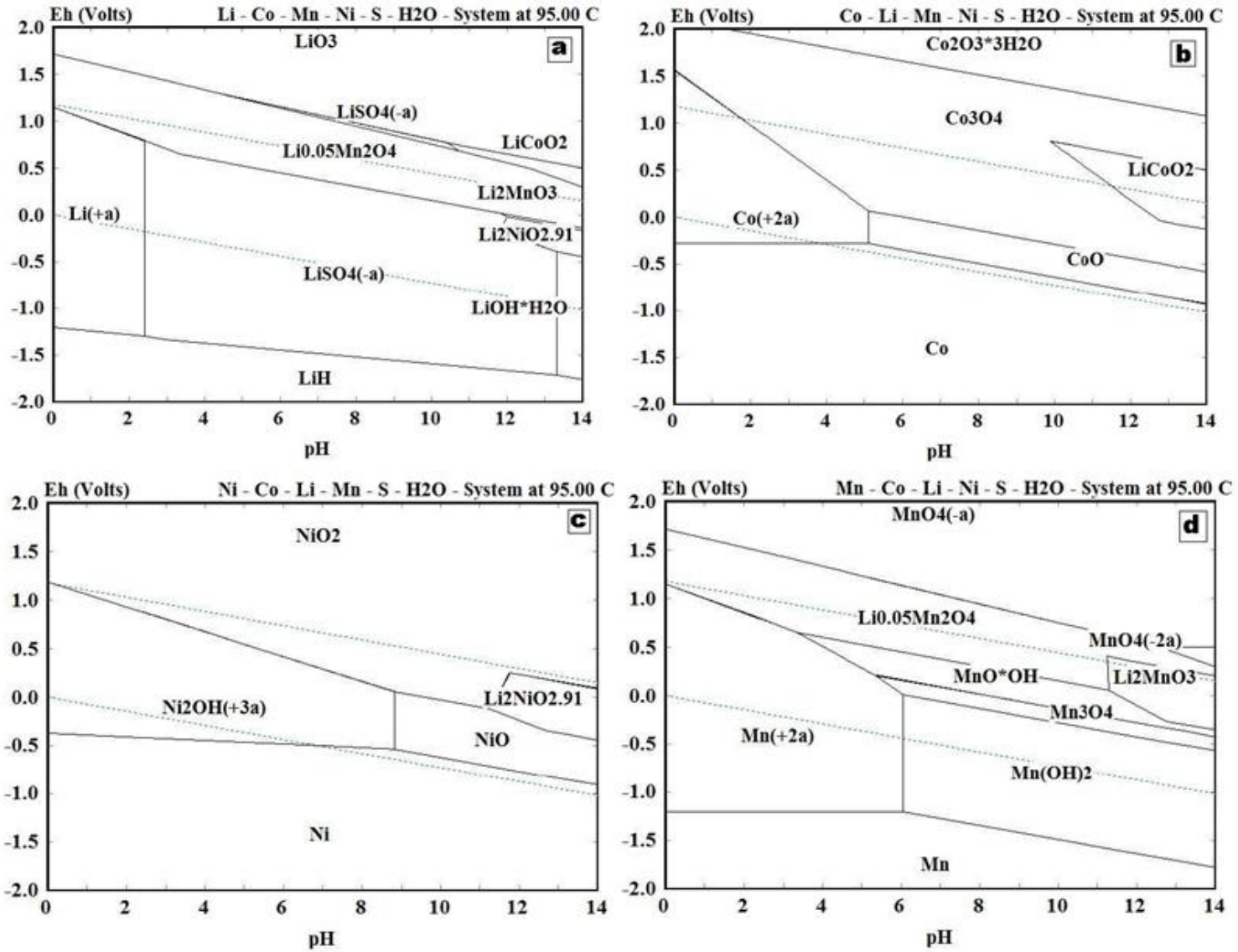

Fig. 3.25: Eh-pH diagrams (368 K) for H_2O_2 system: (a) Li-SO_4, (b) Co-SO_4, (c) Mn-SO_4, (d) Ni-SO_4, in presence of other elements

A comparison of ΔG^{o}_{368} values of - 651.2 kJ and -1025.9, for Eq. 3.6 in the presence of H_2O_2 and Eq. 3.2 for $NaHSO_3$, respectively shows that sodium bisulfite is thermodynamically a better reductant to dissolve the major constituent ($LiCoO_2$) of the cathodic material in sulfuric acid at 368 K. The highly negative values of ΔG^{o} for other reactions with $NaHSO_3$ in relation to the H_2O_2 for the entire temperature range further substantiate this trend. This behavior is also reflected by the lower E_{SCE} value (~400 mV) recorded experimentally with the reductant (0.075 M) $NaHSO_3$ compared to that of (5%) H_2O_2 (580 mV) at 368 K, as discussed in section 3.2.1.

3.3.2 *Effect of pulp density:* The effect of pulp density (5–100 g/L) on the leaching of the metals was studied in 1 M H_2SO_4 at 368 K and 240 min with 5% H_2O_2. The results (Fig. 3.26) clearly show that the leaching efficiency of all the metals decreased as the pulp density increased. The dissolution of these metals is nearly constant in the pulp density range of 5–50 g/L when H_2O_2 is used as the reductant. In particular, 95.8% Li, 80.2% Co, 96.6% Ni and 85.9% Mn were recovered at 20 g/L pulp density. Increasing the pulp density to 50 g/L adversely affected the metal dissolution. The leaching efficiency of Li, Co, Ni and Mn was found to be 94.5, 79.2, 96.4 and 84.6% respectively, at 50 g/L pulp density. Hence, 50 g/L pulp density was considered for the further experiments.

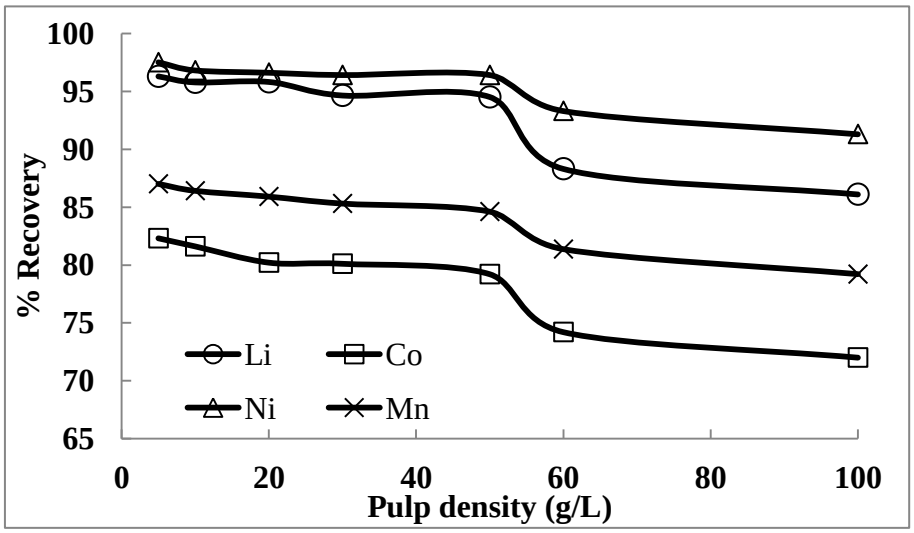

Fig. 3.26: Effect of pulp density on the leaching of metals using 1 M H_2SO_4 and 5% H_2O_2 at 368 K in 240 min.

3.3.3 *Effect of time:* The effect of time on the leaching efficiency of metals was examine under the conditions given in Fig. 3.27. As can be seen the increase in leaching time increases the recovery of all metals. With H_2O_2, 78.4% Li, ~62% Co and Ni and 55.6% Mn were recovered in 60 min leaching time. Maximum leach recovery in 240 min was found to be 94.5% Li, 79.2% Co, 96.4% Ni and 84.6% Mn using H_2O_2 as the reductant with 1 M H_2SO_4 at 50 g/L pulp density. All metals have shown similar effect on the leaching efficiency irrespective of the reductant used except that recovery of cobalt was high (91.6%) when $NaHSO_3$ was used as the reductant at the 20 g/L pulp density (Fig. 3.17); the Co leaching efficiency being 85.1% at 50 g/L pulp density.

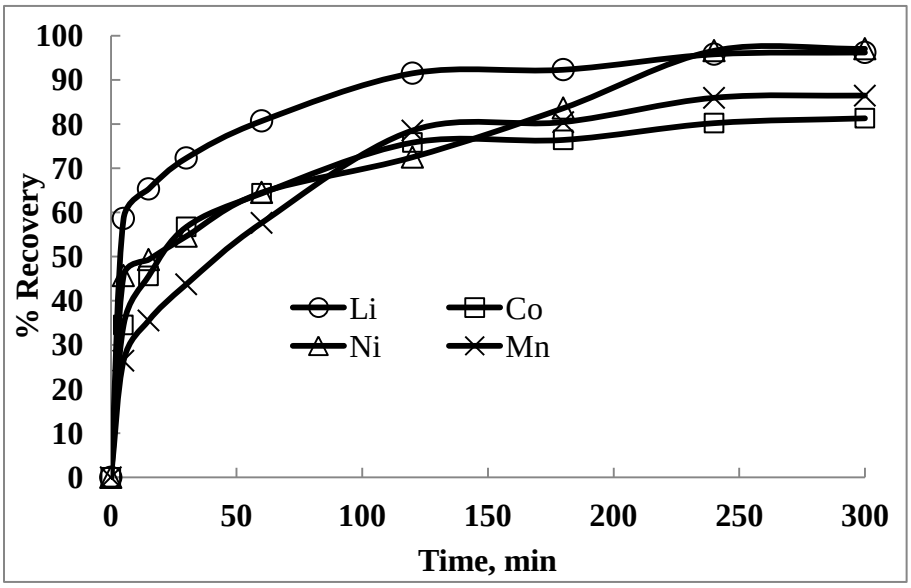

Fig. 3.27: Effect of time on the leaching of metals using 1 M H_2SO_4 and 5% H_2O_2 at 368 K and 50 g/L pulp density.

3.3.4 *Effect of temperature:* The effect of leaching temperature was studied in the range 308–368 K for 240 min with 1 M H_2SO_4, 50 g/L pulp density using 5% H_2O_2 as the reductant. Results plotted in Fig. 3.28 show the increase in leaching efficiency of metals with increase in temperature and maximum dissolution is achieved at 368 K. Thus 94.5% Li, 79.2% Co, 96.4% Ni and 84.6% Mn were leached out under the optimum conditions (1 M H_2SO_4 and 5% H_2O_2, 50 g/L pulp density, 368 K, 240 min). Increasing temperature promotes the mass transfer of acid and reducing agent from solution to the particles. The reaction at the surface of the particles is thus enhanced

thereby increasing the metal dissolution yielding higher extraction efficiency. The optimum temperature can therefore, be maintained at 368 K using 5% H_2O_2.

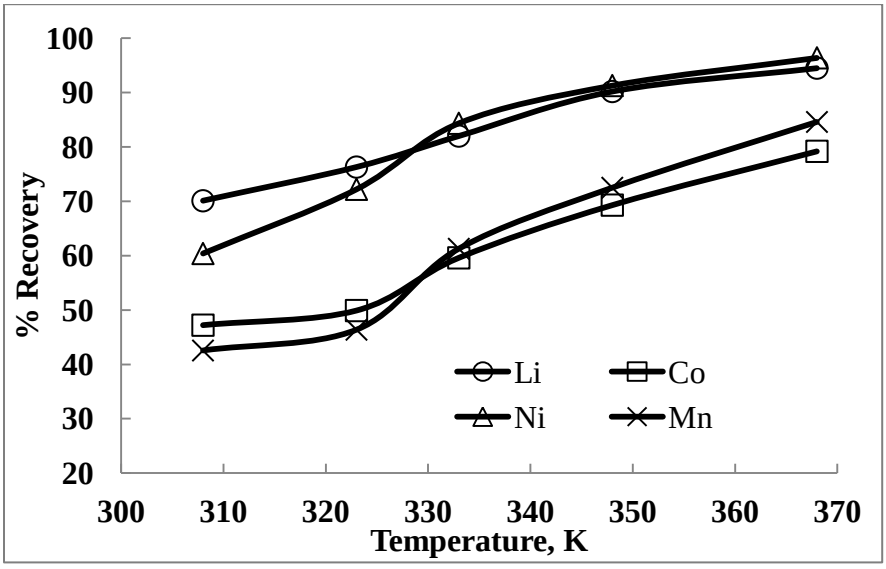

Fig. 3.28 Effect of temperature on leaching of metals in the presence of H_2O_2 as the reductant at 50 g/L pulp density and 1 M H_2SO_4 in 240 min.

3.3.5 *Kinetics of leaching:* In this case also kinetic data showed poor fit to the chemical and diffusion control kinetic models with low correlation coefficients for most metals (Figures not included for the sake of brevity). Therefore, data on the kinetics of leaching were plotted to the empirical model following the logarithmic rate law (Eq. 1.20, Chapter 1). The plots of $(-\ln(1-x)^2$ versus t at different temperatures show that the kinetic data fitted well to this model which is evident from the high R^2 values (Fig. 3.29). Interestingly the leaching kinetics of Mn is also represented by the empirical model in the H_2SO_4-H_2O_2 system unlike the leaching under the H_2SO_4-Na_2SO_3 system. The specific rate constants obtained from the kinetic data of empirical model were used to construct the Arrhenius plot (Fig. 3.30).

The activation energy values (Ea) calculated from the Arrhenius plots using H_2O_2 are found to be 30.7, 29.6, 42.6 and 43.9 kJ/mol for Li, Co, Ni and Mn, respectively. This could be attributed to the resistance of the diffusion layer for acid-hydrogen peroxide on the reaction interface (Seo et al., 2013). A comparison

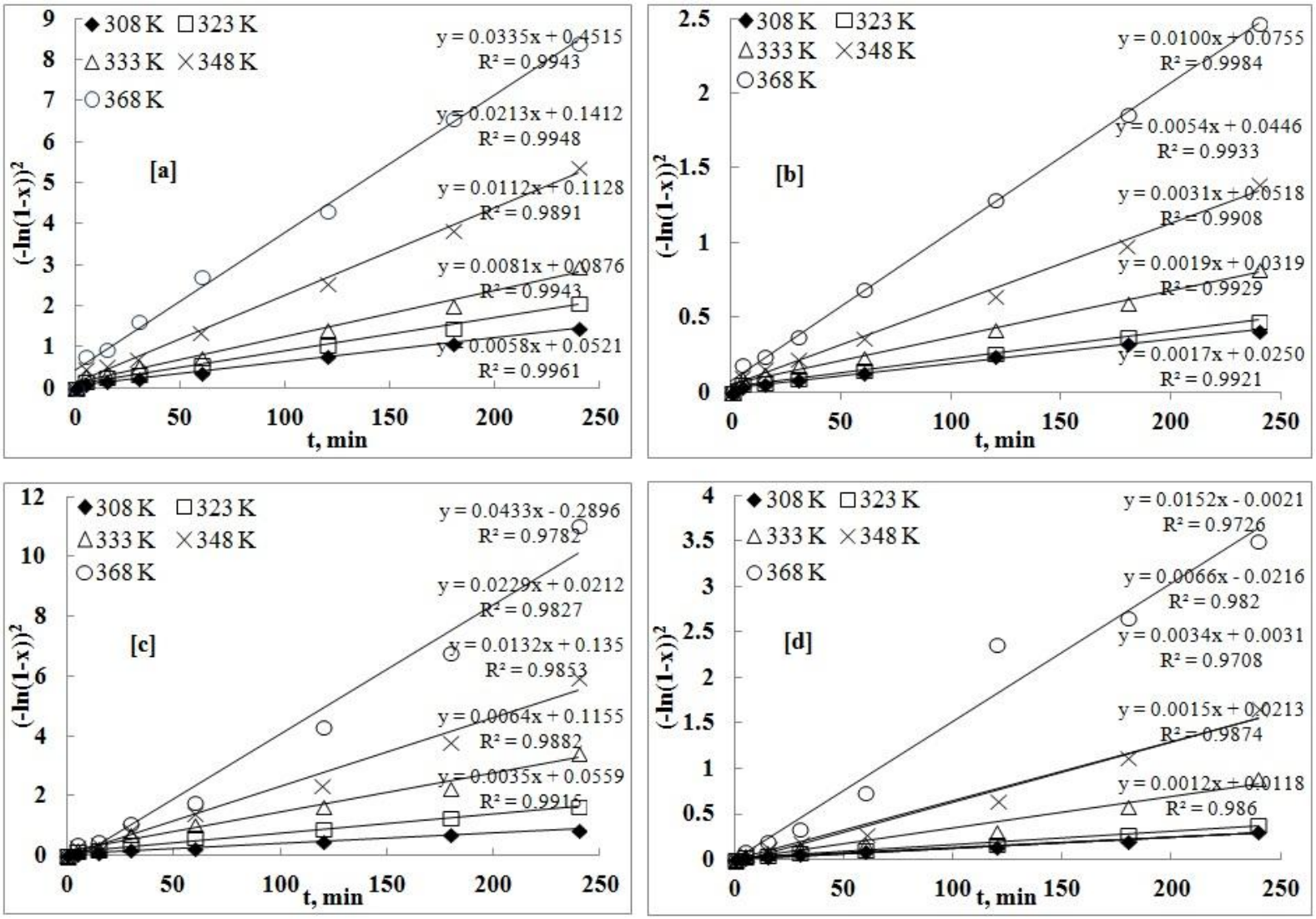

Fig. 3.29: Logarithmic model for leaching of metals (a- Li, b-Co, c-Ni, d-Mn) by H_2O_2-H_2SO_4 in temperature range (308-368 K)

of the activation energy for the two reductants shows that sodium bisulfite acquired lower E_a values at 20.4, 26.8 and 21.7 kJ/mol for Li, Co and Ni, respectively than that of H_2O_2. Thus sodium bisulfite acts as a better reductant for the leaching of metals from cathodic material of spent LIBs in sulfuric acid as compared to H_2O_2.

3.3.6 *Mechanism of metal dissolution in presence of H_2O_2:* XRD patterns for the residues generated in the presence of H_2O_2 in 60 and 120 min at 368 K are given in Fig. 3.31. It is clear that the intensity of the major phases is reduced progressively in leach residues with time (Figs. 3.31a & b). In the leaching with 1M H_2SO_4 and 5% H_2O_2 in 60 min, the major phases detected were $LiCoO_2$ and $Li_2NiO_{2.91}$, whereas the minor phases being non-stoichiometric entities of Li, Co and Ni along with MnO_2 (Table 3.5). After 120 min of leaching the major phases identified above were supplemented with secondary cobalt oxide ($CoCo_2O_4$) and MnO_2 phases, besides the minor phases such as Co_3O_4 and Li_2NiO_2.

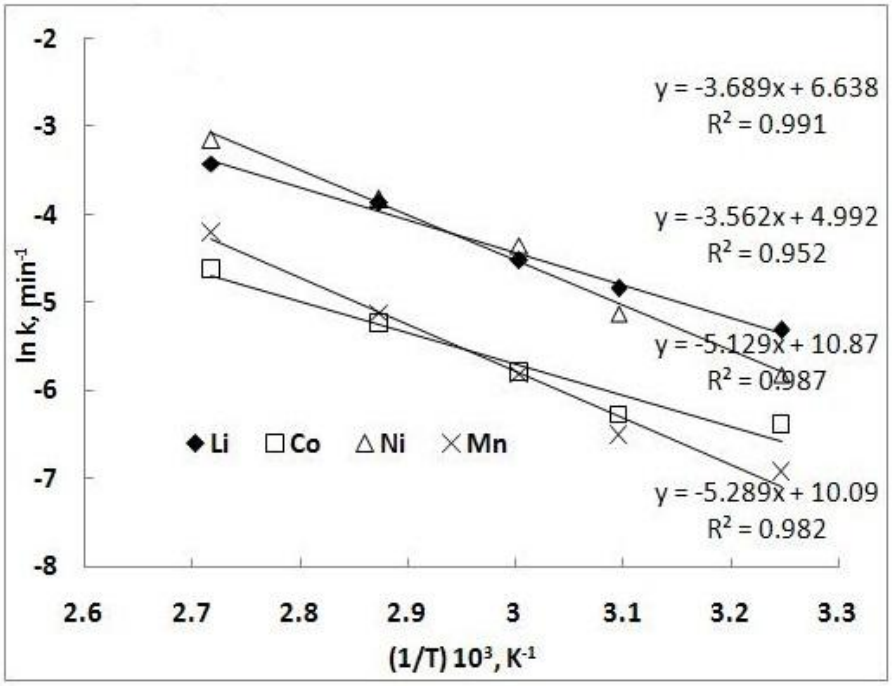

Fig. 3.30: Arrhenius plot for the leaching of Li, Co, Ni and Mn from cathode active material of LIBs at 368 K in presence of H_2O_2

The morphology of the cathode active material after leaching was examined by SEM-EDAX (Fig. 3.32). For the acid leaching in presence of H_2O_2 after 60 min (Fig. 3.32a), minimum degree of corrosion of particles with irregular shape along

with large number of secondary particles, and higher metal content can be seen. SEM image for the residue on subsequent leaching in 120 min show improved corrosion and fragments of particles, besides relatively lower metal contents (Fig. 3.32b-EDAX). Some oxide phases of Co and Mn identified by XRD analysis (Table 3.5) precipitated as the brighter particles can be noticed on the surface (Fig. 3.32b). XRD and SEM–EDAX studies thus substantiate the leaching mechanism proceeding through the surface diffusion of the lixiviant on the reacting particles.

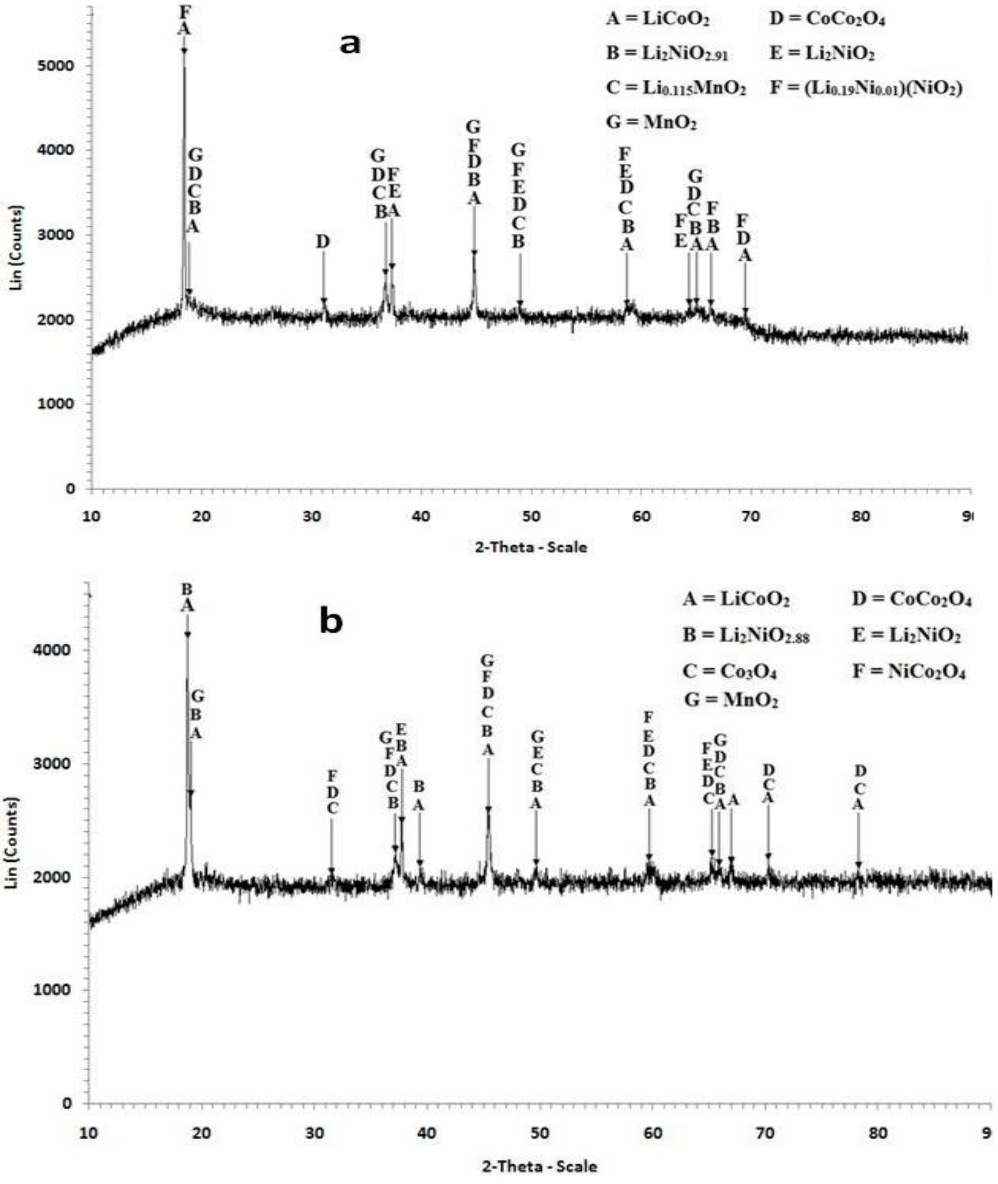

Fig. 3.31: XRD analysis of residue after treatment of spent cathode powder in 1 M H_2SO_4 and 5% H_2O_2 in (a) 1 h, (b) 2 h at 368 K and 50 g/L pulp density

Table 3.5 XRD analyses of leach residues obtained from the acid leaching in presence of H_2O_2 [Conditions: 1 M H_2SO_4 and 5% H_2O_2, 368 K, 50 g/L pulp density]

Residue	Major phase	JCPDS No.	Minor phase	JCPDS No.
After 60 min	$LiCoO_2$	750532	$(Li_{0.19}Ni_{0.01})(NiO_2)$	851975
	$Li_2NiO_{2.91}$	310733	$CoCo_2O_4$	710816
			Li_2NiO_2	460738
			$Li_{0.115}MnO_2$	822168
			MnO_2	421169
After 120 min	$LiCoO_2$	771370	Co_3O_4	781969
	$CoCo_2O_4$	710816	Li_2NiO_2	460738
	$Li_2NiO_{2.88}$	750634		
	MnO_2	421169		

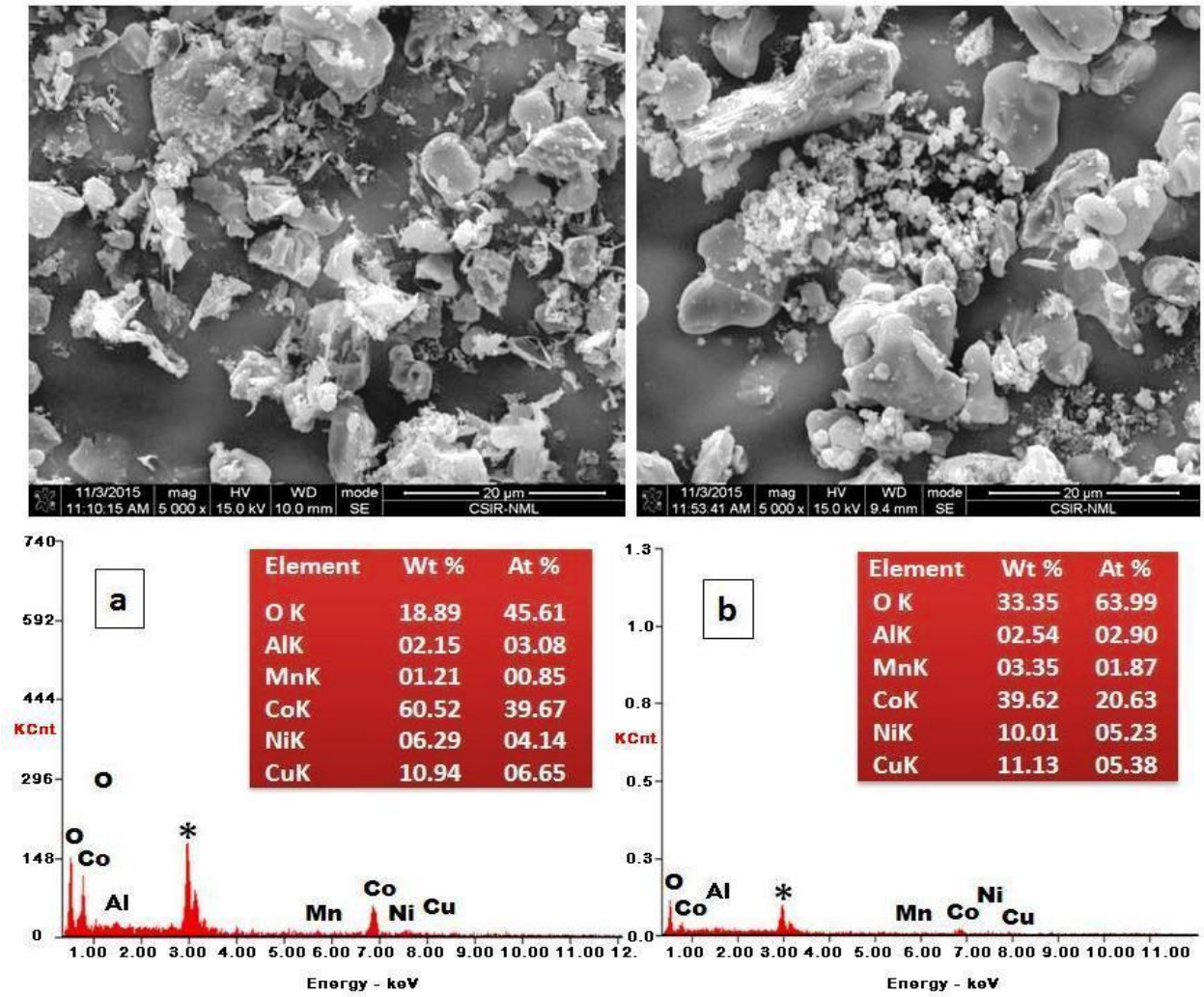

Fig. 3.32: SEM-EDAX of leach residue with H_2O_2 in (a) 60 min, (b) 120 min at optimized conditions (*Ag coating; Li not detected in EDAX)

3.4 Process intensification by acid baking and leaching to extract metals from cathode material

During the sulfuric acid leaching in absence or presence of a reductant, solubilization of almost all the metals takes place simultaneously without any selectivity. For selective recovery of metals an innovative approach such as process intensification by sulfatization through the sulfuric acid baking has been explored to transform prominent metals to their sulfates, thereby breaking the impervious layer and making the material more active. The transformed mass if discharged into water or low concentration of acid could result in selective leaching of some metals (in transformed matrix) to the bulk solution phases (Guo et al., 2009). Thus the sulfuric acid baking-water leaching of the spent cathode active material, a novel process that can operate at comparatively lower temperature than that of the alkali roasting processes, besides ensuring lower acid consumption in relation to the direct sulfuric acid leaching. Moreover, selective dissolution of metals has the merit of the lesser metal contamination at each stage resulting in ease of separation. Accordingly, a two-step process involved sulfuric acid baking to convert major components of spent battery material to water soluble phases yielding selective recovery of a set of metals like Li and Co over other metals (Ni and Mn) in water leach stage. The dissolution of remaining metals is attempted in the second stage of leaching.

3.4.1 Sulfuric acid baking and water leaching

The low temperature (100–300 °C) sulfuric acid baking was carried out in order to assess /improve the selective leaching of some of the metals over others from the cathode active material. On baking with the acid, the phases in the material were transformed and identified by XRD studies as $Li_2Co(SO_4)_2$, Li_2MnO_3 and Co_3O_4 in the major amount; the phases of the baked material at 300 ^oC are presented in Table 3.6. The effects of various baking parameters (amount of sulfuric acid, and baking temperature and duration) on the dissolution of Li, Co, Ni and Mn were studied. All the baked samples were thereafter leached with distilled water under the respective parametric conditions, unless otherwise stated.

3.4.1.1 *Effect of amount of sulfuric acid*: The effect of sulfuric acid on the recovery of metals was investigated by adding different amounts of the acid (0.5–3.5 mL) for 5 g of cathodic material keeping other conditions constant (baking temperature-300 ^{o}C, time-30 min). The collected baked material was leached in water at 95 ^{o}C for 120 min. Results presented in Fig. 3.33 show that 2 mL H_2SO_4 (0.37 M) is enough to dissolve ~79.0% Li and 91.1% Co in 120 min during the water leaching while the dissolution of Ni and Mn is less than 16% under this condition. The pH of the leaching medium remained unchanged (~3) after 120 min, whereas the redox potential decreased from 521 mV to 490 mV indicating the dissolution of the highly oxidized sulfates of Li and Co leaving only the relatively lesser oxidized phases in the leached slurry.

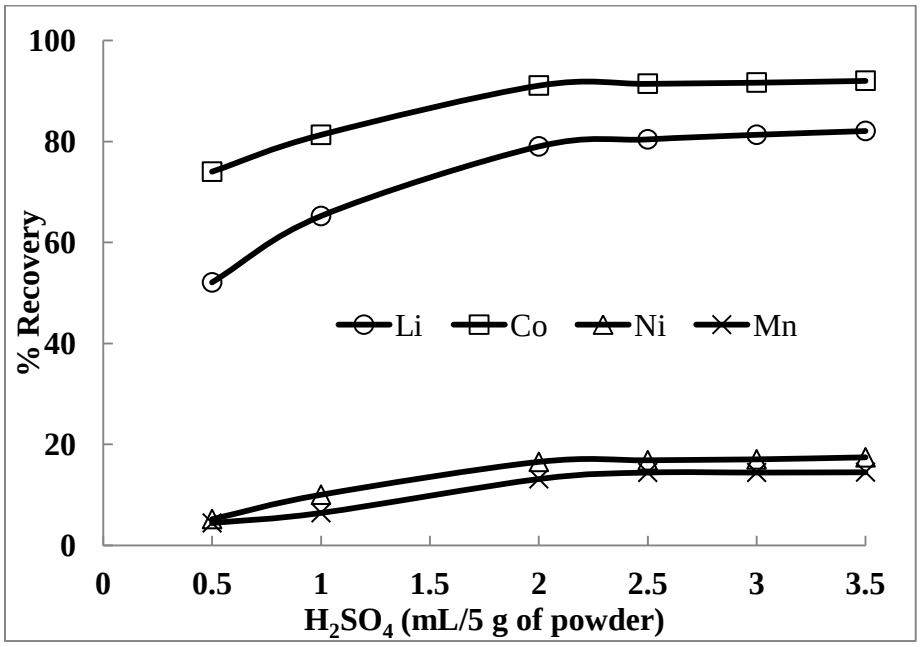

Fig. 3.33: Effect of amount of sulfuric acid during baking on the recovery of metals during leaching at 25% PD, 95 ^{o}C in 120 min.

3.4.1.2 *Effect of baking temperature:* The effect of temperature was studied in the range 200-400 ^{o}C when the cathodic material was baked for 30 min using 2 mL of sulfuric acid (per 5 g material). Results show that the recovery of metals increases initially with an increase in the baking temperature till 300 ^{o}C and after that the leaching efficiency decreases (Fig. 3.34). The recovery of metals from the baked

material (at 300 ^{o}C) during the water leaching at 95 ^{o}C and 25% pulp density in 120 min was recorded to be 79.0 % Li and 91.1 % Co along with 16.5 % Ni and 13.1% Mn. Increasing the baking temperature increases the weight to a maximum of ~16% at 400 ^{o}C; whereas increasing the temperature from 100 to 300^{o} C increases the weight of baked material slightly by ~2%. This could possibly be due to the increased rate of evaporation of sulfuric acid (boiling point of H_2SO_4: 327 ^{o}C) exceeding the rate of sulfation of metal oxides (Kim et al., 2009; Safarzadeh et al., 2012).

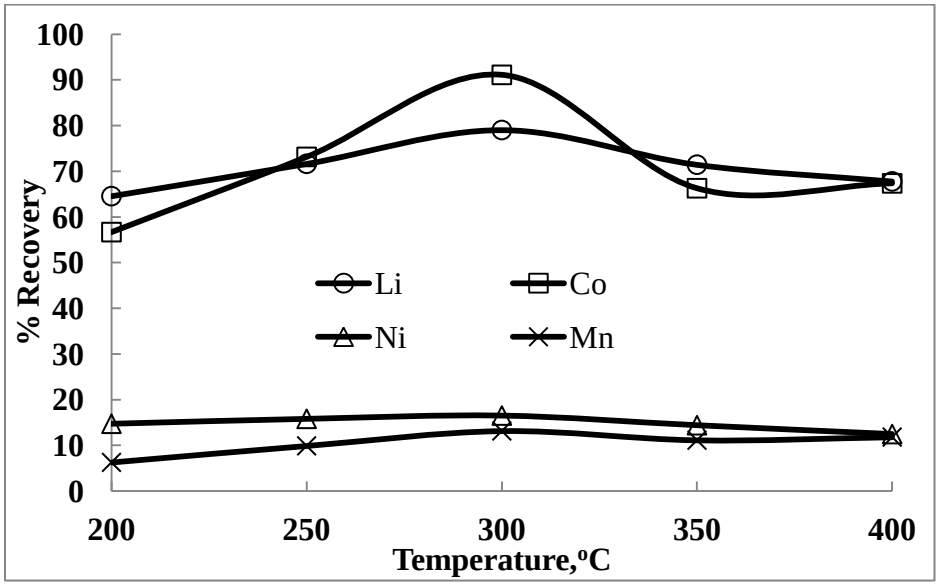

Fig. 3.34: Effect of baking temperature on the recovery of metals during leaching at 25% PD, 95 ^{o}C in 120 min.

3.4.1.3 *Effect of baking duration:* The effect of baking duration on the leaching efficiency of metals was investigated by baking the 5 g battery material at 300 ^{o}C with 2 mL sulfuric acid for different time intervals. The results shown in Fig. 3.35 indicate that 30 min baking time is sufficient to optimally transform the phases of the spent batteries which can solubilize maximum amount of lithium (79.0%) and cobalt (91.1%) along with lower recovery of other metals (16.5% Ni and 13.4% Mn) during the water leaching at 95 ^{o}C. During the baking, the formation of certain phases of Li and Co which can selectively dissolve in water over Mn and Ni, can be identified by calculating the standard free energy change (ΔG^{o}) for the reactions of the cathodic

Table 3.6: XRD analysis of cathode active material after baking and different leaching stages

Sample		**Major phases**		**Minor Phases**	
		Phases	*JCPDS file No.*	*Phases*	*JCPDS file No.*
Baked cathode material (300 ^{o}C, H_2SO_4)		$Li_2Co(SO_4)_2$	48-0868	$NiMnO_3$	12-0269
		Li_2MnO_3	84-1634	$NiSO_3.2H_2O$	34-0315
		Co_3O_4	78-1969 80-1541		
Leach-I residue after water leaching (75 ^{o}C, 60 min, 25% PD)		$Li_2NiO_{2.88}$	75-0634	$Li_{0.115}MnO_2$	82-2168
		$Li_2NiO_{2.91}$	31-0733	Co_3O_4	78-1969
		$NiMnO_3$	12-0269		
		$LiNi_{0.5}Mn_{1.5}O_4$	32-0581		
2^{nd} stage acid leaching with mixed acid and glucose (50 ^{o}C, 45 min, 10% PD)	*Leach-II residue in 60 min*	MnO_2	42-1169	$(Li_{0.19}Ni_{0.01})(NiO_2)$	85-1975
		$Li_{0.115}MnO_2$	82-2168		
	Leach-II residue in 120 min	MnO_2	42-1169	$(Li_{0.19}Ni_{0.01})(NiO_2)$	85-1975
				$Li_{0.115}MnO_2$	82-2168

material with the acid. The feasibility of the reactions in the system is accordingly predicted (HSC Chemistry 7.14).

Equations 3.9-3.13 describe the most likely reactions of Li, Co, Mn and Ni with sulfuric acid in the baking process (ΔG^o calculated at 573 K). The values of ΔG^o determined at various temperatures (473-677 K) are also included in Table 3.7 for these reactions. As can be seen, the major phases ($LiCoO_2$, $Li_2CoMn_3O_8$ and NiO_2) present in the spent LIBs may form water soluble sulfates of lithium and cobalt during the acid baking while converting nickel and manganese to relatively less soluble or insoluble nickel hydroxyl sulfate, $NiMnO_3$ and Li_2MnO_3, respectively, among others at 573 K (300 ^{o}C).

$$2LiCoO_2 + 3H_2SO_4 = Li_2SO_4 + 2CoSO_4 + 3H_2O + \tfrac{1}{2} O_2, \quad \Delta G^o_{573} = -684.8 \text{ kJ} \qquad (3.9)$$

$$Li_2CoMn_3O_8 + H_2SO_4 = CoSO_4 + Li_2MnO_3 + 2MnO_2 + H_2O, \quad \Delta G^o_{573} = -78.4 \text{ kJ} \qquad (3.10)$$

$$2NiO_2 + MnO_2 + H_2SO_4 = NiMnO_3 + NiSO_4 + H_2O + O_2, \quad \Delta G^o_{573} = 90.96 \text{ kJ} \qquad (3.11)$$

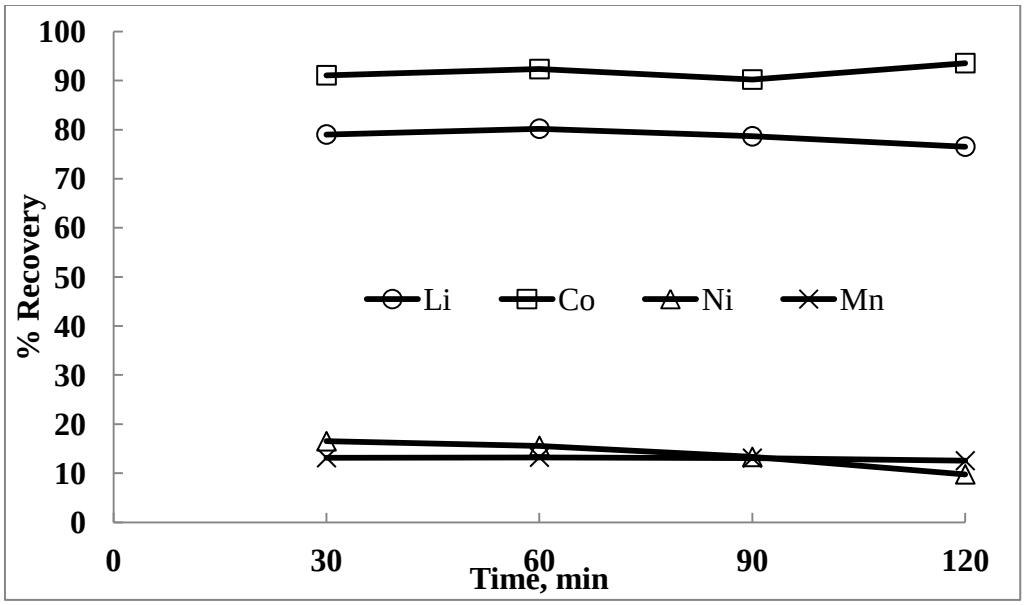

Fig. 3.35: Effect of baking duration on the recovery of metals during leaching at 25% PD, 95 ^{o}C in 120 min.

$NiO_2 + H_2SO_4 = NiO.SO_2.2H_2O$, ΔG^{o}_{573}=-214.8 kJ (3.12)

$CoO + H_2SO_4 = CoSO_4 + H_2O$, ΔG^{o}_{573}= -108.2 kJ (3.13)

Table 3.7: ΔG^{o} for chemical reactions during baking of cathode active material in temperature range 473-673 K

T (K)	ΔG^{o} values for the equations 3.9-3.13 (kJ)				
	Eq.3.9	Eq.3.10	Eq.3.11	Eq.3.12	Eq.3.13
473	-676.7	-81.9	87.6	-231.8	-110.9
523	-680.5	-80.1	88.2	-223.4	-109.6
573	-684.8	-78.4	90.9	-214.8	-108.2
623	-690.1	-76.8	91.1	-206.3	-106.9
673	-696.6	-75.6	91.4	-197.6	-105.8

Table 3.7 shows the values of standard free energy change for Eqs. 3.9, 3.10, 3.12, 3.13 making these reactions thermodynamically feasible in the baking process while forming a few of the chemical entities that are potentially leachable in water. Further the most reactions are feasible even at the lower baking temperature excepting Eq. 3.9 which is more favorable at the higher temperature. This can be further concurred with the residue characterization. However, the positive value of the standard free energy

change for Eq. 3.11 indicates that this reaction is thermodynamically unfavorable. Thus the formation of $NiMnO_3$ is less likely as per Eq. 3.11, but this phase has been identified in the XRD analysis discussed later, which might have formed by some other chemical reaction not considered here.

3.4.1.4 *Effect of optimized baking conditions on the metal recovery (Leach-I):* As can be seen in the preceding section, the dissolution of lithium and cobalt from the acid baked material is selective in the water leaching (leach-I) while the nickel and manganese dissolution is much lower. Keeping the optimized conditions of baking and using 2 mL H_2SO_4 (per 5 g cathodic material sample) at 300 ^oC for 30 min, leaching parameters like type of lixiviants, time, temperature and pulp density were optimized and results are discussed here.

3.4.1.5 *Effect of lixiviant type*: In order to examine the dissolution behavior of metals from the baked material, different types of lixiviants were used in the presence and absence of a reductant. The metal recovery (%) using different lixiviants is shown in Table 3.8. As can be seen, the water leaching results in a better selectivity for Li and Co as against the acid or acid-reductant mixture; this ensured neither any further consumption of a reducing agent nor the acid. The leaching of cobalt can, however, be increased (> 90%) when the baked material is leached in sulfuric acid in the presence of a reductant (H_2O_2 or $NaHSO_3$), but this entails further consumption of the acid along with slightly higher leaching of manganese as well.

Table 3.8: Effect of various lixiviants on the leaching of metals from the baked cathode active powder in leach-I at 95 ^oC for 120 min (Standard deviation: ±2% max)

Lixiviants used	**% Metal Recovery**			
	Li	**Co**	**Ni**	**Mn**
Water	79.02	91.09	16.52	13.14
1 M H_2SO_4	78.63	83.61	16.8	13.4
1 M H_2SO_4 + 5% H_2O_2	78.6	90.2	17.03	14.95
1 M H_2SO_4 + 0.075 M $NaHSO_3$	80.3	91.3	14.6	16.2

3.4.1.6 *Effect of leaching temperature:* The leaching temperature might play a significant role in metals extraction from the baked material. Fig. 3.36 shows the effect of temperature on the leaching with distilled water for 60 min at 25% pulp density. It can be seen that the extraction of all the metals increases steadily with the increase in temperature till 75 °C; the leaching efficiency being 78.6% Li, 80.4% Co, 15.8% Ni and 12.9% Mn. Further increase in the temperature to 95 ^{o}C has appreciable influence only on the recovery of Co which rose to 91% from that of ~80% recorded at 75 °C. However, with a cumulative steady state achieved for other metals, the optimum leaching temperature for further experiments is considered to be 75 ^{o}C.

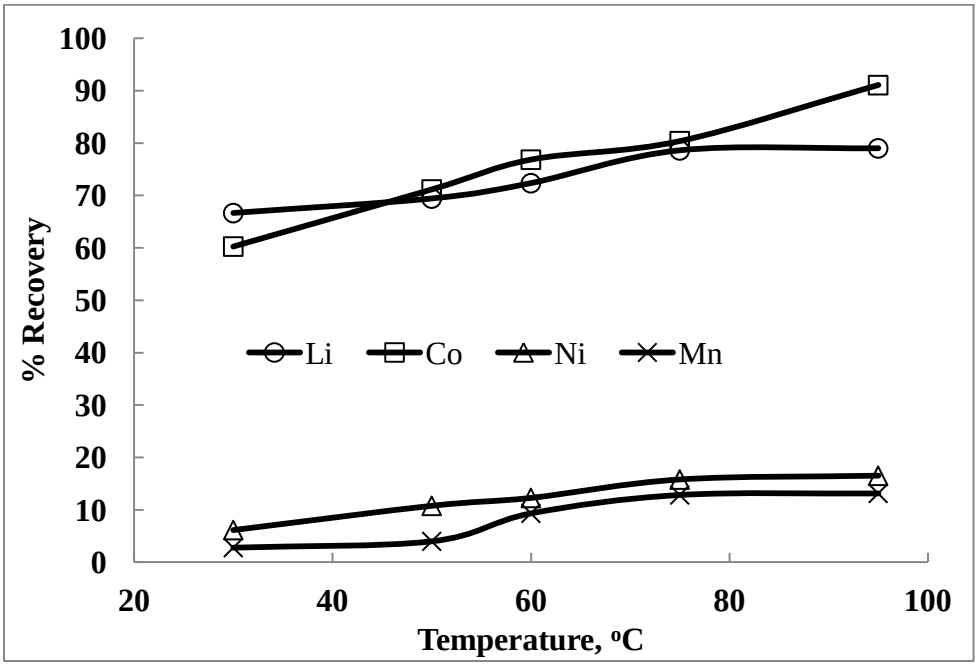

Fig. 3.36: Effect of leaching temperature on the recovery of metals by water leaching of baked cathode active material in 60 min and 25% PD.

3.4.1.7 *Effect of pulp density*: The effect of pulp density on the metal dissolution of the baked material is shown in Fig. 3.37. As is apparent, the leaching efficiency of Li, Co, Ni and Mn decreased slightly with the rise in pulp density; the dissolution of manganese is much less affected compared to other metals. At the pulp density of 25%, about 78.6% Li, 80.4% Co, 15.8% Ni and 12.9% Mn are recovered in 60 min at 75 ^{o}C, whereas at the higher pulp density of 50%, the recovery of metals being 63.7% Li, 70.7% Co, 4.9% Ni and 9.6% Mn. The higher recovery of Li and Co at 25% (w/v) pulp density can be termed as the optimum for further experiments.

3.4.1.8. *Effect of leaching time:* The baked cathode material is leached with distilled water at 75 °C and 25% (w/v) PD for different time periods (5-120 min), and results are shown in Fig. 3.38. It is observed that the extraction of Li and Co increases apparently by leaching time up to 60 min. Further increasing the duration of leaching has a marginal effect on the dissolution of lithium and cobalt. It is also observed that with the increase in leaching time, dissolution of all the metals increased. More than 50% of cobalt and lithium were dissolved in 5 min while the dissolution of Ni and Mn was very low (< 5%) under this condition. The selective dissolution of Li (78.6%) and Co (80.4%) over Ni (15.8%) and Mn (12.9%) is clearly noticed in 60 min of leaching.

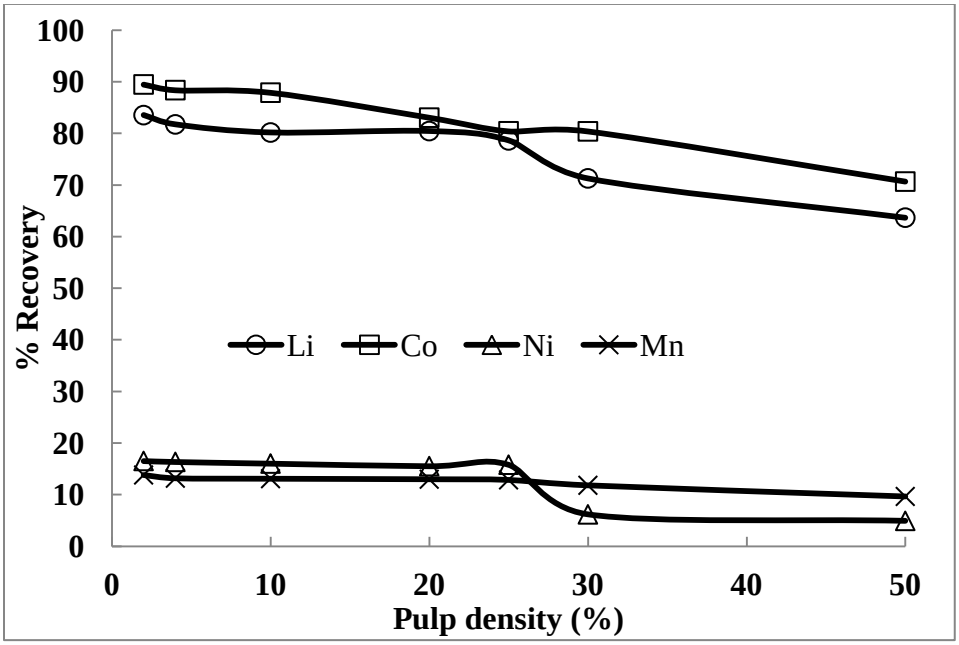

Fig. 3.37 Effect of pulp density on the recovery of metals by water leaching of baked cathode active material in 60 min and 75 ^{o}C.

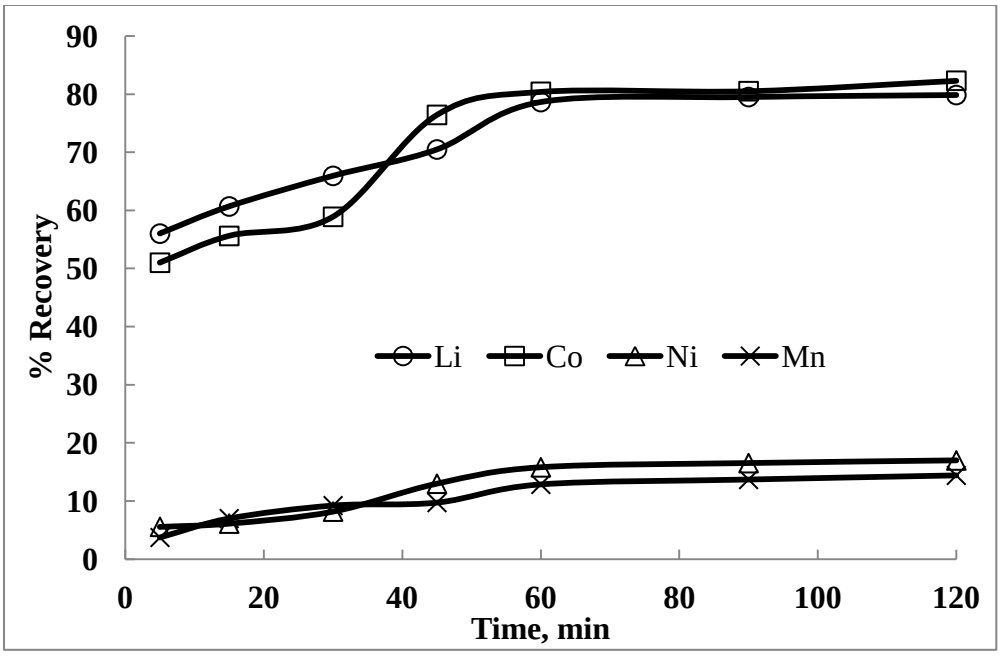

Fig. 3.38: Effect of time on the recovery of metals water leaching of baked cathode active material at 75 ^{o}C. 25% PD

3.4.1.9 *Optimum conditions and residue characterization:* Based on the optimized conditions for the water leaching of baked cathodic powder performed at 75 °C temperature, 60 min time and 25% (w/v) PD, the leaching efficiencies of lithium and cobalt were found to be 78.6 and 80.4%, respectively, besides the low dissolution of nickel (15.8%) and manganese (12.9%). The composition of the residue obtained from the leach-I under the above conditions was analyzed to be: 1.4% Li, 7% Co, 8.4% Ni and 9.7% Mn. In order to prevent the loss of residual metals- Li and Co in the leach-I residue while achieving the maximum recovery of major un-leached components viz., Ni and Mn, a second stage leaching can be adopted. In leach-II, recovery of nickel and manganese present mainly as lithium nickelate and lithium manganese oxide, respectively (Table 3.6), besides a few other phases, are particularly stressed upon.

It is necessary to understand the thermodynamics of reaction during the leaching of the acid baked phases in water. Formation of Li_2SO_4 or $CoSO_4$ in water has a very little consequence and as such a salt dissolves in water as the aquo-complex. However, if we consider $Li_2Co(SO_4)_2$, then the products formed would be aquo-complexes like, $Li_2(H_2O)_x.SO_4$ and $[Co(H_2O)_4]$ $[SO_4]$ with a change in free

energy value of -124.8 kJ favoring the dissolution of Li and Co (Eq. 3.14). These potentially leachable entities of metals such as Li and Co formed in the acid baking step can give rise to their selective dissolution in the first stage (water leach), making the leach-I residue rich in Ni and Mn. The thermodynamically less favourable dissolution of entities (Eq.3.15,3.16,3.17) like, $NiSO_3.2H_2O$, $NiMnO_3$ and Li_2MnO_3 with ΔG^o of -37.3 kJ, -87.6 kJ and -144.6 kJ, respectively reflect for the low dissolution of Ni and Mn in leach-I. Minor solubility of Ni and Mn may be attributed to the small amount of their sulfates formed during the baking. The recovery of cobalt is only due to $CoSO_4$ (and not Co_3O_4), which is still the major phase after baking. Since cobalt is present in high concentration (35.8%) in the untreated sample, the reactant is the $CoSO_4$ phase present as double salt- $Li_2Co(SO_4)_2$. The reaction of Co_3O_4 with water is thermodynamically unfavourable with ΔG^o_{348} of 762.9 kJ (Eq. 3.18).

$$Li_2Co(SO_4)_2 + 2H^+ = 2Li^+ + Co^{+2} + 2HSO_4^- \qquad \Delta G^o_{348} = -124.8kJ \qquad (3.14)$$

$$NiSO_3.2H_2O + H^+ = Ni^{+2} + SO_3^{-2} + 2H_2O \qquad \Delta G^o_{348} = -37.3\ kJ \qquad (3.15)$$

$$NiMnO_3 + 2H^+ = Ni^{+2} + MnO_2 + 2OH^- \qquad \Delta G^o_{348} = -87.6\ kJ \qquad (3.16)$$

$$Li_2MnO_3 + 2H^+ = 2Li^+ + MnO_2 + H_2O \qquad \Delta G^o_{348} = -144.6\ kJ \qquad (3.17)$$

$$Co_3O_4 + 4H_2O = Co^{+2} + 2Co^{+3} + 8OH^- \qquad \Delta G^o_{348} = 762.9\ kJ \qquad (3.18)$$

3.4.2 *Second stage leaching (leach-II):* The results of the treatment of water leach residue (rich in nickel and manganese) obtained above with different lixiviants are presented and discussed.

3.4.2.1 *Effect of concentration of lixiviant (acid/mixtures):* The effect of various lixiviants on the leaching of metals from the leach-I residue generated at 75 ^oC, 25% PD and 60 min, was tested. Initial experiments (leach-II) were carried out using the H_2SO_4 in the concentration range 0.25-3 M at 10% PD and 50 ^oC. With 1 M H_2SO_4 only the trace amounts (< 2-3 %) of Ni and Mn were leached in the solution (Table 3.9), although the solubilization of Li and Co was a little higher (5.5-7.8%). On adding a reducing agent viz., 5% H_2O_2 or 0.075M $NaHSO_3$ in 1 M H_2SO_4, leaching of cobalt improved to ~15% because of better solubility of Co(II) sulfate as highlighted

in previous sections (3.1.2 and 3.2.2) along with dissolution of 10-12% Li, but recovery of Ni and Mn remained still poor (4-8%). In place of H_2SO_4, different concentrations (0.25 M -3 M) of HNO_3 however, improved the metal recovery only slightly, but still the higher leaching efficiency targeted for Ni and Mn could not be achieved. The effect of the addition of the reductant ($NaHSO_3$, H_2O_2) to the lixiviant containing HNO_3 solution for the recovery of metals was not very significant and hence not included here.

A mixture of both acids was then tested for the recovery of all the metals of leach-I residue. At a fixed concentration of H_2SO_4 (1 M), the relative concentration of HNO_3 was varied from 0.25 to 2 M. It is observed that a mixture of 1 M H_2SO_4 and 0.5 M HNO_3 was sufficient of dissolving 11.04% Ni and 9.68% Mn, besides the leaching of Li (4.3%) and Co (2.3 %) values in the solution.

Table 3.9: Effect of various lixiviants on leaching of residue from leach-I stage at 10% PD, 50 ^oC, 45 min.

Lixiviants used	Metal recovery (%)			
	Li	Co	Ni	Mn
1 M H_2SO_4	5.53	7.79	< 3	< 2
1 M H_2SO_4 + 5% H_2O_2	10	14.6	4.2	3.2
1 M H_2SO_4 + 0.075 M $NaHSO_3$	11.8	16.32	8.32	6.44
1 M HNO_3	8.62	9.52	7.22	5.64

3.4.2.2 *Effect of addition of reducing agent:* Reducing sugar (e.g., glucose) facilitates metal dissolution in an acid environment, thereby improving the conversion of the respective metals to their soluble forms (Granata et al., 2012; Chen et al., 2015). In order to examine the effect of glucose (HiMedia™) concentration to the extent of metal dissolution, its concentration was varied in the range 0–5%. Other parameters maintained during the leach-II include 1 M H_2SO_4 + 0.5 M HNO_3, 50 ^oC and 10% (w/v) pulp density. The addition of glucose has significantly improved the dissolution of Ni and Mn as shown in Fig. 3.39. Nearly 14.6% Li, 10.12% Co, 67% Ni and 64.8% Mn were recovered using 2% glucose under the above conditions, which was accompanied by the decrease in redox potential from 782 mV to 585 mV and increase in pH from 0.16 to 0.67. However, when 1 M H_2SO_4 and 0.5 M HNO_3 were used

separately with glucose (2 g) as the reductant for 10 g of leach-I residue at 50 ^{o}C for 45 min, the recoveries of Ni and Mn fell down drastically. Respective leaching of Ni and Mn was recorded to be 4.47% and 2.38% with nitric acid, whereas it was almost negligible (~1% Ni and 1.2% Mn) with sulfuric acid. The redox potential decreased from 906 mV to 692 mV with nitric acid in the presence of glucose as the generated NO alone could not convert lithium nickelate to a soluble phase (nickel sulfate). Similarly with a decrease in redox potential from 810 mV to 640 mV during reductive sulfuric acid leaching could neither favor the dissolution of nickel.

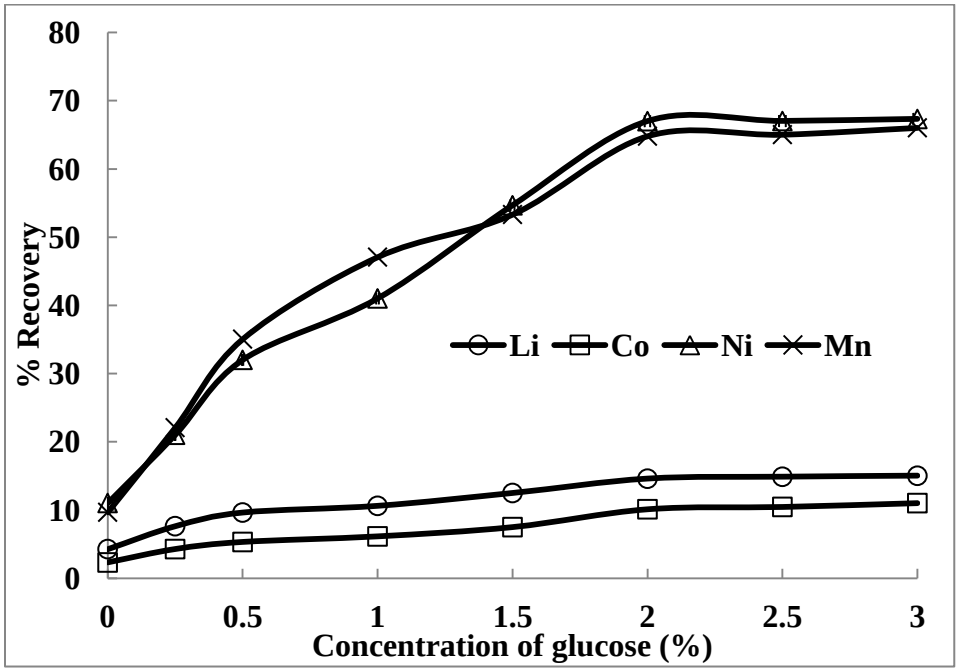

Fig. 3.39: Effect of addition of glucose on 2nd stage leaching of leach-I residue [Conditions: 10% PD, 50 ^{o}C, 45 min, 1 M H_2SO_4 + 0.5 M HNO_3]

Increased recovery of Ni is attributed to the formation of NO by the reaction of HNO_3 with glucose (Pagnanelli et al., 2004; Smith et al., 2012) as shown in Eq. (3.19). The resulting NO species in Eq. (3.19) helped in the dissolution of lithium nickelate as per reaction (3.20) in the presence of H_2SO_4. The overall reaction of lithium nickelate in the presence of glucose and acid mixture can be represented in Eq. 3.21 at 50 ^{o}C. The un-reacted $NiMnO_3$ in leach-I residue can also react with glucose and acid mixture as shown in Eq. 3.22.

$$C_6H_{12}O_6 + 8\ HNO_3 \rightarrow 8\ NO + 6\ CO_2 + 10\ H_2O, \qquad \Delta G^{o}_{323} = -2536.2\ kJ \quad (3.19)$$

$6LiNiO_2+9H_2SO_4+2NO \rightarrow 6NiSO_4+3Li_2SO_4+2HNO_3+8H_2O$, ΔG^o_{323}=-538.2 kJ (3.20)

$24\ LiNiO_2 + C_6H_{12}O_6 + 36\ H_2SO_4 = 24\ NiSO_4 + 12\ Li_2SO_4 + 6\ CO_2 + 42\ H_2O$

ΔG^o_{323}= -6841.9 kJ (3.21)

$12\ NiMnO_3 + C_6H_{12}O_6 + 24\ H_2SO_4 = 12\ NiSO_4 + 12\ MnSO_4 + 6\ CO_2 + 30\ H_2O$

ΔG^o_{323} = -4765.9 kJ (3.22)

In order to assess the thermodynamic feasibility of Eqs. 3.19-3.22 (Table 3.10), the values of ΔG^o for these reactions were also calculated (HSC Chemistry 7.14). As can be seen the values are highly negative at all temperatures considered (303-348 K), reflecting the feasibility of the leaching of lithium nickelate and $NiMnO_3$ by acid mixture with glucose. In particular at the intermediate temperature of 323 K (50 ^oC), most reactions are thermodynamically favorable, which explains for the high recovery of nickel and manganese from water leached residue in the next stage (acid leach).

Table 3.10: ΔG^o for chemical equations in the temperature range 273-573 K

T (K)	ΔG^o values for the equations 3.19-3.22 (kJ)			
	Eq. 3.19	Eq. 3.20	Eq. 13.21	Eq. 3.22
303	-2493.2	-543.5	-6841.4	-4757.3
308	-2503.9	-542.2	-6841.5	-4759.5
313	-2514.7	-540.9	-6841.7	-4761.7
323	-2536.2	-538.2	-6841.9	-4765.9
333	-2557.7	-535.6	-6842.1	-4770.2
348	-2589.8	-531.6	-6842.3	-4776.5

3.4.2.3 *Effect of temperature*: Effect of temperature on the leaching efficiency of the metals was studied using an acid mixture (1 M H_2SO_4 and 0.5 M HNO_3) at 10% PD for 120 min. The results given in Fig. 3.40 show that dissolution of Ni and Mn increased drastically with temperature. At 50 ^oC, the recovery of Ni and Mn was recorded to be 67% and 64.8%, respectively, along with the leaching of 14.6% Li and 10.12% Co.

3.4.2.4 Effect of leaching time: Leach recovery of metals with time in the optimized acid mixture (1 M H_2SO_4 and 0.5 M HNO_3) at 50 ^oC and 10% PD is presented in Fig.

3.41. The increase in leaching time improved the dissolution of all metals. With the increase in duration of leaching from 15 to 45 min, the recovery of metals increased from 8.5% to 14.6% for Li, 6.6 to 10.1% for Co, 60 to 67% for Ni and 30 to 64.8% for Mn. With no increase in the metal recovery beyond 45 min of leaching, the optimum duration of 45 min was used in further experiments.

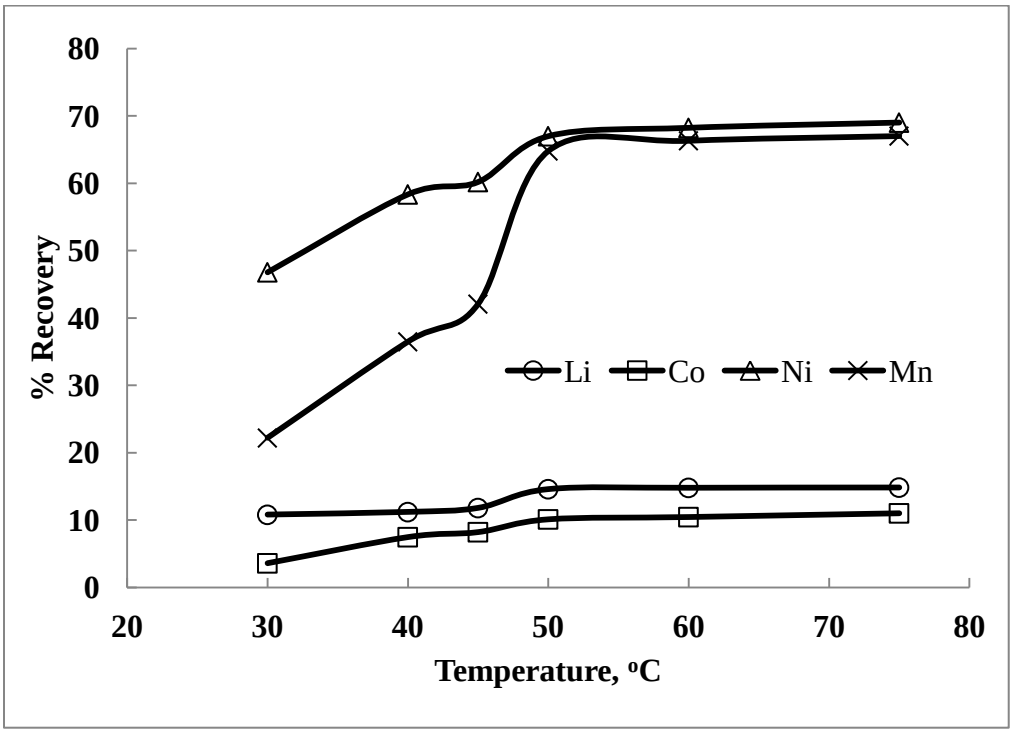

Fig. 3.40: Effect of temperature on 2nd stage leaching of leach-I residue using 1 M H_2SO_4 + 0.5 M HNO_3 and 2 % glucose.

3.4.2.5 *Effect of pulp density:* In order to examine the effect of pulp density variation in the range 2-25%, leach residue obtained after leach-I was subjected to further leaching (leach-II) with an acid mixture (1 M H_2SO_4, 0.5 M HNO_3) for 45 min. The results given in Fig. 3.42 show the solubilization of 69.7% Ni and 66.7% Mn along with 14.2% Li and 11.2% Co at a pulp density of 2%. Increase in pulp density beyond 10% adversely affected the recovery of the metals; the maximum leaching was found to be 67% Ni and 64.8% Mn along with 14.6% Li and 10.12% Co in 45 min at 10% PD.

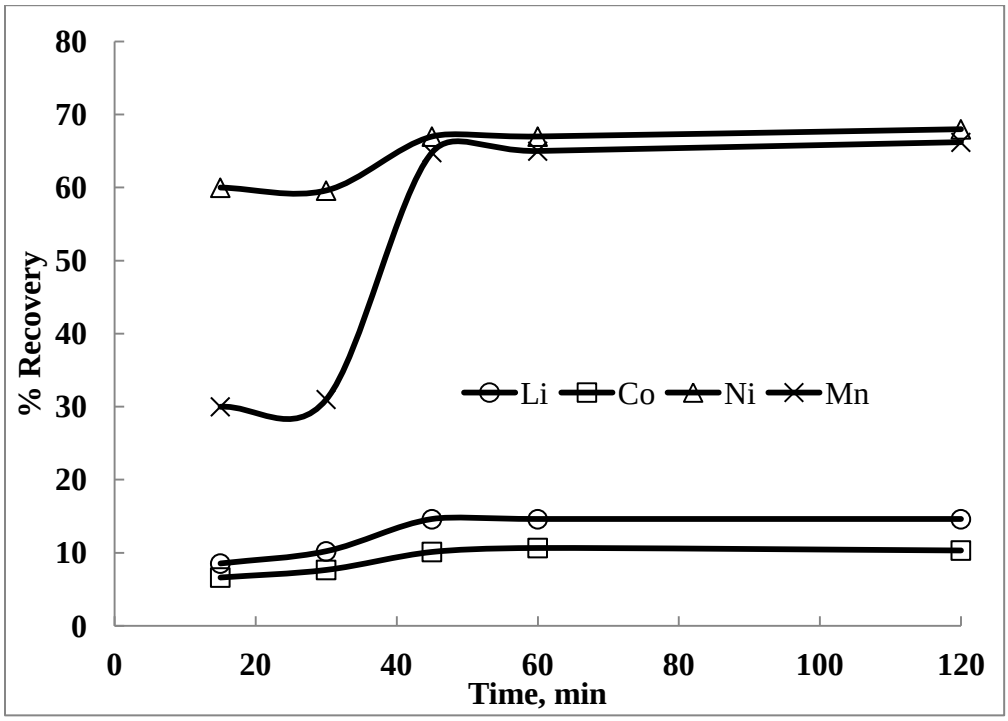

Fig. 3.41: Effect of time on 2nd stage leaching of leach-I residue using 1 M H_2SO_4 + 0.5 M HNO_3 and 2 % glucose.

The two-stage leaching process, thus represents the leaching of the baked cathode material by water in leach-I at 75 ^oC and 25 % PD for 60 min, followed by the leaching with the acid mixture (H_2SO_4+ HNO_3) in leach-II at 50 ^oC and 10 % PD for 45 min. The baking-leaching process seems advantageous because of the selective dissolution of Co and Li over other metals (Ni and Mn) and the lower acid consumption compared to the direct sulfuric acid leaching. The overall recovery in the two-stage leaching of the baked cathode powder could be worked out as: 93.2% Li, 90.5% Co, 82.8% Ni and 77.7% Mn.

3.4.2.6 *Material* characterization: The leach residues obtained from the treatment of the cathode material were characterized using XRD phase analysis (Fig. 3.43). As reported above, the major phases identified in untreated sample are $LiCoO_2$, $Li_2CoMn_3O_8$, $(Li_{0.85}Ni_{0.05})(NiO_2)$ and minor phases being $(Li_{0.69}Ni_{0.01})(NiO_2)$ and CoF_4 (Table 3.1). Baking of cathode active material in 30 min produced relatively

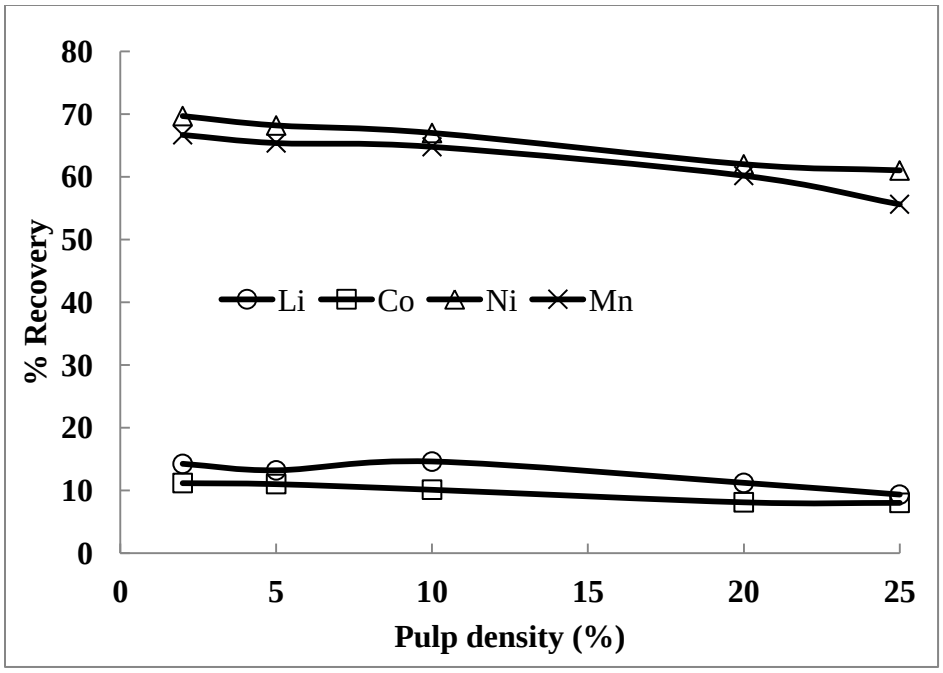

Fig. 3.42: Effect of pulp density on 2nd stage leaching of leach-I residue using 1 M H_2SO_4 + 0.5 M HNO_3 and 2 % glucose.

friable and fluffy materials, wherein the reaction with sulfuric acid led to the conversion of metals to respective sulfates-$Li_2Co(SO_4)_2$ along with Li_2MnO_3 and Co_3O_4 as the major phases while $NiMnO_3$ and $NiSO_3.2H_2O$ being the minor phases (Fig. 3.42a). The phase transformation during the acid baking can be established by XRD analysis which accounts for the selective leaching of Li and Co over Ni and Mn in water (leach-I). As can be seen from the XRD patterns (Fig. 3.43) and the phases identified above (Table 3.6), the intensities of the major peaks decreased progressively in different residues. The leach-I residue at 75 ^oC for 60 min show the presence of lithium nickelate ($Li_2NiO_{2.88}$, $Li_2NiO_{2.91}$) and Ni-Mn rich phases-$NiMnO_3$ and $LiNi_{0.5}Mn_{1.5}O_4$ in the major amounts. This illustrates the presence of un-dissolved Ni and Mn after selective dissolution of Li and Co with their decreased ratio in the lower stoichiometric intermediate phases like $Li_{0.115}MnO_2$ and Co_3O_4 as the minor phases (Fig. 3.43b).

On further leaching (leach-II), the Li-Co depleted residue of stage-I with acid mixture and a reductant at 50 ^oC, the maximum dissolution of Ni and Mn in 60 min can be accounted for the presence of MnO_2 and $Li0_{.115}MnO_2$ as the major phases. Lowering of Li and Co contents in the leach-II residue is further demonstrated by the presence

of minor amounts of $[Li_{0.19}Ni_{0.01}](NiO_2)]$ phase. Increased recovery of metals with time is also evident from the XRD analysis of the residues (Fig. 3.43c). In leach-II residue obtained in 120 min, the Li and Ni contents dropped in the non-stoichiometric entities viz., $(Li_{0.19}Ni_{0.01})(NiO_2)$ and $Li_{0.115}MnO_2$ identified as the minor phases, indicating the dissolution of lithium nickelate (Fig. 3.43d). However, relatively lower recovery of Mn compared to Ni is reflected by the presence of MnO_2 as the major phase in the residue.

The leaching of metals with time was further examined by comparing the morphological changes through the SEM studies and also the elemental distribution in the leach residues with that of the cathodic sample. EDAX data clearly show a progressive decrease in the average content of most metals (Li, Co, Ni, Mn) in the residues as the leaching progressed in 2-stages. Fig. 3.44a reflects the SEM image of the untreated sample showing larger particles present in irregular morphologies. The material baked at the 300 ^oC depicts a porous structure with the formation of new phases as thick segregated needles. Fig. 3.44b depicts the particles reacted to a certain extent, although the fraction reacted is probably lower for the larger secondary particles. The leach-I residue after water leaching performed at 75^oC for 120 min shows low concentrations of Co (EDAX), which clearly indicates the selective dissolution of Li and Co in the porous residue with corroded surface leaving Ni and Mn (Fig. 3.45). Subjecting the leach-I residue to leach-II stage (acid mixture in the presence of glucose), a very high recovery of Ni and Mn besides, the remaining Li and Co is corroborated by a decrease in the particle size (SEM, Fig. 3.46), and low elemental distribution (in the EDAX). The characterization of the cathode material and the residues by SEM-EDAX studies and XRD phase analysis thus provide evidence for the selective leaching of the metals in a two-step process (Fig. 3.47).

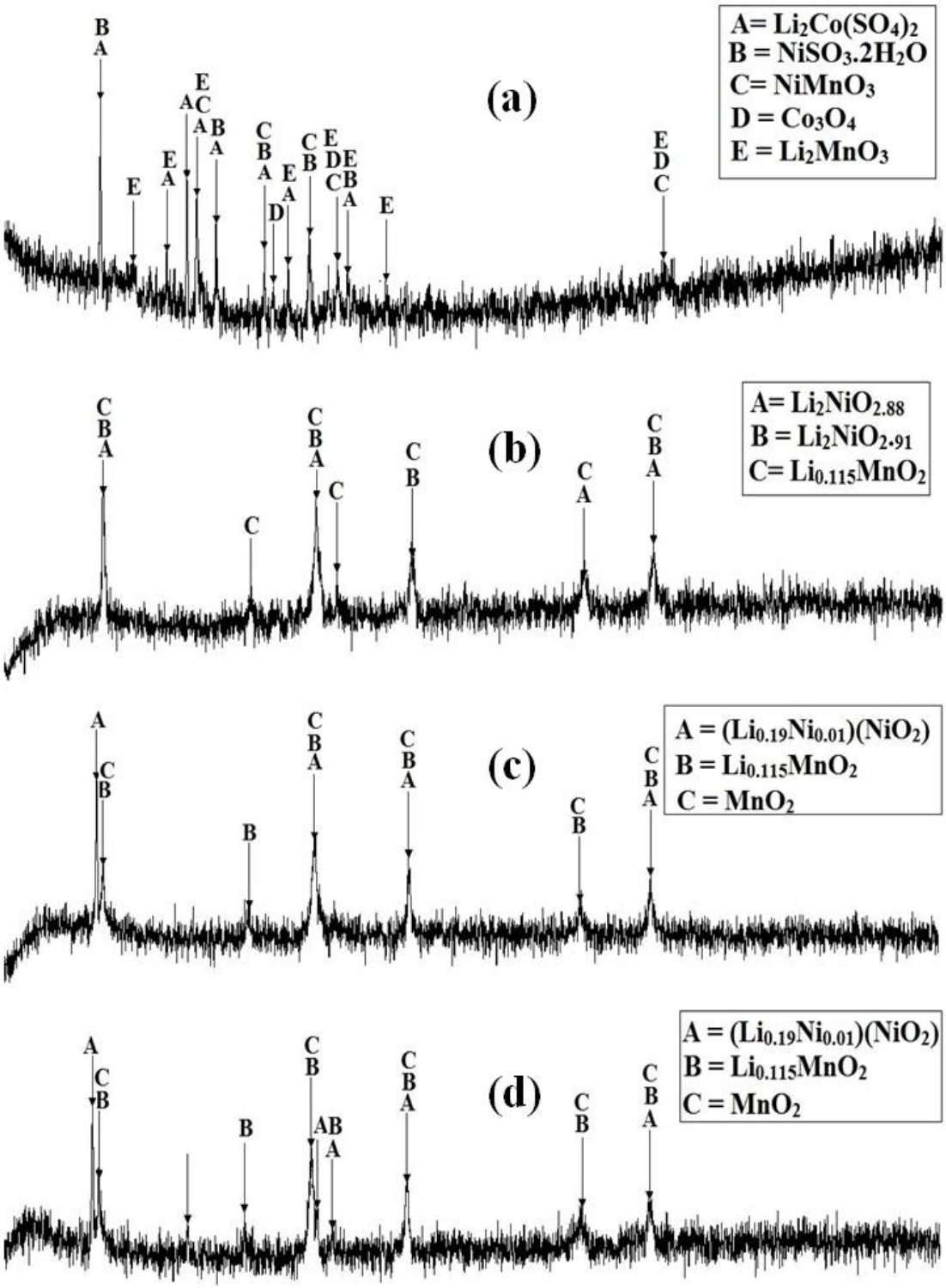

Fig. 3.43: XRD phase analysis of (a) baked cathode material; (b) 1st stage water leached residue; (c) 2nd stage acid leached residue in 60 min at 50 ^{o}C; (d) 2nd stage acid leached residue in 120 min at 50 ^{o}C.

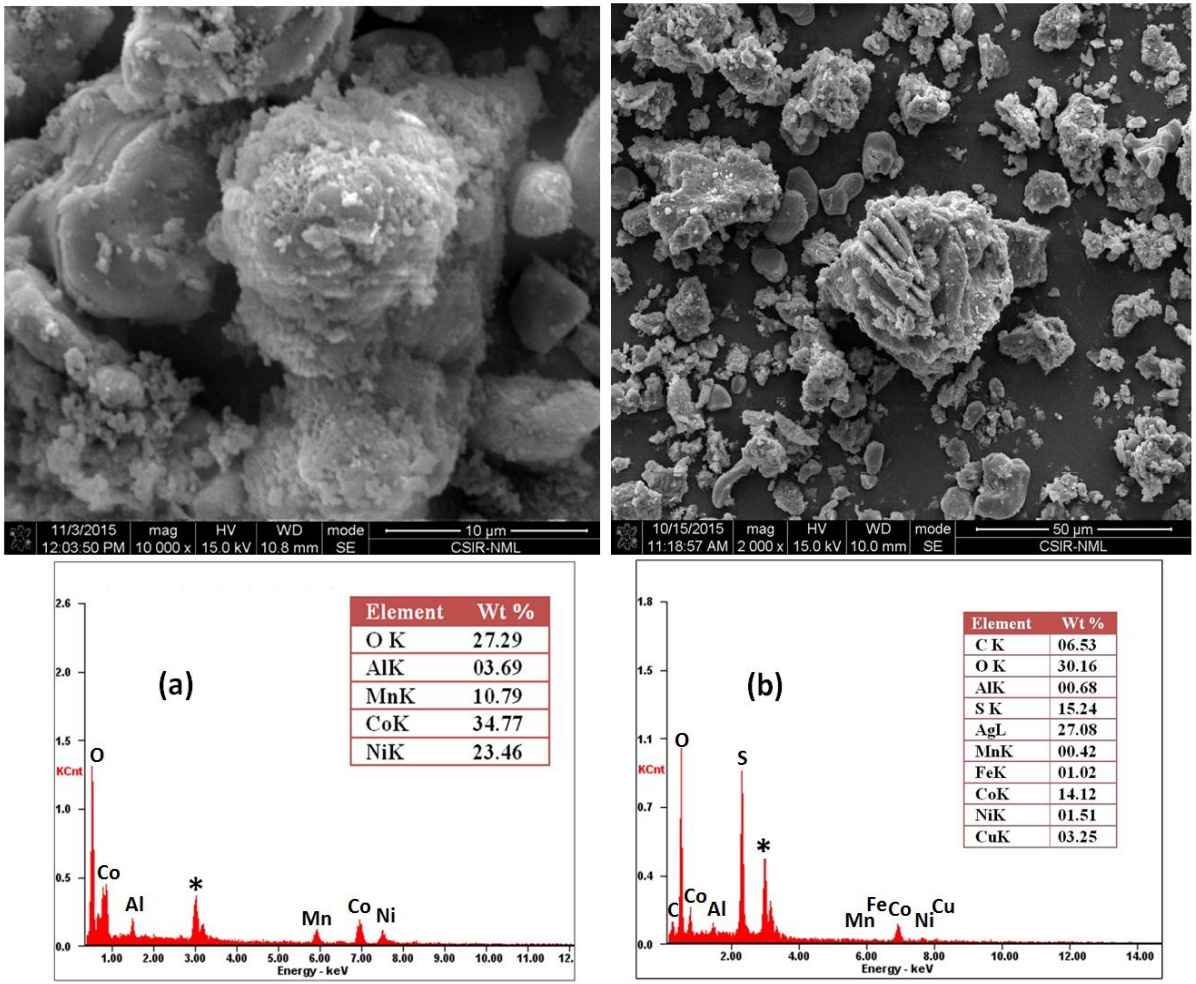

Fig. 3.44: SEM-EDAX analysis of untreated (a) and baked (b) cathode active material (baking temperature: 300 ^{o}C, time: 30 min, acid: 2 mL H_2SO_4/5 g material) [*Ag coating, Li not detected]

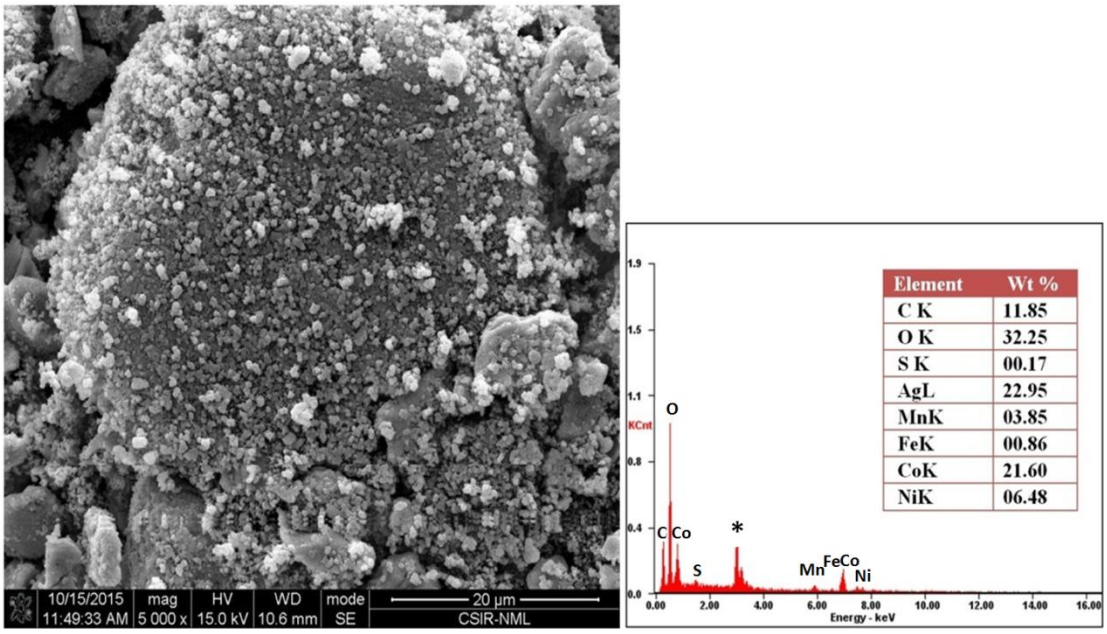

Fig. 3.45: SEM-EDAX analysis of leach-I residue after water leaching of baked material (at 75 ^{o}C and 25 % PD for 60 min)

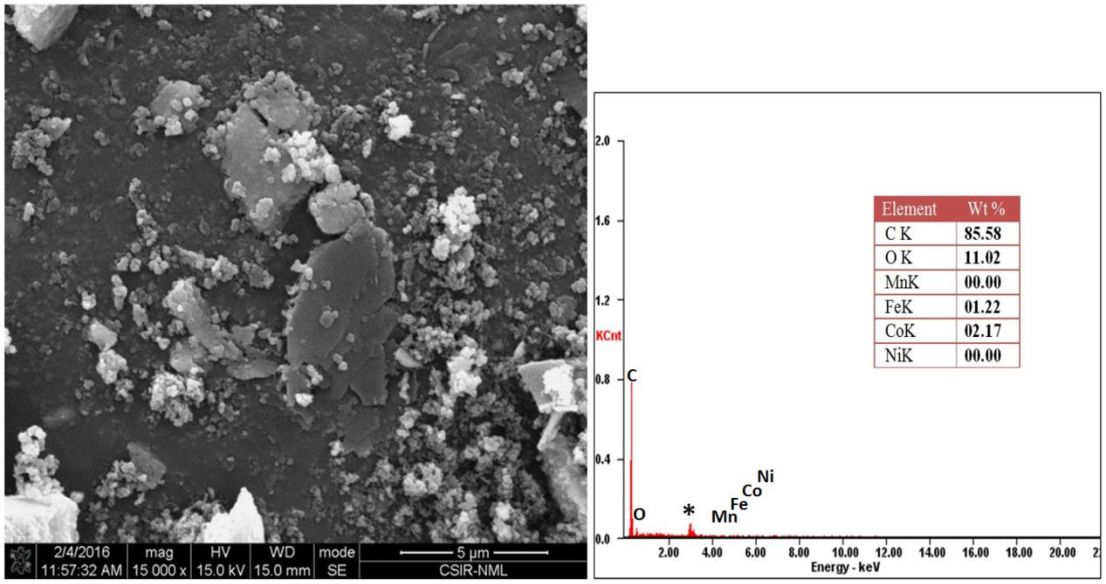

Fig. 3.46: SEM-EDAX analysis of residue obtained after leach-II (2nd stage leach) in 60 min (1M H_2SO_4 + 0.5 M HNO_3 and glucose, 50 ^{o}C, 10% PD) [*Ag coating, Li not detected]

Fig. 3.47: Flowsheet of process intensification by acid baking followed by leaching to extract metallic values from LIB cathode materials

3.5 Separation and synthesis of metal salts from the solution generated during the leaching in presence of $NaHSO_3$ as the reductant

The leach liquor obtained during the optimization process discussed above could be treated by various methods such as precipitation, solvent extraction, ion exchange, membrane separation etc. to separate and recover the valuable metals (Chagnes and Pospiech, 2013). Precipitation process being simple has been investigated to achieve the separation and recovery of individual metal from the leach liquor produced under the leaching system H_2SO_4-$NaHSO_3$ as a typical case which can be suitably modified to treat other leach solutions.

3.5.1 *Precipitation of cobalt oxalate:* Cobalt oxalate was precipitated by adding oxalic acid drop by drop to the leach solution (6.56 g/L Co, 1 g/L Li, 2 g/L Ni, 2 g/L Mn; pH 1.4) generated under the optimum conditions. The effect of temperature on the precipitation efficiency of cobalt was examined. With increase in temperature from 308 to 323 K the recovery of cobalt increased from 78.42 to 98.93% (data not shown). Further increase in the temperature (>323 K) caused a decrease in its recovery because of the dissolution of precipitated cobalt oxalate. The pH of solution slightly increased (up to 1.52) initially during the precipitation process, but no further change was noticed after the initial increase as reported earlier also (Sohn et al., 2006). The optimum conditions to recover cobalt oxalate ($CoC_2O_4.2H_2O$) were worked out to be: 1 M oxalic acid, equilibrium pH 1.5, temperature 323 K and time 2 h. The polycrystalline pink precipitate was obtained at 50 ^oC and pH 1.5. Based on the chemical analysis using ICP and other techniques the composition was found to be 37.2 % Co and 14.21 % C, indicating a product purity of 98.8% with the traces of Ni and Mn. Monoclinic phase of $CoC_2O_4.2H_2O$ can be characterized by the presence of a doublet peak ($2\theta=18.745^o$) in the XRD powder diagram (Wisgerhof and Geus, 1984). The powder XRD (Fig. 3.48a) corresponds to the reported pattern for the orthorhombic phase of cobalt oxalate dihydrate (JCPDS file: 25-0250). The cobalt oxalate dihydrate precipitate (Fig. 3.48b) has tubular rod-like morphology (Fig. 3.48c) generated by self-assembly of needle-like microcrystals; the EDAX analysis (inset in Fig. 3.48d) depicts the sample to be cobalt dominant matrix.

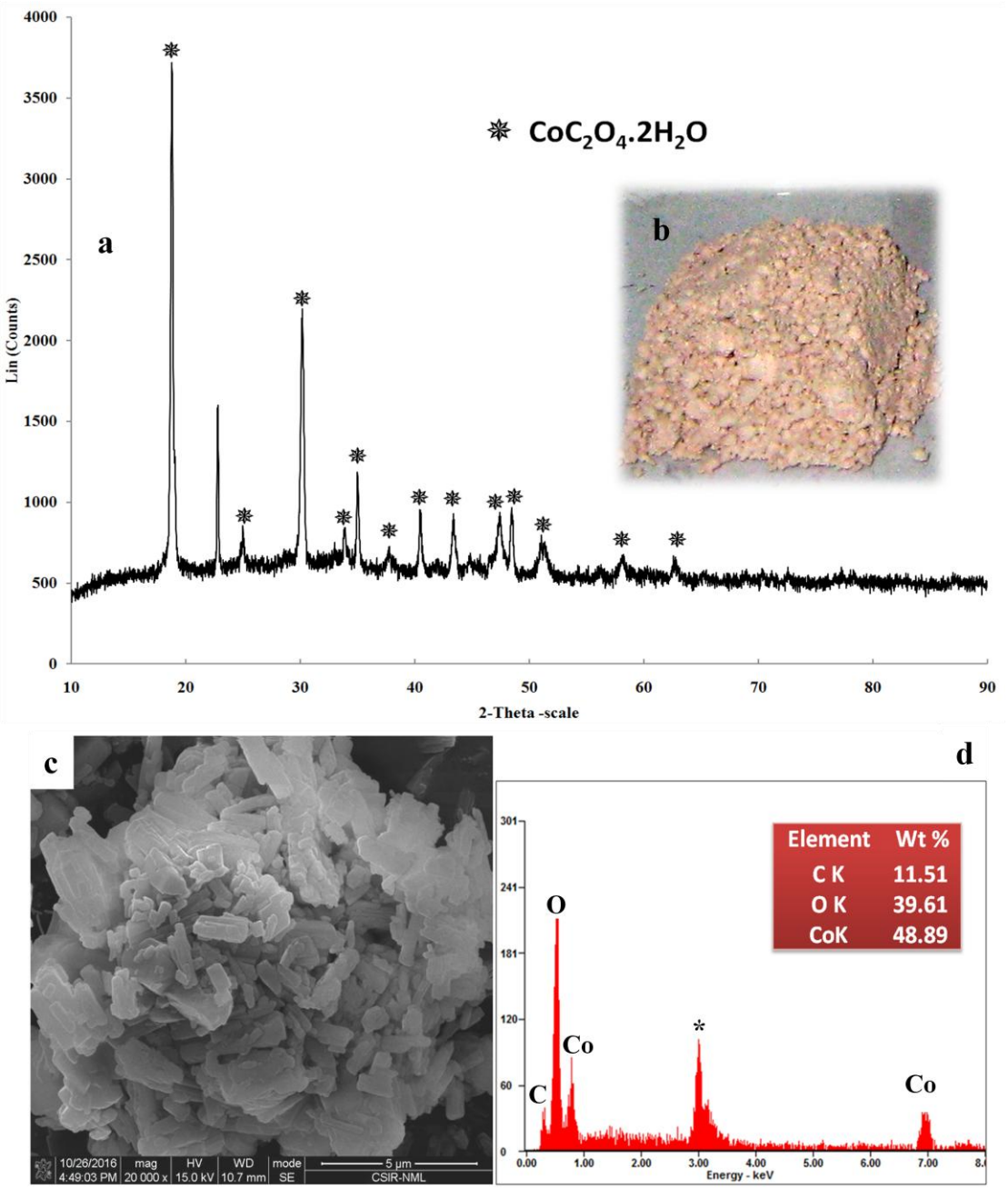

Fig. 3.48: Cobalt oxalate synthesized at pH 1.5 using oxalic acid (a-XRD; b-pink precipitate of $CoC_2O_4.2H_2O$; c-FESEM of tubular rod like Co-oxalate; d-EDAX of Co-oxalate)

3.5.2 *Precipitation of Mn and Ni:* Leach liquor after cobalt precipitation was then used for precipitation of Mn and Ni. The pH of the cobalt depleted solution was adjusted to 7.5 by adding 5 M NaOH solution and manganese was selectively precipitated with the saturated solution of Na_2CO_3 (Sayilgan et al., 2010). Light brownish - pink precipitate of $MnCO_3$ so obtained was washed and was dried in an oven for 24 h. A 99.6% pure Mn carbonate was recovered from the leachate as analyzed by ICP and other relevant techniques (47.4 % Mn, 18.91 % C and a minor amount of Ni, 0.22%). Fig. 3.49a reflects the presence of manganese carbonate ($MnCO_3$) matching to JCPDS File (no. 86-0172) while indicating the hexagonal symmetry of particles. The light brown precipitate of $MnCO_3$ (Fig. 3.49b) has the morphology resembling to the aggregates of microspheres (Fig. 3.49c) while EDAX (inset in Fig. 3.49d) reflecting the dominant Mn peaks.

The pH of the raffinate (Co-Mn depleted solution) was again adjusted to 9.0 by adding the 2 M NaOH solution. This was followed by the addition of saturated solution of Na_2CO_3 while stirring for 2 h at room temperature. A light green precipitate of $NiCO_3$ so obtained was dried in oven at 363 K for 24 h and was analyzed; the composition was found to be: 46.38% Ni and 10.3% C apart from <0.5% Mn and Li as impurity. Fig. 3.50a corresponds to the purity of 99.5% Ni as carbonate ($NiCO_3$) (JCPDS File no. 10-0272 and 78-0210) indicating the hexagonal symmetry of the particles. The light green powder (Fig. 3.50b) exhibits the flakes of $NiCO_3$ (Fig. 3.50c) and EDAX (inset in Fig. 3.50d) reflects the strong peaks of Ni dominating the matrix.

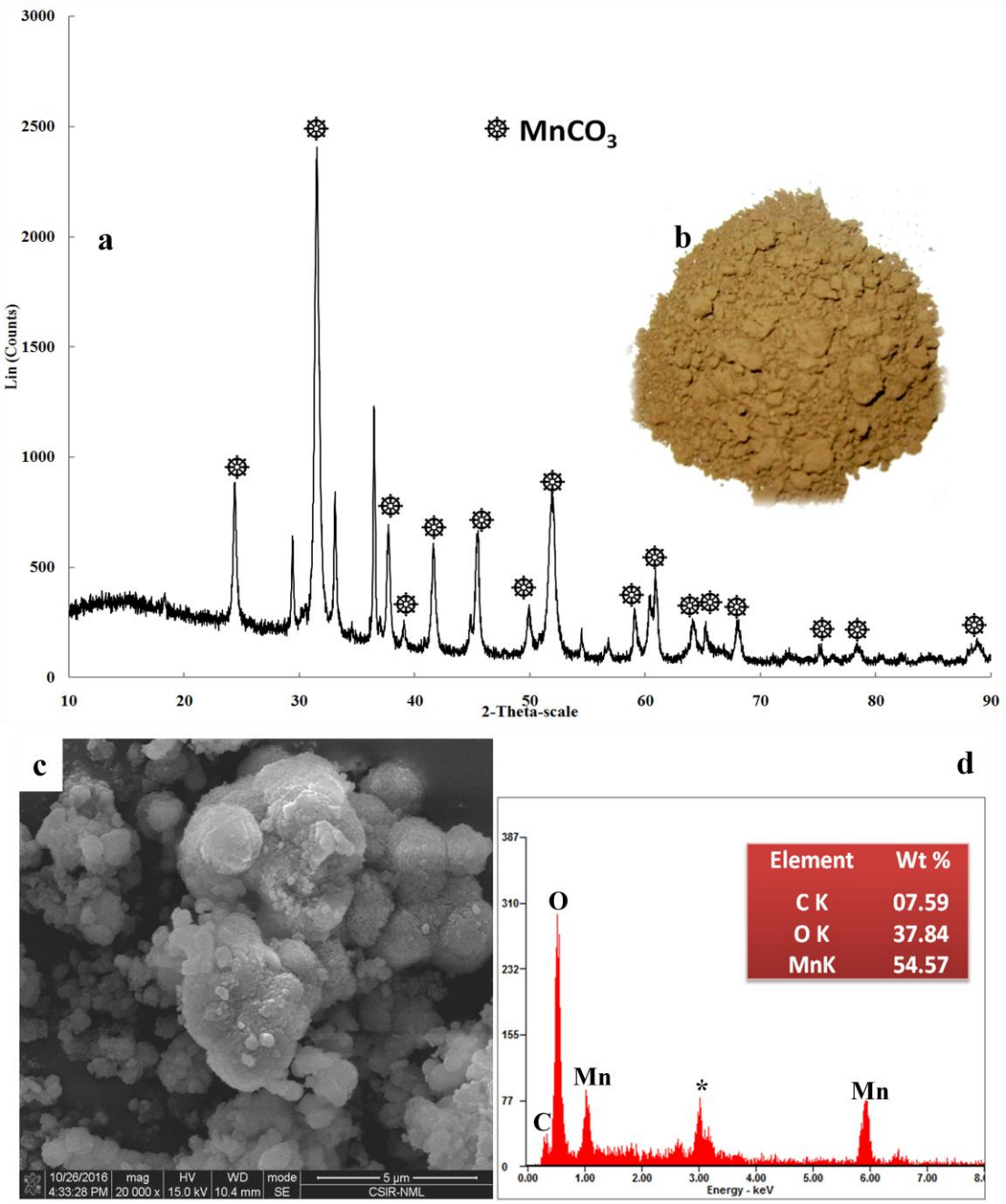

Fig. 3.49: Manganese carbonate synthesized at pH 7.5 (a-XRD; b-brownish-pink precipitate of $MnCO_3$; c-FESEM showing microspheres of Mn-carbonate; d-EDAX of $MnCO_3$)

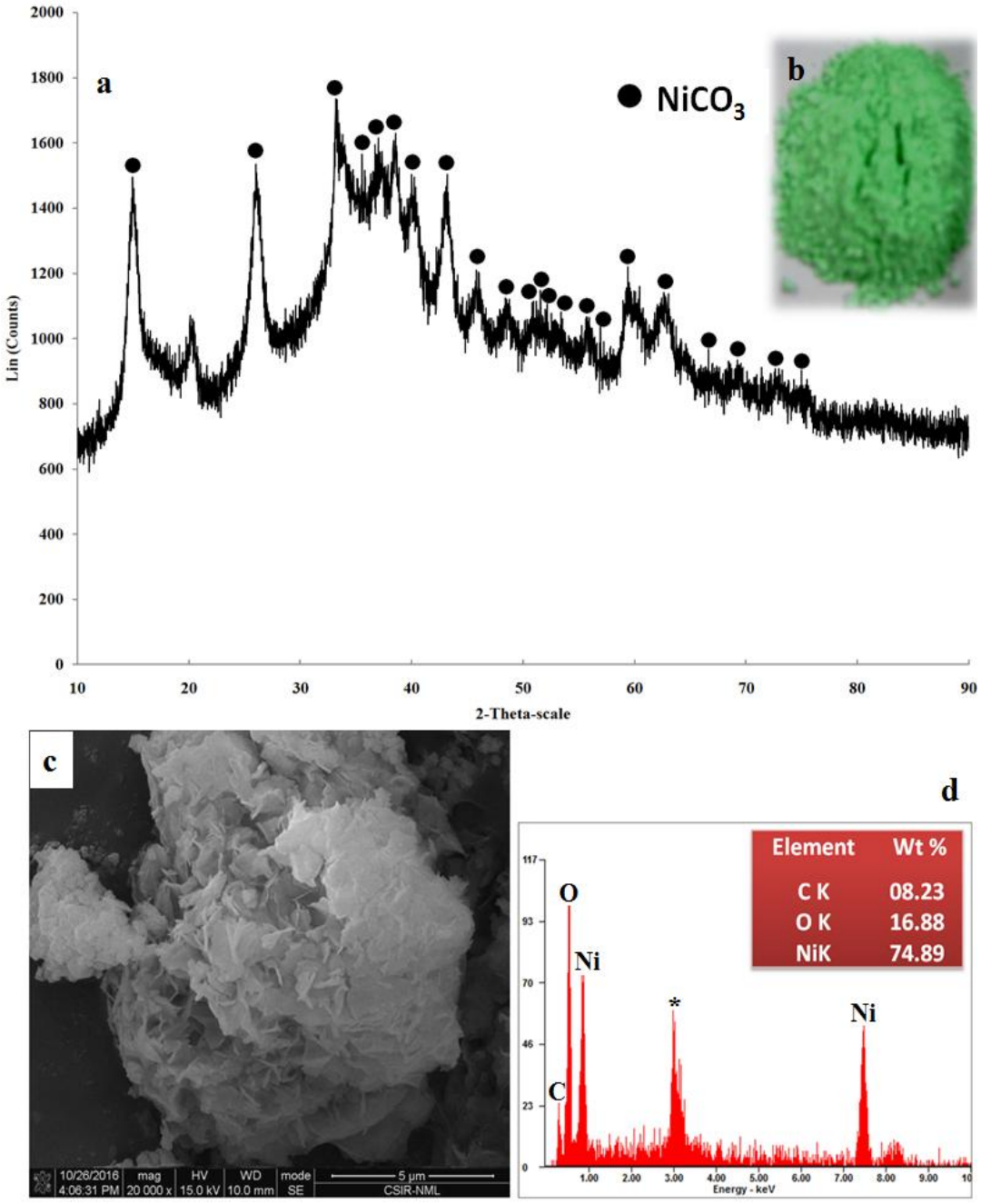

Fig. 3.50: Nickel carbonate synthesized at pH 9 (a-XRD; b-light green $NiCO_3$; c-FESEM of flakes of nickel carbonate; d-EDAX of $NiCO_3$ powder)

3.5.3 Recovery of lithium as Li_2CO_3: After recovering Co, Mn and Ni, lithium carbonate was precipitated by adding an excess amount of sodium carbonate in the filtrate. The precipitation process can be expressed as Eq. (3.23):

$$2Li + Na_2CO_3 \rightarrow Li_2CO_3 \downarrow + 2Na^+ \quad (3.23)$$

Because of the lower concentration of Li^+ in the leach solution, the filtrate after recovering Co, Mn and Ni was condensed to 50% (by vol.) in order to precipitate Li_2CO_3 as much as possible. The white precipitate obtained at pH 14 was filtered and was washed with hot water. The material was then dried at 363 K for 5 h to recover lithium. The XRD pattern of lithium carbonate shown in Fig. 3.51a matched quite well with that of JCPDS Files (no. 22-1141 and 09-0359). The chemical analysis of the white precipitate (Fig. 3.51b) conformed to the 99.6% purity of Li as carbonate with the presence of 30.91 % Li, 16.2 % carbon and traces of Ni (<0.002%).The SEM image (Fig. 3.51c) shows the agglomerates (rectangular flakes) with the mean crystal size ranging from 4-6 μm consisting of sub-nanosized primary particles. Although the EDAX (Fig. 3.51d) confirmed the presence of carbonate salt, but the detector couldn't analyze lithium.

All the bulk products synthesized in this work has great potential which can be further improved for their respective purity. The possibility also exists to alter the state of the carbonates to the suitable salts of the recovered metals for subsequent application prospects in the lithium-battery industry and paving the way for sustainable battery recycling approach.

A general flow-sheet of the entire process is given in Fig. 3.52 to recover important metallic values from the dissembled batteries and selectively precipitating cobalt as its oxalate and Mn, Ni and Li as carbonates.

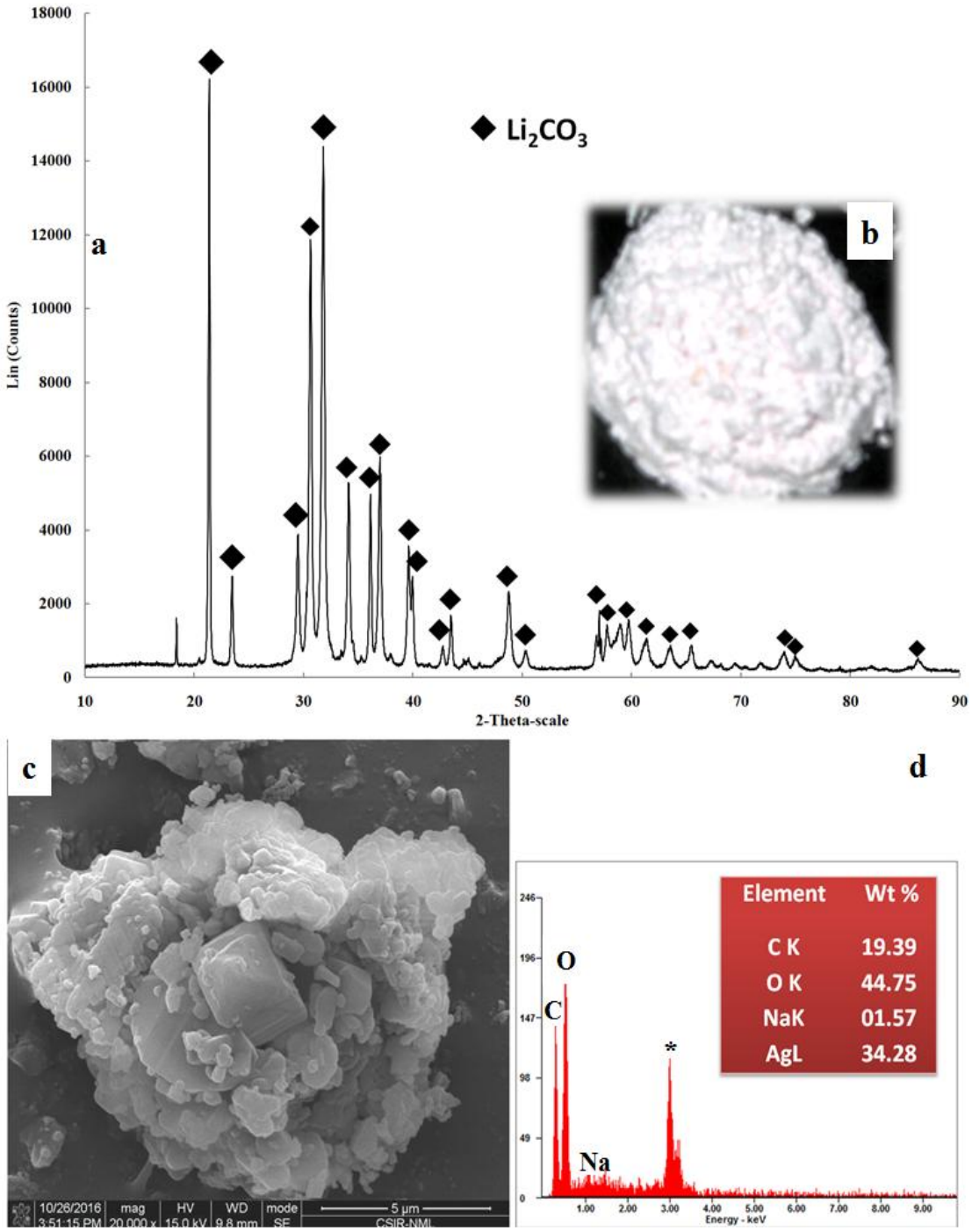

Fig. 3.51: Lithium carbonate synthesized at pH 13-14 (a-XRD; b- picture of Li_2CO_3; c-FESEM of agglomerates of Li-carbonate; d-EDAX of Li_2CO_3)

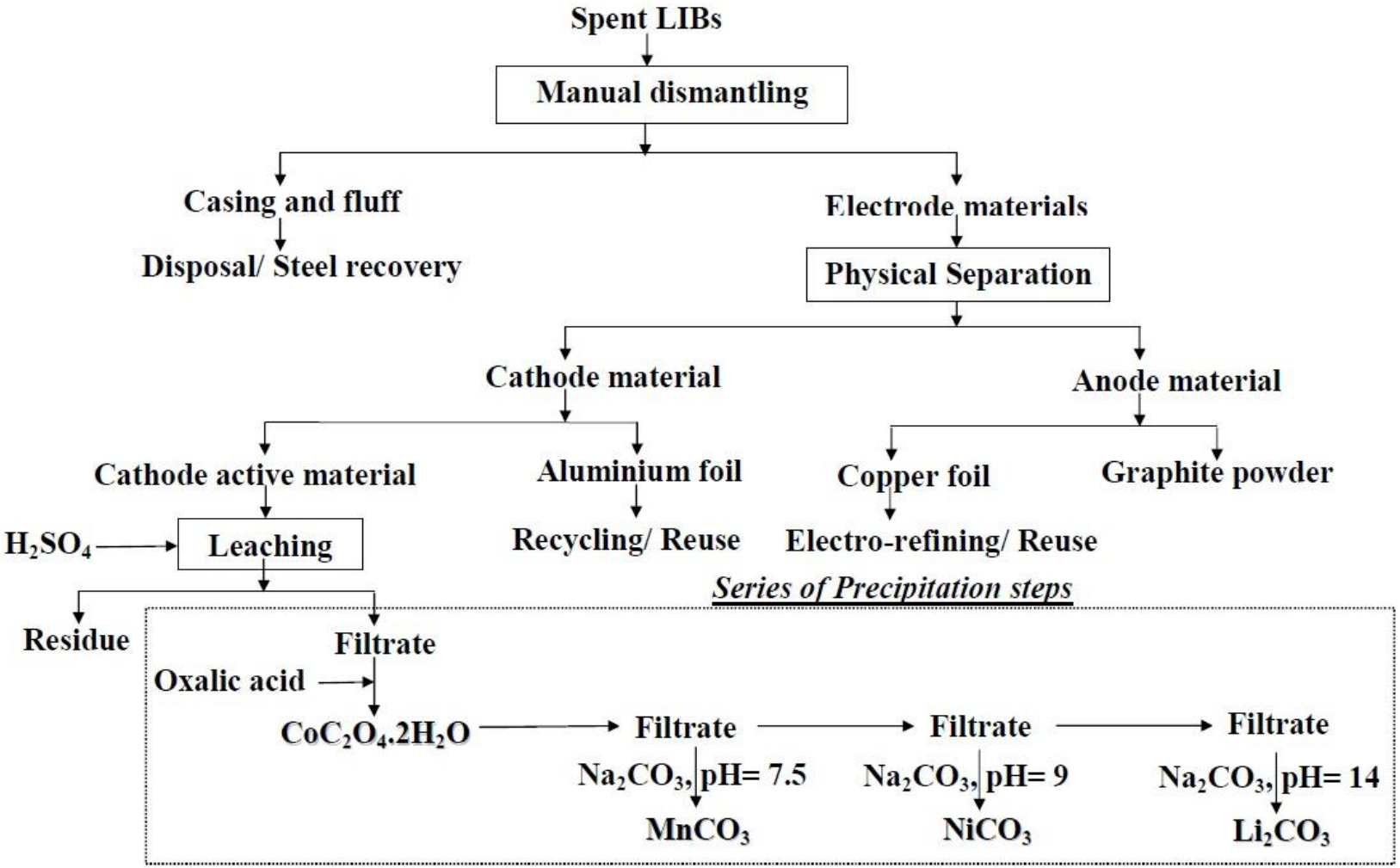

Fig. 3.52: A general flow-sheet developed for extraction and precipitation of Li, Mn, Ni and Co from waste lithium ion batteries

Highlights

- Cathode active material of spent LIBs can be treated to recover the valuable metals by leaching in sulfuric acid in absence and presence of a reducing agent.
- Leaching efficiency of ~90% Li, 49% Co, 94.6% Ni and 48.5% Mn can be achieved when the cathodic material is leached only in 1 M H_2SO_4 at 368 K and 20 g/L pulp density for 240 min. Leaching kinetics following the logarithmic rate law with diffusion control mechanism is corroborated by XRD phase analysis and SEM-EDAX studies. The activation energy (Ea) for the leaching of Li, Co and Ni is found to be 16.4, 7.4 and 18.5 kJ /mol, respectively in the temperature range 308-368 K.
- Leaching efficiency with H_2SO_4 (1 M) in the presence of sodium bisulfite (0.075 M) as a reductant at 368 K and 20 g/L pulp density, is found to be ~96.7 % Li, 91.6 % Co, 96.4 % Ni and 87.9 % Mn in 240 min. The logarithmic rate law representing the kinetic data is supported by the XRD and SEM-EDAX studies. The leaching of Li, Co and Ni acquired activation energy of 20.4, 26.8 and 21.7 kJ /mol, respectively in the same temperature range. Use of H_2O_2 (5% v/v) as a reductant in H_2SO_4 (1M) however, yields the leaching of 94.5% Li, 79.2% Co, 96.4% Ni and 84.6% Mn at 50 g/L pulp density and 368 K in 240 min. While applying the above kinetic model, Ea values were found to be 30.7, 29.6, 42.6 and 43.9 kJ /mol (308-368 K). A comparison of the ΔG^{o}_{368} (-651.2 and -1025.9 kJ in the presence of H_2O_2 and $NaHSO_3$, respectively) for the reaction with $LiCoO_2$, also infers that the latter is thermodynamically a better reductant.
- Process intensification by baking of cathodic material (300 °C, 2 mL H_2SO_4 /5 g powder, 30 min) followed by water leaching (leach-I) selectively recovers 78.6% Li and 80.4% Co over Ni and Mn with low (<15%) dissolution in 60 min at 25% PD and 348 K. With 67% Ni and 64.8% Mn recovery using 1M H_2SO_4 and 0.5M HNO_3 plus glucose (2% w/v) at 323 K in 45 min (leach-II), the overall leaching efficiency is found to be 93.2% Li, 90.52% Co, 82.8% Ni and 77.7% Mn.

- From the leach liquor obtained after acid leaching in presence of $NaHSO_3$, ~96% pure cobalt oxalate (>98% Co) can be precipitated with oxalic acid at 323 K, followed by recovery of Mn and Ni- carbonates at pH 7.5 and 9.0, respectively. Li_2CO_3 (99.6% purity) is then recovered from the filtrate by the addition of Na_2CO_3.